

(2)

**DEPARTMENT OF  
MATERIALS SCIENCE AND MINERAL ENGINEERING**

AD-A214 460

AIRBORNE ELECTROMAGNETIC SENSING OF SEA ICE THICKNESS

Final Report  
prepared for NORDA  
Under U.C.B. contract #N00014-87-K-6005  
482456-25867 (GF-25867)

by  
A. Becker and G. Liu

Engineering Geoscience  
December 1988



Hearst Mining Building  
University of California, Berkeley

89 11 16 114

# REPORT DOCUMENTATION PAGE

Form Approved  
OMB No. 0704-0188

Public reporting burden for this collection of information is estimated to average 1 hour per response, including the time for reviewing instructions, searching existing data sources, gathering and maintaining the data needed, and completing and reviewing the collection of information. Send comments regarding this burden estimate or any other aspect of this collection of information, including suggestions for reducing this burden, to Washington Headquarters Services, Directorate for Information Operations and Reports, 1215 Jefferson Davis Highway, Suite 1204, Arlington, VA 22202-4302 and to the Office of Management and Budget, Paperwork Reduction Project (0704-0188), Washington, DC 20503.

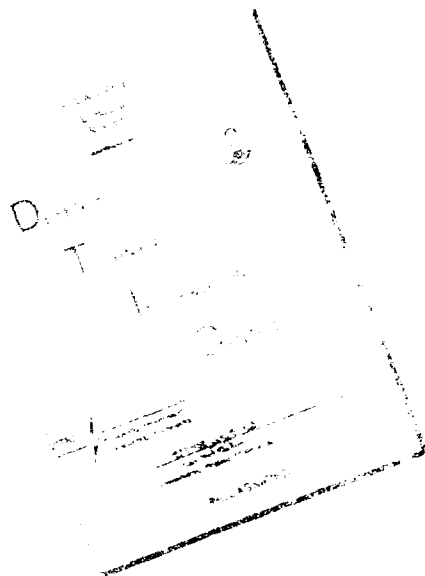
<b>1. Agency Use Only (Leave blank).</b>			<b>2. Report Date.</b> Dec. 14, 1988		<b>3. Report Type and Dates Covered.</b> Final	
<b>4. Title and Subtitle.</b> Airborne Electromagnetic Sensing of Sea Ice Thickness			<b>5. Funding Numbers.</b> Program Element No. DE63704 Project No. R129905 Task No. 300 Accession No. DN257087			
<b>6. Author(s).</b> A. Becker and G. Lire						
<b>7. Performing Organization Name(s) and Address(es).</b> Department of Materials Science and Mineral Engineering Hearst Mining Building University of California, Berkeley			<b>8. Performing Organization Report Number.</b>  CR N00014-87-K-6005			
<b>9. Sponsoring/Monitoring Agency Name(s) and Address(es).</b> Naval Ocean Research and Development Activity Code 311 SSC, MS 39529-5004			<b>10. Sponsoring/Monitoring Agency Report Number.</b>  CR N00014-87-K-6005			
<b>11. Supplementary Notes.</b>						
<b>12a. Distribution/Availability Statement.</b> Approved for public release; distribution is unlimited.			<b>12b. Distribution Code.</b>			
<b>13. Abstract (Maximum 200 words)</b>						
<b>14. Subject Terms.</b> electronic/electrical engineering, physical oceanography snow, ice and permafrost			<b>15. Number of Pages.</b> 121		<b>16. Price Code.</b>	
<b>17. Security Classification of Report.</b> Unclassified			<b>18. Security Classification of This Page.</b> Unclassified		<b>19. Security Classification of Abstract.</b> Unclassified	
<b>20. Limitation of Abstract.</b>						

## Summary

A conventional frequency domain helicopter-borne electromagnetic (HEM) system can be used to map sea ice keels with a reasonable degree of accuracy. A preliminary interpretation of the acquired data can be made manually with the help of a nomogram or automated with the use of a table look-up routine on a small computer. Such data may also be more accurately interpreted with the use of an adaptation of Occam's inversion. This scheme allows for the practical non-uniqueness of the inverse solution but selects the smoothest keel shape that is consistent with the field data. The inversion method is much more computationally intensive than the table look-up technique. While the latter can be implemented on a small computer to form an interactive in-flight interpretation system, the inversion technique involves many forward computations and, for the present, is best reserved for post flight data analysis. It is possible that this difficulty can be resolved with the use of specialized computing equipment.

In the strict sense both the proposed interpretation techniques are only suitable for use on data acquired over two dimensional features whose strike length (measured in a direction perpendicular to the flight line) is much greater than the flight height. An examination of the anomalies for three-dimensional keels however, reveals that good data interpretation is possible whenever the keel strike length exceeds the system height by a factor of three.

# **DISCLAIMER NOTICE**



THIS DOCUMENT IS BEST  
QUALITY AVAILABLE. THE COPY  
FURNISHED TO DTIC CONTAINED  
A SIGNIFICANT NUMBER OF  
PAGES WHICH DO NOT  
REPRODUCE LEGIBLY.

## Table of Contents

Table of Illustrations.....	i
1.0 Introduction.....	1
2.0 AEM Anomalies for Ice Keels.....	2
3.0 Charts for Data Interpretation.....	4
4.0 Inversion of AEM Data .....	7
4.1 Theory .....	8
4.2 Inversion of synthetic data.....	13
4.3 Application to low frequency data.....	17
4.4 Discussion.....	20
5.0 The Three Dimensional Keel.....	21
5.1 The keel model.....	22
5.2 Airborne electromagnetic profiles .....	22
5.3 Discussion.....	26
References.....	26
Appendix A Computational Methods .....	55
Appendix B Computer Programs .....	67

Accession For	
NTIS GRA&I	
DTIC TAB	
Unannounced <input type="checkbox"/>	
Justification .....	
By .....	
Distribution/ .....	
Availability Codes .....	
Dist	Avail and/or
	Special
A-1	23

## Table of Illustrations

	page
Figure 1 HX and HZ systems over sea ice.....	29
Figure 2 System geometry and the traversed feature (A = 3.4m, w= 21m) .....	30
Figure 3 HX system response for two different ice keels (solid line: A = 12m, W = 28m. dashed line: A = 12m, W = 14m) ..	31
Figure 4 HZ system response for the same ice keels as shown in Figure 3 .....	32
Figure 5 HX system response for two different ice keels (solid line: A = 12m, W = 28m. dashed line: A = 6m, W = 28m) .....	33
Figure 6 HZ system response for the same ice keels as shown in Figure 5 .....	34
Figure 7 (a) HX system responses. (b) Cross sections of the model keel (solid line) and the interpreted keel (dashed line) 35	
Figure 8 Two-dimensional interpretation chart for the HX system response. Point C for the theoretical data shown in Figure 8, point D for the 930 Hz field data shown in Figure 11 .....	36
Figure 9 Two-dimensional interpretation chart for the HZ system response .....	37
Figure 10 Field data for a part of line F6L3 .....	38
Figure 11 Comparison of the interpreted result of field data with the drill-hole measurements .....	39

Figure 12 (a) Synthetic data for the HX system and inversion results. Model 1. (b) Synthetic data for the HZ system and inversion results. Model 1 .....	4 0
Figure 13 (a)Synthetic data for the HX system and inversion results. Model 2. (b) Synthetic data for the HZ system and inversion results. Model 2 .....	4 1
Figure 14 (a) Synthetic data with 5% added noise and inversion results for the HX system. Model 1. (b) Synthetic data with 5% added noise and inversion results for the HZ system. Model 1 .....	4 2
Figure 15 (a) Synthetic data with 10% added noise and inversion results for the HX system. Model 1. (b) Synthetic data with 10% added noise and inversion results for the HZ system. Model 1 .....	4 3
Figure 16 (a) Synthetic data with 5% added noise and inversion results for the HX system. Model 2. (b) Synthetic data with 5% added noise and inversion results for the HZ system. Model 2 .....	4 4
Figure 17 (a) Height of the system over the ice/water interface during the flight. (b) Synthetic data and inversion results for the HX system. Model 3. (c) Synthetic data and inversion results for the HZ system. Model 3 .....	4 5
Figure 18 Synthetic data at 2500Hz and inversion results for the HX system. Model 4. The data shown are the scaled sum of the in-phase and quadrature components of the secondary magnetic field .....	4 6
Figure 19 Scaled in-phase data at 16,290Hz and the inversion results for the HZ system .....	4 7
Figure 20 Sea ice keels of Model Set 1. A=3m, w=24m. (a) s= inf.; (b) s=96m; (c) s=48m; (d) s=24m; (e) s=12m .....	4 8

Figure 21 (a) HX system response over the ice keels shown in Figure 20. (b) HZ system response. (c) Cross section of the ice directly below the flight line .....	49
Figure 22 Current flow pattern on a flat water surface below a horizontal-axis transmitter. The length of the arrows corresponds to the strength of the current .....	50
Figure 23 Sea ice keels of Model Set 2. A=6m, w=24m. (a) s= inf.; (b) s=96m; (c) s=48m; (d) s=24m .....	51
Figure 24 (a) HX system response over the ice keels shown in Figure 23. (b) HZ system response. (c) Cross section of the ice directly below the flight line .....	52
Figure 25 Sea ice keels of Model Set 3. A=3m, w=12m. (a) s= inf.; (b) s=96m; (c) s=48m; (d) s=24m; (e) s=12m .....	53
Figure 26 (a) HX system response over the ice keels shown in Figure 25. (b) HZ system response. (c) Cross section of the ice directly below the flight line .....	54

## Airborne Electromagnetic Mapping of Sea Ice Keels

*Alex Becker and Guimin Liu*

### 1.0 Introduction

Sea ice is a unique environment encountered in most Arctic work. This includes the transportation of vehicles through ice-covered waters, the construction of offshore drilling structures, and the safe operation of submarines. In such circumstances, knowledge of the thickness and properties of sea ice is important. This is true especially for ice keels, which constitute a local downward indentation of the ice-water interface.

Recently, Canpolar consultants (1985) reviewed the possible techniques for remotely measuring sea ice thickness, among these they included airborne impulse radar and airborne electromagnetics. The impulse radar technique has been very successful in some areas (Kovacs and Morey, 1985). It may however, occasionally yield erroneous data when saline moisture zones exist within the ice cover. Becker et al. (1983), on the other hand, examined the feasibility of using frequency-domain airborne electromagnetics to determine sea ice thickness. At low frequencies, sea ice is practically transparent to electromagnetic waves and the observed secondary magnetic field can be used to estimate the distance from the EM system boom to the ice-water interface. At the same time, a laser altimeter installed on the boom measures the distance to the surface of the ice, so that the difference of these two distances is the sea ice thickness. This technique was successfully used in mapping the average sea ice thickness in Prudhoe Bay, Alaska, but it failed in an area of a multi-year pressure keel because of the inappropriate one-dimensional (1-D) techniques used to interpret data (Kovacs, et al., 1986; Becker, et al., 1987). In order to recover

the geometry of the keel, two- or three-dimensional interpretation techniques are required.

In this report we primarily concern ourselves with the development of techniques for interpreting AEM data for two-dimensional keels which are assumed to be infinitely long in a direction perpendicular to the flight line. The computational methods used to construct the necessary forward solutions are outlined in the Appendix. These serve either for the construction of interpretation nomograms or in the impletation of a numerical inversion scheme. In order to establish the validity of the two-dimensional interpretation scheme we also examine the effects of finite keel length on the observable anomalies.

In terms of computer time, the modeling technique we employ is particularly well suited for the interpretation of the AEM data collected over sea ice keels. Using the conventional finite element method, 30 minutes CRAY II CPU time is required to compute the AEM system response along a traverse line over an ice keel. However, for a similar problem, using an approach rooted in potential theory, the computation takes about 10 seconds on IBM 3090 (equivalent to about 3 seconds on CRAY) with a gain more than two orders of magnitude in speed. We will show that the assumption of a perfectly conducting sea water model is not a significant drawback since it can be used for any system operation frequency greater than 30 KHz.

## 2.0 AEM Anomalies for Ice Keels

Let us first briefly examine the airborne electromagnetic response to two-dimensional sea ice keels as a function of their size and shape (cf. Fig.1). For these calculations, the electromagnetic system has a coil separation of 6.5m and is "flown" 25m above the upper ice surface which is flat. With the exception of the zone containing the keel, the sea ice is 5m thick and is assumed to have negligible electrical conductivity. The data is calculated for both the vertical-coaxial coil configuration (HX system) and the horizontal-coplanar one (HZ system). The keel is assumed to have

the shape of a Gaussian curve and its parameters and geometry are shown in Figure 2.

Figure 3 shows the HX system response for two different keels with parameters  $A = 12m$ , and  $W = 28m$  (solid line) or  $14m$  (dashed line). The observed secondary magnetic field is expressed in parts per million (ppm) of the primary field at the receiver. There is a big anomaly in the system response due to either of these ice keels. For a keel width  $W = 28m$ , the maximum anomaly is about 35% of the background response and we define this to be the "percent anomaly". In order to characterize the shape of the observed anomaly, we define the "anomaly width",  $q$ , to be the width of the anomaly at one half of its maximum value. For a keel width  $W = 28m$ , the anomaly width  $q$  is  $45m$ . When the keel width  $W$  is halved and other conditions are kept unchanged, the HX system anomaly is significantly reduced. In this case, the maximum anomaly (or percent anomaly) decreases by 37%, and the anomaly width decreases by 33%.

The situation for the HZ system is similar. Figure 4 shows the HZ system response due to the same two ice keels that were previously examined. For a keel defined by  $A = 12m$  and  $W = 28m$ , the percent anomaly for the HZ system response is 32%. The anomaly width  $q$  is  $66m$  in this case, which is much larger than that seen for the HX system. When the keel width is halved, the HZ system anomaly also decreases greatly. In this case, the anomaly amplitude (or percent anomaly) drops by 32% and the anomaly width decreases by 20%. From the comparison of Figures 3 and 4, we can see that the HX system response tracks the shape of the the keel closely, while the HZ system anomaly is much wider.

Next, the keel drawdown  $A$  is halved while the keel width is kept constant at  $W = 28m$ . The corresponding HX system response is shown in Figure 5 (dashed line), and HZ system response is shown in Figure 6 (dashed line). The anomaly amplitude contracts by 29% for the HX system and by 37% for the HZ system. However, the

corresponding decrease in the anomaly width is small, 8% for the HX system, and 3% for the HZ system.

From the above model studies, we find that the amplitude of the anomaly (or accordingly the percent anomaly) is sensitive to both the thickness and the width of the keel. Thus, it is essentially a function of the area of the cross section of the keel. In contrast, the anomaly width is primarily related to the keel width. It is not sensitive to the keel thickness as long as the shape of the keel does not change. It is also noticed that the HX system response is more sensitive to keel shape than the HZ system response. The curve of HX system response resembles the keel shape and the change in the anomaly width due to the change of the keel width is much larger than that for the HZ system (33% compared to 20%).

It is worthwhile to compare the result calculated with the above technique to that obtained by the finite element method (Lee and Morrison, 1985) that allows a finite conductivity for both the sea ice and the sea water as well as a low operation frequency. This is done in Figure 7 for a triangular sea ice keel. The ice is uniformly 5m thick except for the keel area and it has a conductivity of 0.002 S/m. The conductivity of the sea water is 4 S/m and the HX system flies at 30m above the surface of the ice and operates at 2500 Hz. The dashed line in Figure 7 (upper part) represents the in-phase component of the response, and the solid line corresponds to the system response that would be observed if the sea water conductivity were infinite and sea ice conductivity were zero. Notice the similarity of these two curves and that the percent anomalies and anomaly widths are almost identical for these two curves. Thus it appears appropriate to use the perfect conductor model to interpret low frequency data observed in practice.

### 3.0 Charts for Data Interpretation

From the above analysis of numerical data, it is seen that the percent anomaly is a function of the cross area of a sea ice keel and the anomaly width is primarily a function of the keel width. To

interpret field data, we need a strategy to relate the observed electromagnetic anomaly to the keel geometry. In terms of the smooth keel used in this analysis (see Figure 2), we need to estimate the two keel parameters A and W from the observed anomaly of the system response. In the following, we are going to concentrate on the HX system configuration which appears superior in terms of sensitivity of the keel geometry. Parallel analysis can be carried out for the HZ system. .

From the computation and analysis of the HX system response for model keels with systematic values of A and W, one can construct an interpretation chart as shown in Figure 8. The vertical axis of the chart is the percent anomaly, while the horizontal axis represents the ratio of the anomaly width q to the flight height h above the flat part of the ice-water interface. Here, the two sets of parametric curves intersect each other clearly and are well separated. The solid lines are for constant values of the drawdown A, and the dashed lines are for constant keel width W. The charted values of a and w are the keel drawdown "A" and width "W" normalized by h, the system height above the flat seawater surface. As shown, the percent anomaly decreases with the decrease of the keel drawdown and keel width. In fact, the line  $a = 0.8$  tends to zero fast and intersects the lines  $a = 0.4$ ,  $a = 0.2$ , etc.. For purpose of clarity, this is not shown in Figure 8. Nonetheless, this does not pose a serious problem in practice since such narrow and sharp keels are highly improbable. Although the interpretation chart is constructed for  $h = 30m$ , it can be used for the range  $h = 25m - 50m$  with an error less than  $\pm 4\%$ . .

As pointed out at the end of last section, the anomaly shape for low frequency data is almost identical to that obtained in case of the perfect conductor model. This makes the interpretation chart shown in Figure 8 applicable for a wide range of frequencies. We expect that the interpretation chart is useful for the frequency range between 1 - 100 kHz. A similar interpretation chart can be constructed for the HZ system response. It is shown in Figure 9.

Now consider the 2500 Hz theoretical data shown in Figure 7 (dashed line) for an assymmetric triangular keel. From the in-phase component of the AEM response, the percent anomaly and anomaly width are calculated to be 7% and 27m respectively. Thus  $q/h = 27/35 = 0.72$ . We draw this point in the interpretation chart (point C in Figure 8) and find the corresponding values of  $a$  and  $w$  to be 0.1 and 0.35 respectively. Hence  $A = a \times h = 3.5\text{m}$ , and  $W = w \times h = 12.3\text{m}$ . The estimated keel is drawn (symmetrically about the maximum anomaly of the data) in the lower portion of the illustration (dashed line in Figure 7). We can see that the size of the interpreted keel is close to that of the model keel. But since we have assumed that the keel is symmetric in the interpretation, the position of the maximum of the interpreted keel is misplaced 3.5m to the right.

The field data collected over an ice keel in the Prudhoe Bay by Geotech Ltd. for CRREL (Kovacs et al., 1986) are interpreted next. The AEM system used consists of two pairs of vertical coaxial coils (HX system) and two pairs of horizontal coplanar coils (HZ system). The former operate at 930 Hz and 4158 Hz respectively, and the latter operate at 530 Hz and 16290 Hz respectively. The transmitter-receiver separation of each coil pair is about 6.5m.

A part of the 930 Hz and 16290 Hz data for line F6L3 is shown in Figure 10. The altitude is the distance from the system boom to the ice surface measured by a laser altimeter. Note that the quadrature component of the 16290 Hz data is of bad quality. As we can see in the figure, the data are highly correlated with the altitude as expected. First, we interpreted the data using a 1-D technique (Becker et al, 1987). The result shows an average of 3m thick ice (see Figure 11) but no ice keel is apparent in the interpretation. However, we notice that there is an anomaly in the system response from fiducial numbers 2668 - 2675, which can not be related to the small altitude variation in that area. Moreover, the 1-D interpreted results also show thicker ice in that region. For the 930 Hz data, the anomaly width  $q$  is found to be 31.4m and the percent anomaly is 6.5%. Since  $h$  is about 38.5m (altitude + average

ice thickness),  $q/h = 0.83$ . The corresponding point is found in the interpretation chart (point D in Figure 8), which gives  $a = 0.08$  and  $w = 0.42$ . Hence  $A = a \times h = 3.08\text{m}$ ,  $W = w \times h = 16.2\text{m}$ . The interpreted keel is plotted symmetrically about the maximum anomaly in Figure 11 (dashed line). The solid line in the figure is the average of the drill hole measurements along three parallel lines 11.5 meters apart. As we can see, the interpreted keel is an good approximation of the real feature. Note, however, that the effect of the variation of the altitude of the system boom has been neglected in the interpretation.

The interpretation of 4158 Hz data yields similar result to the above. But difficulty was encountered in interpreting the HZ system data which were acquired at 530 and 16290 Hz. As shown in Figure 10, there is also an anomaly in the 16290 Hz data from fiducial numbers 2668 - 2675. If we calculate the percent anomaly and anomaly width in this case, the corresponding point will fall off the interpretation chart shown in Figure 9 and can not be interpreted.

Generally speaking, the chart interpretation method gives an overall estimate of the size and shape of an ice keel. In order to recover the detail shape of an ice keel, we consider in the next section an iterative technique for data inversion. The chart interpretation can be used to obtain an initial model for the iterative technique where the variation of the system altitude can be easily accounted for.

#### 4.0 inversion of AEM Data

Now consider the determination of sea ice keel shape by data inversion. In order to overcome the problem associated with 1-D data interpretation, we present a two-dimensional (2-D) AEM data inversion scheme where ice thickness may vary along the flight direction of the AEM system. In the perpendicular direction, however, the geometry of the ice/water interface is assumed to be invariant. Although the actual ice bottom topography is three dimensional (3-D), most ice keels do exhibit a dominant extension in

one direction which is called the strike because they are formed by the interaction of two ice plates (Canpolar, 1985). Indeed, as will be shown in the next section, if the strike length of an ice keel of Gaussian shape is greater than three times the AEM system flight height 2-D interpretation may be quite appropriate.

The interpretation scheme that we have developed is based on the principle of the Occam's inversion presented by Constable et al. (1987). Due to practical non-uniqueness of the inverse problem, there may be many sea ice keels that may fit the observed data within a specified error. This scheme yields the smoothest among these. The smooth keel shows the basic features of the actual keel although small bumps on its surface may not appear in the inversion results. Because the process of the data acquisition however constitutes a low-pass filter, it is also possible that the information needed to define the keel in detail is absent from the acquired data.

We first examine the theory of constrained smooth inversion and then use it to interpret synthetic field data which are generated with our numerical modeling program (cf. Appendix). Both noise free and artificially contaminated data are used to test the scheme. Finally we propose a procedure to apply this inversion scheme to low frequency data. In addition to this field data sets (collected in Prudhoe Bay by Geotech,Ltd. in 1985) are also interpreted using this procedure.

#### 4.1 Theory

Let  $x$  denote the traverse direction of the AEM system,  $y$  the strike direction of the ice keel and  $z$  the downward pointing vertical. The interface of the ice and the water is described by  $z = h(x)$ . Our purpose here is to reconstruct this interface from the airborne electromagnetic data  $d(x)$  while the upper surface of the ice is mapped by a laser device. The difference in elevation between the bottom and the top surface of the ice is the required ice thickness. The data  $d(x)$  can be either the horizontal or/and the vertical secondary magnetic field recorded during the flight.

Now consider  $h(x)$  as the only unknown. This is true when the two assumptions used in our previous modeling algorithm (see the Appendix) are valid. These are: 1) the sea ice is transparent to the electromagnetic wave, and 2) the sea water can be treated as a perfect electric conductor. With these considerations, the AEM data can be written as

$$d(x) = F[h(x)] \quad \dots (1)$$

where  $F[ ]$  is the functional for forward modeling. Equation (1) immediately reveals that the inversion problem is actually one-dimensional (1-D) with the direction of variation along  $x$  instead of along  $z$ . Fortunately there is a large amount of geophysical literature dealing with 1-D inversion. One particular scheme that well suits our needs is Occam's inversion presented by Constable et al. (1987).

The basis for Occam's inversion is the search for the smoothest solution that fits the observed data within a specified tolerance. This principle applies particularly well to our work because electromagnetic wave propagation in sea water is a diffusion process, so that the resolution of sharp edges on the ice/water interface can not be expected from the data. Furthermore, any information on the sharp edges is contained in the high wave-number range of the data, which is contaminated by noise. Because inversion implies downward continuation (Parker, 1977), the attempts to reconstruct the fine structures of the interface will amplify any noise and result in unstable solutions. Hence a stable solution is necessarily smooth.

In order to find the smoothest solution, let us first define the roughness of the ice/water interface. Physically the rougher the interface is, the larger the magnitude of its derivatives. Thus we define

$$R = \int_{p_1}^{p_2} \left| \frac{dh(x)}{dx} \right|^2 dx$$

to be the roughness of the interface  $h(x)$ ;  $(p_1, p_2)$  define the lateral keel extent outside of which the interface is assumed to be flat. In the discrete sense,

$$R = \sum_{i=2}^N (h_i - h_{i-1})^2 = \|\partial h\|^2 \quad \dots (2)$$

where  $h_i = h(x_i)$  and  $\|\cdot\|$  denotes the  $L^2$  norm, and

$$\partial = \begin{vmatrix} 0 & 0 & 0 & \dots & 0 \\ -1 & 1 & 0 & \dots & 0 \\ 0 & -1 & 1 & \dots & 0 \\ \ddots & \ddots & \ddots & \ddots & \ddots \end{vmatrix}$$

$$h = (h_1, h_2, \dots, h_N)^T$$

Note that  $p_1 = x_1$ ,  $p_2 = x_N$  and that the points  $x_1, x_2, \dots, x_N$  are usually equally spaced.

Suppose that there are  $M$  data points recorded over an ice keel,  $d_j = d(X_j)$ ,  $j=1, 2, \dots, M$ . The corresponding computed predictions from the discrete model  $h$  are  $F_j(h)$ . The goodness of fit of the predictions to the actual data can be evaluated using the least-squares criterion

$$E = \sum_{j=1}^M [d_j - F_j(h)]^2 = \|d - F(h)\|^2 \quad \dots (3)$$

where

$$\begin{aligned} d &= (d_1, d_2, \dots, d_M)^T \\ F(h) &= (F_1(h), F_2(h), \dots, F_M(h))^T \end{aligned}$$

The ice/water interface  $h$  can only vary within some physical bounds. If we assume that the  $z = 0$  plane is chosen such that it coincides with the flat part of that interface then a reasonable lower bound is:

$$h_i \geq 0, \quad i = 1, 2, \dots, N \quad \dots (4)$$

since the ice keel protrudes downward. An upper bound can also be set for each individual case

$$h_i \leq T_i, \quad i = 1, 2, \dots, N \quad \dots (5)$$

In the Arctic, small ice keels may protrude several meters into the water, whereas large keels can protrude tens of meters (Lowry and Wadhams, 1979). The values of  $T_i$  should be estimated for each specific ice keel encountered. Note that  $h_1 = h_N = 0$  should be included in the constraints in order for the solution to be smooth at the two end points. This condition can be met by simply letting  $T_1 = T_N = 0$ .

Now the mathematical problem to be solved can be stated as follows: find a solution  $h$  which minimizes the roughness  $R$  and brings the misfit  $E$  within an acceptable tolerance, while the bound constraints (4) and (5) are satisfied. Without the bound conditions (4) and (5), this problem is exactly identical to the one solved by Constable et al. (1987).

The condition for the data misfit is

$$\|d - F(h)\|^2 \leq E_* \quad \dots (6)$$

where  $E_*$  is the tolerance. If we treat this inequality as an equality and apply the method of Lagrange multipliers, the above problem can be reduced to the minimization of

$$U = \|\partial h\|^2 + \mu^{-1} (\|d - F(h)\|^2 - E_*) \quad \dots (7)$$

with constraints (4) and (5). Here  $\mu^{-1}$  is the Lagrange multiplier. As interpreted by Constable et al,  $\mu$  is a smoothing parameter. The larger the  $\mu$  is, the less the solution is affected by the misfit. On the contrary, if  $\mu$  is small, the data misfit is minimized with little influence from the roughness term.

The original problem can now be solved with the following procedures: Solve the above minimization problem for a series of  $\mu$

values to obtain a set of solutions of the ice/water interface. Among these solutions, choose the one which satisfies the tolerance condition (6). If more than one solution satisfies (6), choose the one with the largest  $\mu$  value for this corresponds to the smoothest solution desired.

Such solutions can not however be easily obtained by the direct minimization of the objective function  $U$  ( equation (7) ) since the minimization is non-linear. It is first necessary to transform the non-linear problem into a problem of quadratic programming, for which existing mathematical tools can be used.

Let us linearize the  $F(h)$  about an initial model  $h^0$

$$F(h) = F(h^0) + J \Delta \quad \dots (8)$$

Here  $h = h^0 + \Delta$ , and the Jacobian matrix is

$$J = \begin{vmatrix} \frac{\partial F_1}{\partial h_1} & \frac{\partial F_1}{\partial h_2} & \cdots & \frac{\partial F_1}{\partial h_N} \\ \frac{\partial F_2}{\partial h_1} & \frac{\partial F_2}{\partial h_2} & \cdots & \frac{\partial F_2}{\partial h_N} \\ \cdots & \cdots & \cdots & \cdots \\ \frac{\partial F_M}{\partial h_1} & \frac{\partial F_M}{\partial h_2} & \cdots & \frac{\partial F_M}{\partial h_N} \end{vmatrix} \quad \dots (9)$$

Substituting (8) into (7) and dropping the constant term  $\mu^{-1}E$ , we obtain

$$U = ||\partial h||^2 + \mu^{-1} ||\tilde{d} - J h||^2$$

where  $\tilde{d} = d - F(h^0) + J h^0$  is the modified data. Rearrangement of the above equation gives

$$V = \frac{1}{2} \mu U - \frac{1}{2} \tilde{d}^T \tilde{d} = \frac{1}{2} h^T H h - \frac{1}{2} \tilde{d}^T C^T h \quad \dots (10)$$

Here  $V$  is the new objective function and

$$\mathbf{H} = \mu \partial^T \partial + \mathbf{J}^T \mathbf{J}$$

$$\mathbf{C} = \mathbf{J}^T \tilde{\mathbf{d}}$$

Note that  $\mathbf{H}$  is a symmetric positive-definite matrix. The minimization of the new objective function  $V$  is equivalent to the minimization of  $U$  for a fixed value of  $\mu$ .

Now that the new objective function is in quadratic form the problem of optimization with bound constraints (4) and (5) can be solved using quadratic programming (Gill et al., 1981). There are subroutines available in existing mathematical software libraries which can be used for this purpose. These are E04AF in the NAG Fortran Library and VE04A in the Harwell Fortran Library. We selected VE04A because of its simplicity.

The smoothest solution can now be actually obtained in the following way. Starting from an initial model  $\mathbf{h}^0$ , solve the minimization problem for different  $\mu$  values. From these solutions choose the one that minimizes the actual misfit  $E$  instead of  $V$ . (Minimizing  $V$  may result in divergence of the solution (Constable et al., 1987)). Use this solution for the next initial model and iterate until the solution for the ice/water interface that brings the misfit below a specified tolerance is found.

The initial model  $\mathbf{h}^0$  can be chosen arbitrarily since it does not affect the convergence of the inversion to the smoothest solution. This is one of the beauties of the smooth inversion scheme which sets out to seek a unique solution. In our problem we set the initial model to be a flat ice cake, i.e.,  $\mathbf{h}^0 = (0, 0, \dots, 0)^T$ .

#### 4.2 Inversion of synthetic data

In this section we will apply the above scheme to invert some synthetic data which are generated with the fast modeling algorithm (see Appendix). To test the stability of the inversion scheme white

noise will also be added to the numerical data. Most inversion schemes require the knowledge of solutions to the forward problem in the computation of the Jacobian matrix. Here these are obtained with the fast forward modeling algorithm. The partial derivatives in the Jacobian are computed using the forward finite-difference of two numerical solutions. Thus one iteration of the inversion process requires  $N+1$  forward calculations for  $M$  data points.

Before considering the inversion results let us first describe the geometry of the problem for all the synthetic models. Unless otherwise specified, the transmitter and the receiver are both small circular loops separated by 6.5 meters, and both are maintained at 25 meters above the upper ice surface. For convenience the vertical co-axial coil system is referred to as the HX system because the axes of the coils are in the  $x$  direction while the horizontal co-planar coil system is referred to as the HZ system. The receiver measures the secondary magnetic field which is expressed in parts per million of the received primary field. The inversion is performed for the HX and the HZ system data independently although the joint inversion can be easily accomplished. Except in the keel area the ice thickness is assumed to be five meters. Note that for the synthetic data generation we assume the induction limit to hold so that the system frequency is not involved. Applications to low frequency data, however, will be shown in the next section.

The position of the end points  $p_1$  and  $p_2$  of the ice keel must now be chosen. These can be arbitrary as long as they are located outside the range of the keel. They should not be too far apart however, because the computation of the Jacobian matrix can be quite expensive and convergence of the inversion may be slow. From our experience, locating these two points at the one quarter of the peak HX system anomaly points, and at the two points at half of the peak HZ system anomaly yields good results. Note that this condition may need to be relaxed for field data because they may be acquired at fluctuating flight heights, which will distort the shape of the observed anomaly.

The sampling interval of  $h(x)$ ,  $\Delta x$ , is taken to be 3 meters for all the examples shown in this report. The data  $d(x)$  is sampled at an interval of 3.5 meters unless otherwise specified, which at a helicopter speed of 68 knots corresponds to a recording rate of 10 samples/second.

Figure 12(a) shows the inversion results of the HX system data for a triangular model keel (Model 1), which is symmetric and is located between 60 and 90 meters along the profile. The keel drawdown at the peak is 5 meters and its two sides slope at 18 degrees from the horizontal. The solid line in the upper graph is the synthetic data corresponding to the ice keel shown in solid line in the lower graph, while the dashed line is the system response from the inverted keel shown in dashed line in the lower graph. Similar results for the HZ system data are shown in Figure 12(b). In the inversion the two end points  $p_1$  and  $p_2$  are taken at 45 and 105 meters respectively. The tolerance criterion for convergence is set at 1 ppm for the HX system data and 2 ppm for the HZ system data. Three iterations in the inversion yield the convergent solutions shown in Figure 12 from an initial guess of a flat ice cake that is 5 meters thick. As we can see the interpreted keels have smooth vertices as can be expected for the constrained smooth inversion. The interpreted keels are about 1.5 meters too shallow, and the independent results for the HX and the HZ system data are almost identical.

In the next example we invert the synthetic data for an irregular trapezoidal ice keel (Model 2). The steep side of the keel is 34 degrees from the horizontal while the slope of the other side is 16 degrees (Figure 13). The keel protrudes 6 meters down into the water with a flat bottom of 12 meters. Again both the HX and the HZ system data are inverted independently and the results shown were obtained after three iterations. Misfit for the HX system data is again held below 1ppm, and that for the HZ system data is below 2ppm. For the HX system the inverted maximum keel thickness is correct although the two vertices on the steep side are smoothed out. The

other side however is imaged correctly. For the HZ system, the results are similar except that the maximum keel thickness is a half meter too small.

Now white noise of 5% to 10% of the peak anomaly is added to the Model 1 and Model 2 theoretical data. Here system noise may be small but "geological noise" is estimated to be about 5 percent of the anomaly amplitude. The tolerance criterion for the inversion is set at the RMS noise level and the convergence is usually achieved within 4 - 5 iterations. The inversion results are shown in Figures 14 - 16. As demonstrated in these figures the inversion still yields good results except at the 10% noise level where the keel interpreted from the HZ system data is flat at the bottom (Figure 15). Our experience with noisy data shows that the inversion results obtained from the HX system data are usually better than those obtained from the HZ system data. In practice 5% noise is probably excessive.

We next examine the case where the height of the system varies during a flight, as is usually the case in practice. The model keel is a symmetric trapezoid in shape with a maximum drawdown of 3 meters (Model 3). The flat bottom is 12 meters wide and the two sides of the keel slope at 12 degrees from the horizontal (Figure 17). The system height over the flat part of the ice/water interface, shown in Figure 17(a), varies between 37 and 41 meters. This height variation was taken from a test flight in Prudhoe Bay. Here it is assumed that the transmitter and the receiver are always at the same level although in practice the instrument pod may tilt in space. The inversion results for the HX and the HZ system response are shown in Figures 17(b) and (c). As can be seen the inverted keels agree very well with the model keel in this case. The final data misfit is 0.3ppm for the HX system and 0.8ppm for the HZ system.

### 4.3 Application to low frequency data

The inversion procedure can also be extended to the interpretation of low frequency field data. As mentioned earlier, the synthetic data used above were generated in the induction limit where the secondary field only exhibits an in-phase component. In practice however, this can not be realized because the sea water is not a superconductor and the operating frequency of the system must be low enough for the EM wave to penetrate the ice freely. Hence the measured secondary magnetic field has both an in-phase and a quadrature component. Ideally the in-phase and quadrature components can be inverted simultaneously using the above scheme if a fast modeling algorithm for a general conductivity distribution exists. The finite-element and finite-difference methods have been very successful in solving such problems (Lee and Morrison, 1985; Stoyer and Greenfield, 1983). The computational costs associated with these methods however, are prohibitive so that they can not be used in solving this problem as too many forward computations must be carried out even for one iteration.

Although the fast modeling algorithm that we developed generates theoretical data at the induction limit it can be used to invert low-frequency data. For data collected at 30 kHz the arithmetic sum of the in-phase and quadrature components gives a good approximation of the data that would be obtained at the induction limit (Becker et al, 1983). This sum can be directly interpreted using the previous scheme, but it must first be multiplied by a scale factor prior to interpretation. The same scheme can be used since the anomaly shape changes but little with frequency (Becker and Liu, 1987). The scale factor can be computed as the ratio of the response at the induction limit to the sum of the in-phase and quadrature components at that frequency for a 1-D model. Note that this factor varies with the system altitude. If the altitude does not change much in a flight over the ice keel this factor can be taken as a constant.

Let us now consider an example of synthetic data of the HX system at the frequency of 2500 Hz which was generated by the finite-element method (Lee and Morrison, 1985). The conductivities of the ice and water are 0.002 S/m and 4 S/m respectively. The ice is uniformly 5 meters thick except at the keel area where it protrudes 5 meters into the sea water. The shape of the keel is step-triangular as shown in Figure 18 and the HX system is flown at 30 meters above the ice surface. The scaled sum of the in-phase and quadrature components of the theoretical data and the inversion results are also shown in Figure 18. There are ten unevenly spaced data points and the scale factor is 1.044 in this case. As we can see the inverted ice keel is close to the model although it is somewhat shallower. We consider this an encouraging success of the application of the above proposed procedure.

We have not yet had the opportunity to experiment with large quantities of low frequency data. Thus it is not clear in which frequency range the above procedure can be used to yield reasonable results. Furthermore the role of the water conductivity has not yet been investigated although we suspect that its main effect is to decrease the resolution of the inversion results expected from the superconductor assumption. It is worthwhile however to attempt an inversion of the data collected in the Prudhoe Bay by Geotech Ltd. in 1985 (Kovacs, et al., 1987). The data is for line F6L3 collected with the HZ system at the frequency of 16290 Hz. Because the quadrature component is of very poor quality only the in-phase component was scaled by a factor of 1.104 and interpreted. The system altitude, the scaled in-phase component and the inversion results are all shown in Figure 19. The inversion was performed with the two end points of the ice keel fixed at  $p_1 = 54$  meters and  $p_2 = 102$  meters. The background ice thickness was fixed at 3.3 meters which is the average from the 1-D interpretation.

The interpreted ice thickness is 1.5 meters too shallow as compared to the drill-hole measurements (solid line in the bottom of Figure 19) in the keel area. However the keel is clearly visible in the

inversion result, which is encouraging since it is much better than the 1-D inversion that shows but little of the keel (Becker et al., 1987). The inversion was stopped at an RMS data misfit of 15 ppm since more iterations could not reduce the misfit. There may be several causes for such a large misfit:

- 1) The effects of the pitch and roll of the system during the flight was not accounted for in this inversion.
- 2) The time constant of the instrument may be too large for such a small keel to be fully represented in the data. The inversion treats the data as being recorded with a zero time constant, which ignores the integral effect due to the instrument. This effect has been carefully studied by Becker and Cheng (1987).
- 3) The top surface of the ice was treated as a flat plane and the effect of the associated ridge was not considered.
- 4) The assumed 2-D structure of the ice may be incorrect.
- 5) For this frequency channel the operational system noise was large. The quadrature component was quite erratic and was not used in the inversion.

Errors due to 1) can be diminished by improving the computer code. Errors due to 2) and 5) can be reduced to a large extent by improving the instrument. But errors due to 4) can not be reduced in the present 2-D inversion scheme. To do this a 3-D inversion algorithm needs to be developed which can be an extension of the present scheme. The process will be computer intensive and furthermore, the data acquisition will necessarily cover an area instead of a line over the keel. This will be very costly and may not be worthwhile.

Errors due to 3) need to be further investigated. Treating the ice top as a flat plane has an effect of pressing the ridge down into the sea water. The ice thickness probably may not be largely

affected. But it remains to be seen whether a topographic correction is necessary before a 2-D inversion is attempted.

Applying the constrained smooth inversion to the scaled sum of the in-phase and quadrature components of the real data appears to be an attractive simple scheme. If the phase of the response does not change, this is identical to scaling the in-phase component only. The performance, mainly the resolution, of this scheme will deteriorate with lowering the operation frequency. The range of the frequency, in which the above procedure can be applied, needs to be defined by further investigation. Effects of the conductivities of the sea ice and water will also reduce the resolution of the keel geometry expected from the assumption of transparent ice and superconducting sea water, which need be studied in the future.

All the computations in the above inversion have been done on a IBM RT PC computer, which has a comparable speed as the Microvax. A typical case of inversion of  $M = N = 20$  takes about 4 hours of the CPU time. At the present the computer code is not optimized and it can be shown that its optimization may sharply reduce the CPU time by a factor of 5. It appears that in flight data interpretation will require some highly specialized computing equipment.

In all our examples the ice keel position was assumed known. In practice the position of the ice keel may be obtained from the videocamera record of the associated ridge. If this is not possible the AEM data itself can be used to estimate the position of the ice keel prior to the inversion. To do this the influence of the altitude should first be removed from the data so that the remaining anomaly will indicate the position of the keel.

#### 4.4 Discussion

The 2-D inversion scheme can successfully recover the ice keel information, which is usually lost in 1-D inversion. Because the electromagnetic induction is a diffusion process, sharp edges can not

be resolved from the data and we set out to seek a smooth ice keel, which retains the major features of the true ice keel. Although the scheme is designed to work for data collected in the induction limit with transparent ice and superconducting sea water, it can be applied to low frequency data, where the sum of the in-phase and quadrature components is scaled to approximate the required data. At the present the range of the frequency, in which this procedure can be applied, remains unclear and needs further investigation. With refinements and optimization of the computer program however, there is no doubt that this algorithm can be used routinely to process field data.

## 5.0 The Three-Dimensional Keel

Under usual circumstances the ice-water interface in arctic seas exhibits the same irregular topography that is normally associated with land forms. In areas covered by young ice however, the topographic features are minimal and a one-dimensional data interpretation technique for the average thickness of the ice sheet from airborne electromagnetic data (Kovacs, et. al. , 1987) can be used. This technique fails in areas of even moderate ice-water interface topography (Kovacs, et al, 1987). In cases where the axial length of the keel is very large (compared to the AEM system altitude) it is possible to remedy this situation with the use of interpretation charts that allow for a two-dimensional description of the keel. If necessary, a 2-D data inversion outlined above may be carried out to delineate ice keels in more details. Because the two-dimensional data interpretation method appears to produce adequately accurate results it appears worthwhile to find the minimal keel axis length that is necessary for its proper application. This is done below where theoretical data for three-dimensional (3-D) keels is presented. In all 14 different keel models are considered.

### 5.1 The keel model

Cartesian coordinates are used and the XY plane is chosen to coincide with the flat part of the ice-water interface so that the Z axis points vertically down into the sea water. The ice is assumed to be transparent to electromagnetic waves and sea water is assumed to be a perfect electric conductor. Both the co-axial (HX) and co-planar (HZ) coil systems are considered.

The 3-D Gaussian keel model is an extension of the 2-D model described above. Its shape is given by

$$t(x,y) = A e^{-\frac{y^2}{0.361 s^2} - \frac{x^2}{0.361 w^2}} \quad (1)$$

where

$t(x,y)$  is the protruding depth of the ice keel into the sea water,  
 $A$  is the keel drawdown or maximum keel thickness,  
 $w$  is the keel width at  $t = A/2$  on the cross section  $y = 0$ ,  
 $s$  is the keel width at  $t = A/2$  on the cross section  $x = 0$ .

Here we define the  $y$  direction as the strike direction of the ice keel and hence designate  $s$  as the strike length of the keel. An infinite value of  $s$  corresponds to a 2-D ice keel. When  $s = w$ , the keel is a body of revolution. The numerical calculations were carried out as outlined in the Appendix.

### 5.2 Airborne electromagnetic profiles

In this section, we examine AEM profiles over three sets of model ice keels. Except in the keel area, the sea ice is assumed to have a uniform thickness of 5 meters. The keel parameters  $A$ ,  $w$ , and  $s$  are varied to demonstrate the corresponding changes in the AEM system response. For each model set, the keel drawdown  $A$  and keel width  $w$  are fixed, while the keel strike length is varied. Model Set 1 represents a shallow keel, where  $A = 3m$ ,  $w = 24m$ , and keel

strike lengths of 12, 24, 48, 96, and inf. meters respectively (Figure 20). The corresponding theoretical AEM response for the HX and HZ system over the center of these features along a line perpendicular to the keel strike is shown in Figure 21, where curves 1, 2, 3, 4, and 5 correspond to  $s = 12, 24, 48, 96$ , and inf. meters respectively. Both the transmitter and the receiver, which are separated by 6.5m, are "frown" 25m above the upper ice surface. The system response is plotted at a point located mid-way between the transmitter and receiver, and is expressed in parts per million of the primary field at the receiver. Figure 21 (c) shows the cross section of the ice directly below the flight line.

It is evident in Figure 21(a) that as the strike length  $s$  decreases the HX system anomaly becomes smaller but the general shape of the anomaly curve changes little. If these system anomalies for 3-D ice keels are interpreted using the 2-D chart given in our previous report, the interpreted cross section of the keel will be smaller than that in the 3-D model. The significant effect here is a reduction of the interpreted keel drawdown. The keel width however is less affected since the anomaly width does not contract significantly with the keel strike.

As shown in Figure 21(a), the HX system response for a keel strike length  $s$  of 96m (curve 4) closely resembles the response for an infinitely long keel (curve 5). In fact the maximum difference in the relative amplitude or percent anomaly (c.f. Becker and Liu) is of the order of 1.5% and would result in an under-estimation of the keel depth of about 10%. In fact the relative error in the percent anomaly size is also of this order and suggests that a 10% value for this quantity be used as a threshold value for the definition of a two-dimensional keel. Thus, If the maximum relative difference in the relative anomaly is less than 10%, the finite strike keel can be effectively considered as two-dimensional, and hence 2-D interpretation techniques can be applied.

Using this criterion, any ice keel whose strike length exceeds 96m can be effectively considered as two-dimensional for the purpose of data interpretation. In general, the ratio of the strike length to the system height over the ice-water interface must be larger than 96/30. This value is much greater than the value expected from the footprint for the HX system (see Becker, et al., 1987), which is 1.4. At the first sight, this may seem puzzling. A careful look at the current distribution on the water surface, however, will yield the explanation.

The current pattern for a horizontal-axis transmitter is shown in Figure 22 (from Becker, et al., 1987). It consists of two circular current rings while most of the current flows in a direction parallel to the strike of the ice keel. For a keel of finite-strike, this major current flow is distorted. The footprint however was computed on the basis of the unaltered current flow so that it is not surprising to find that the strike/height ratio needed for 2-D interpretation is much larger than the footprint of the HX system.

Now let us look at the HZ system response and see how it changes as the keel strike length is varied. Curves 1, 2, 3, 4, and 5 in Figure 21(b) correspond to  $s = 12, 24, 48, 96$ , and inf. meters respectively. As expected, the HZ system response also decreases when the strike length of the keel is reduced. The major change is the decrease of the anomaly amplitude. The anomaly width, in contrast, stays almost constant. Nonetheless, as the keel strike is further decreased, the anomaly shape also changes and the lower part of the anomaly flattens out.

The HZ system response for  $s = 96$ m is also close to that for the 2-D keel. The maximum relative difference in the relative anomaly in this case is about 12%. Thus taking 10% as the threshold, the keel strike should be somewhat longer than 96m in order to use the 2-D interpretation. Roughly speaking, we may again take the strike/height ratio to be approximately  $96/30 = 3.2$  for the 2-D interpretation to be valid. This is the same as that for the HX system.

and is very close to the value obtained from the footprint of HZ system which is 3.7 . As a matter of fact, the current pattern on a flat water surface for a vertical-axis transmitter consists of concentric circles so that a 3-D ice keel will distort this pattern as much as a 2-D ice keel does.

Now let us increase the keel drawdown A to 6m and keep the keel width at  $w = 24\text{m}$ . Figure 23 shows the deeper ice keels with different strike lengths (Model Set 2). The corresponding HX and HZ system responses are shown in Figure 24 (a) and (b) respectively. Now both the HX and HZ system responses are much larger than those for Model Set 1 due to the larger cross section of these keels. But the characteristics of these anomalies are similar to those discussed for Model Set 1. Therefore, the analysis for Model Set 1 still holds in this case.

Figure 25 shows the narrower keels that make up Model Set 3, where  $A = 3\text{m}$  and  $w = 12\text{m}$ . The keel strike, again, is 12, 24, 48, 96, and inf. meters respectively. Figure 26 (a) and (b) displays the HX and HZ system response and curves 1, 2, 3, 4, and 5 correspond to  $s = 12, 24, 48, 96$ , and inf. meters. Figure 26 (c) shows the cross section of the keel below the flight line.

Now the HX system response is much smaller than those shown in Figure 21 (a) because of the smaller size of the ice keels. But the relative characteristics remain unaltered and the analysis for Model Set 1 still applies here.

The HZ system anomaly also reduces with the decrease of the strike length of the keel. Furthermore, it is observed that a minor feature begins to appear at the center of the anomaly when the keel strike is small. This feature, however, may not be real as it may be caused by numerical errors in the calculation. At present, we are unable to make this point clear due to computational limitations.

### 5.3 Discussion

- 1) The strike length of an ice keel must be at least three times the flight height of the AEM system in order to successfully use the 2-D techniques to interpret both HX and HZ systems response.
- 2) For the HX system, the anomaly amplitude decreases as the keel strike shortens, but the anomaly width changes little.
- 3) For the HZ system, the anomaly amplitude also decreases as the keel strike contracts. At the same time, the lower part of the anomaly tends to become flat.

### References

- Becker, A., Morrison, H.F., and Smits, K., 1983, Analysis of airborne electromagnetic systems for mapping thickness of sea ice: NORDA technical note 261.
- Becker and Cheng, 1987, Detection of repetitive electromagnetic signals, *Electromagnetic Methods in Applied Geophysics*, Vol. 1, Edited by M.N. Nabighian, pp.443-465.
- Becker, A., and Liu, G., 1987, Airborne electromagnetic mapping of sea ice keels, First Interim Report to NORDA.
- Becker, A., Liu, G., and Morrison, H.F., 1987, Airborne electromagnetic sensing of sea ice thickness: Report prepared for CRREL under UCB contract #DACA89-85-K-0008.
- Bergeron, C.J., Juliette, W.I., and Gus, A.M., 1987, Lateral resolution of the modified image method for sea-ice thickness, Extended Abstracts of the SEG 57th International Meeting, New Orleans.
- CANPOLAR Consultants Ltd., 1985, Review of floating ice thickness measurement: Report prepared for the Department of Fisheries and Oceans, Canada under contract 01SE.FP921-3-0624.

Gill, P.E., Murray, W., and Wright, M.H., 1981, *Practical Optimization*, Academic Press, Inc..

Graham,I.G., 1980, Some application areas for Fredholm integral equations of the second kind: The Application and Numerical Solution of Integral Equations, Anderssen et al. ed., 75-101.

Kovacs,A., and R.Morey, 1985, Electromagnetic measurements of multi-year sea ice using impulse radar: CRREL Report 85-13.

Kovacs., A., Valleau, N., and Holladay, J.S., 1987, Airborne electromagnetic sounding of sea ice thickness and sub-ice bathymetry, CRREL Report 87-23, pp.1-40.

Kovacs, A., Morey, R.M., Gordon, F.N.C., and Valleau, N.C., 1986, Modeling the electromagnetic property trends in sea ice and example impulse radar and frequency-domain electromagnetic ice thickness sounding results: CRREL report in preparation.

Lee, K.H., and Morrison, H.F., 1985, A numerical solution for the electromagnetic scattering by a two-dimensional inhomogeneity: Geophysics, 50, 466-472.

Liu, G., and Becker, A., 1988, Effect of three-dimensional sea ice keels on airborne electromagnetic system response, Second Quarterly Report to NORDA.

Liu, G., and Becker, A., 1987, Airborne electromagnetic sensing of sea ice thickness, presented at the 57th SEG Annual International Meeting.

Lowry, R.T., and Wadhams, P., 1979, On the statistical distribution of pressure ridges in sea ice, Journal of Geophysical Research, Vol.84, No. C5, pp.2487-2494.

Mikhlin,S.G., 1964, Integral equations: Pergamon Press, 7-15.

Parker, R.L., 1977, Understanding inverse theory, Ann. Rev. Earth Sci., vol.5, pp35-64.

Parry, J.R., and Ward, S.H., 1971, Electromagnetic scattering from cylinders of arbitrary cross-section in a conductive half-space Geophysics, 36, 67-100.

Rikitake,T.K., and K.Whitham, 1964, Interpretation of the Alert anomaly in geomagnetic variations: Canadian Journal of Earth Sciences, vol.1, 35-62.

Rossiter, J.R., and Lalumiere, L.A., 1988, Evaluation of sea ice thickness sensors, Canpolar Inc., Toronto, Project 1027.

Stoyer, C.H., and Greenfield, R.J., 1976, Numerical solutions of the response of a two-dimensional earth to an oscillating magnetic dipole source, Geophysics, Vol.41, No.3, pp.519-530.

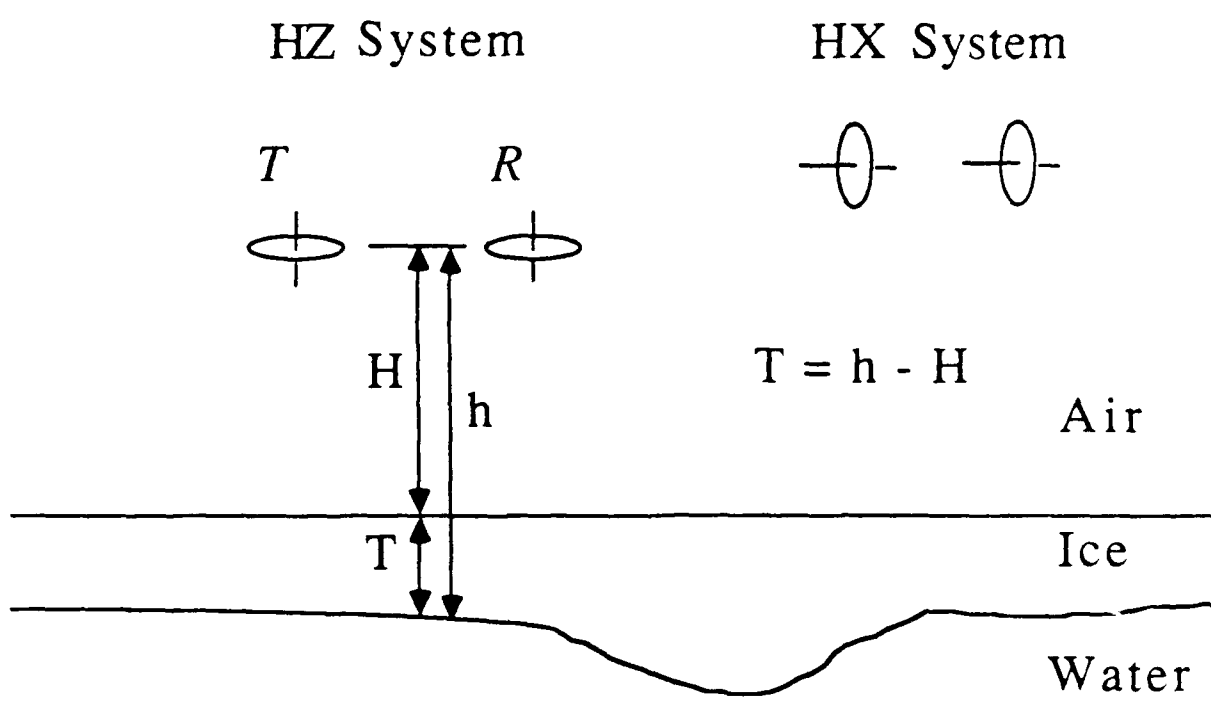


Fig.1 HX and HZ systems over sea ice

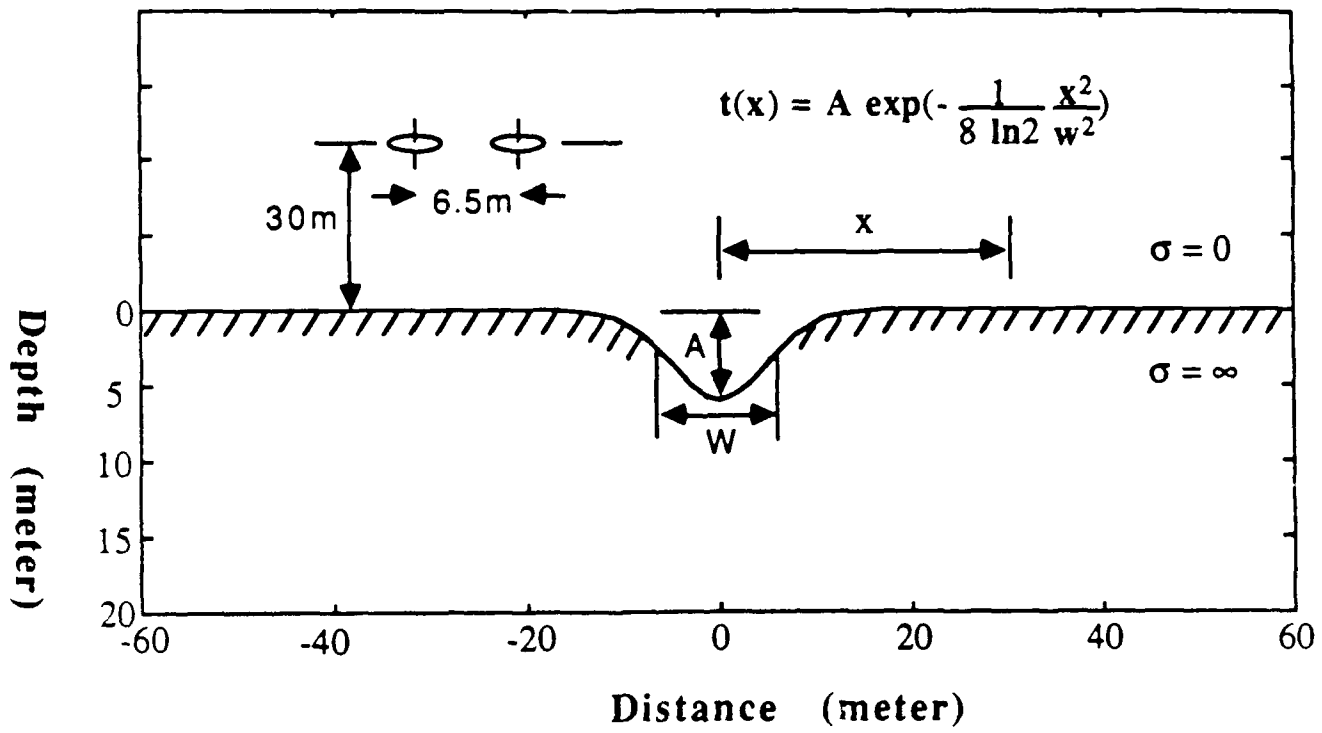


Fig.2 Cross section of a smooth keel

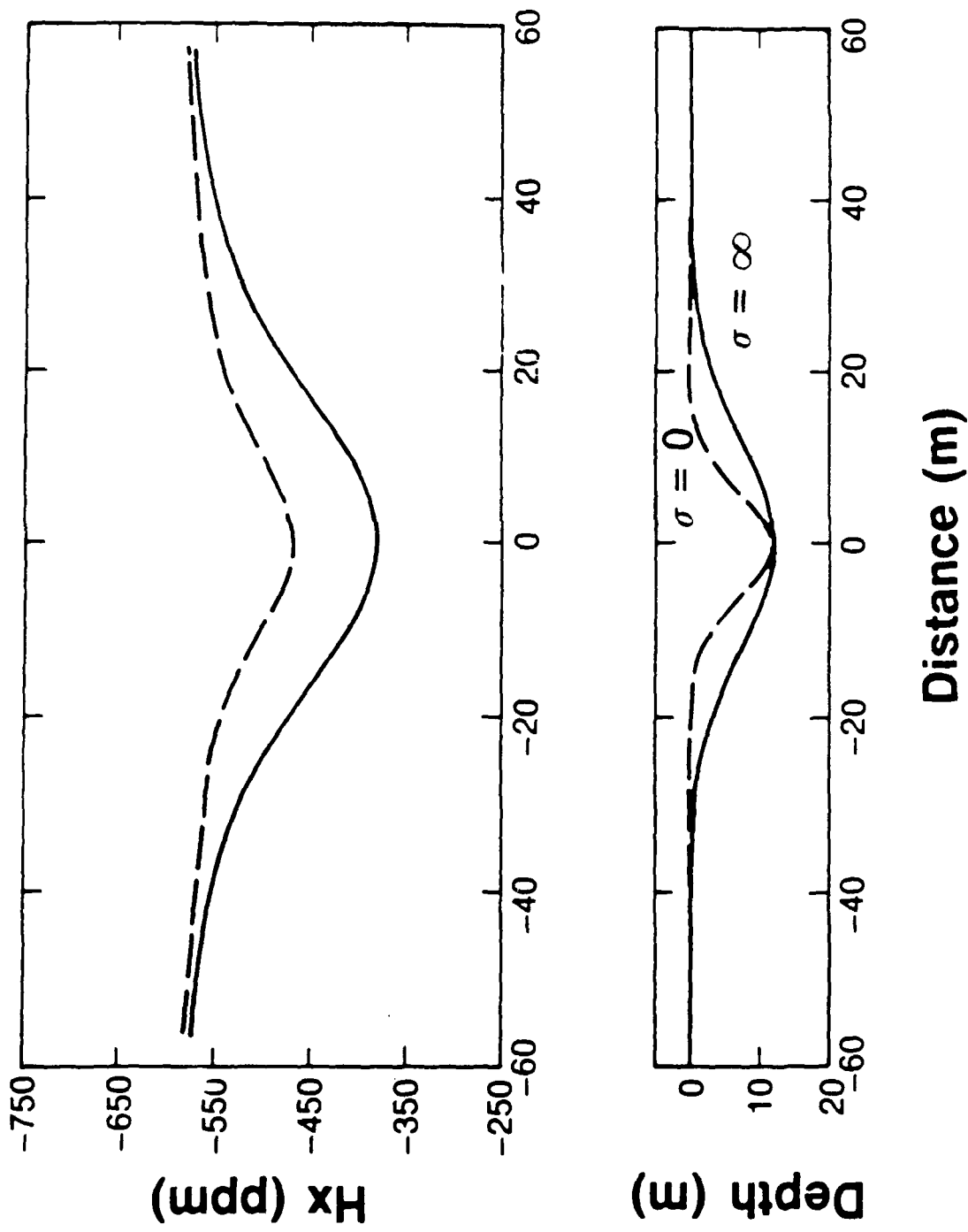


Fig.3 Effect of Keel Width on IIx System Response

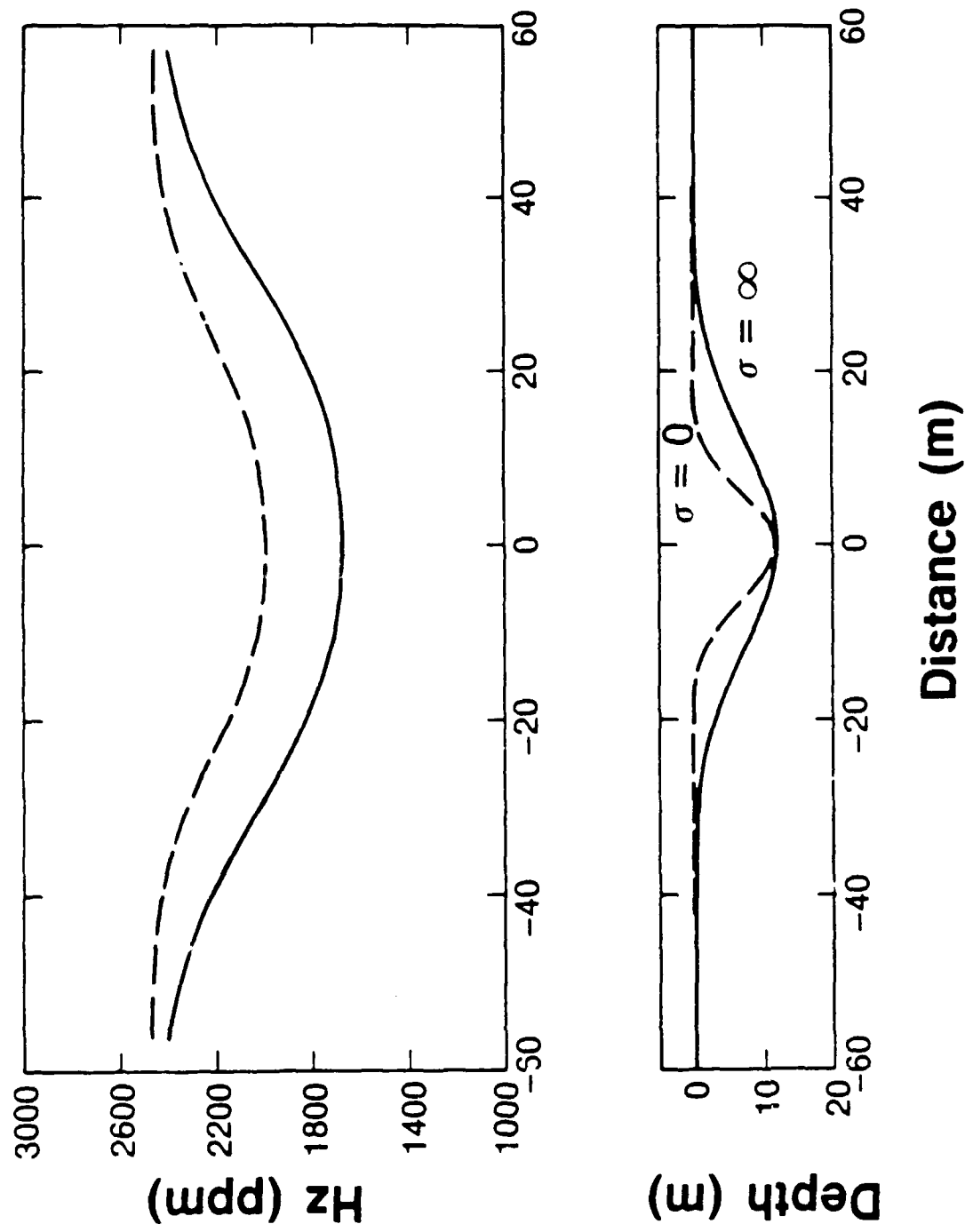


Fig.4 Effect of Keel Width on Hz System Response

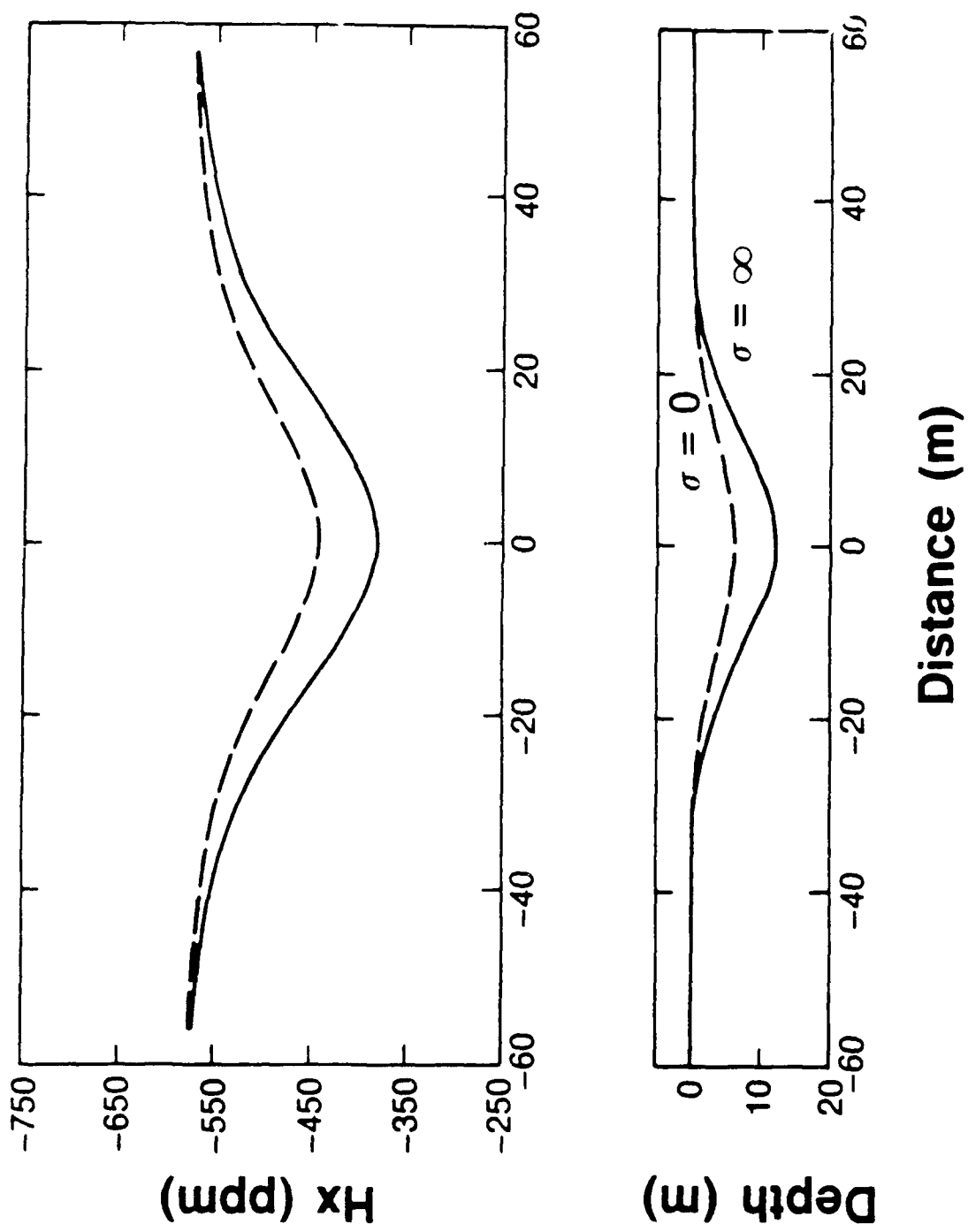


Fig.5 Effect of Keel Drawdown on HX System Response

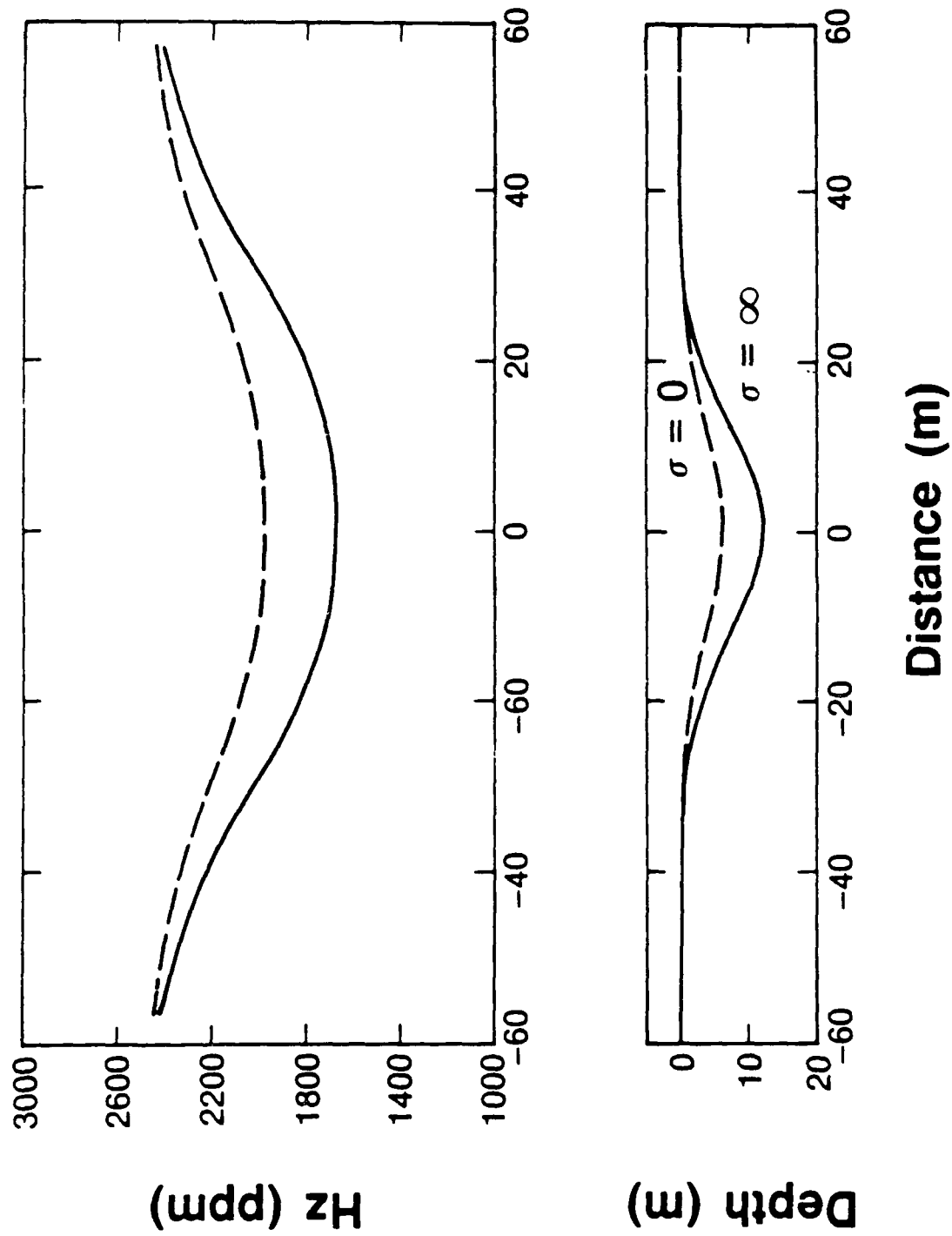


Fig.6 Effect of Keel Drawdown on HZ System Response

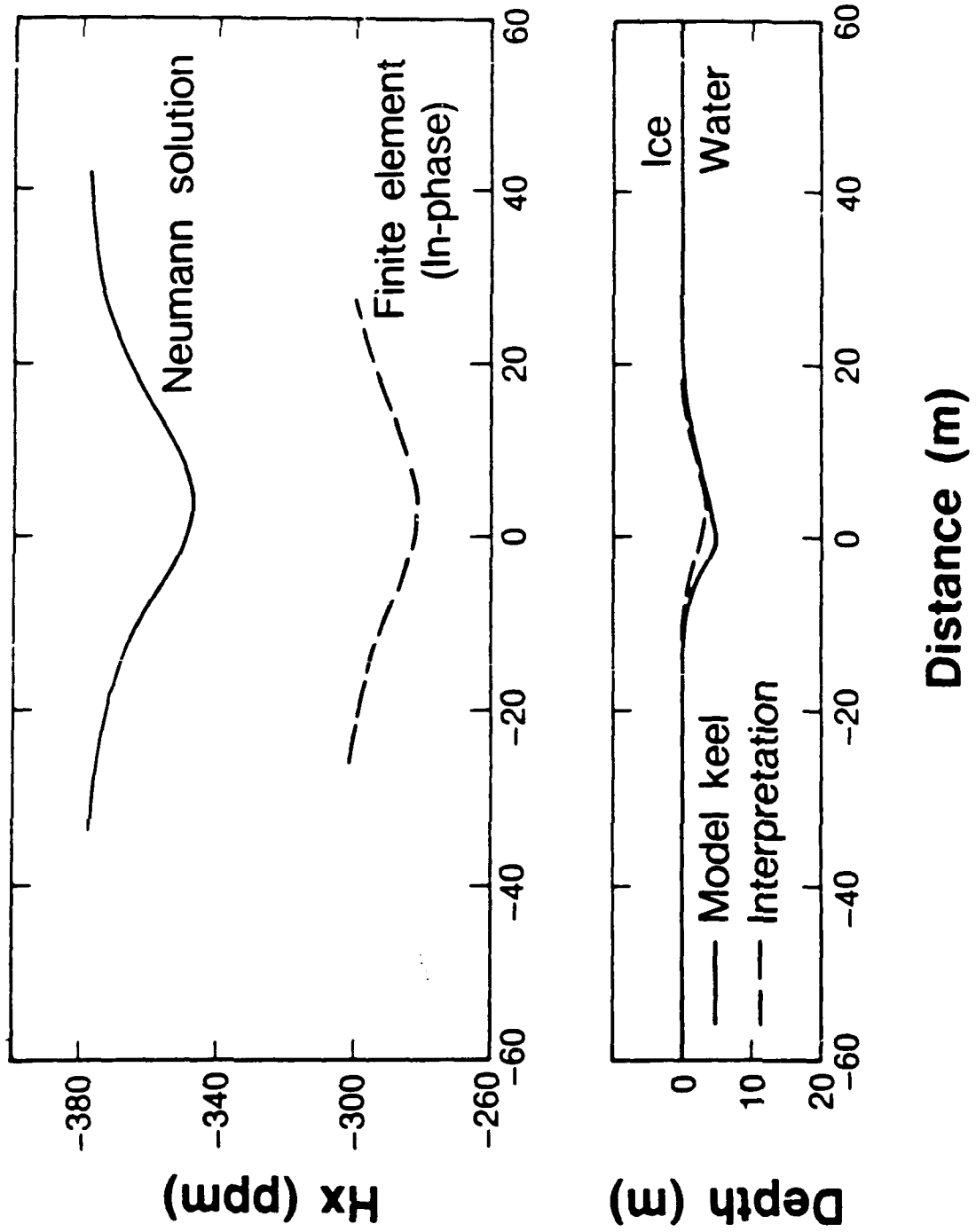


Fig.7 Model Response

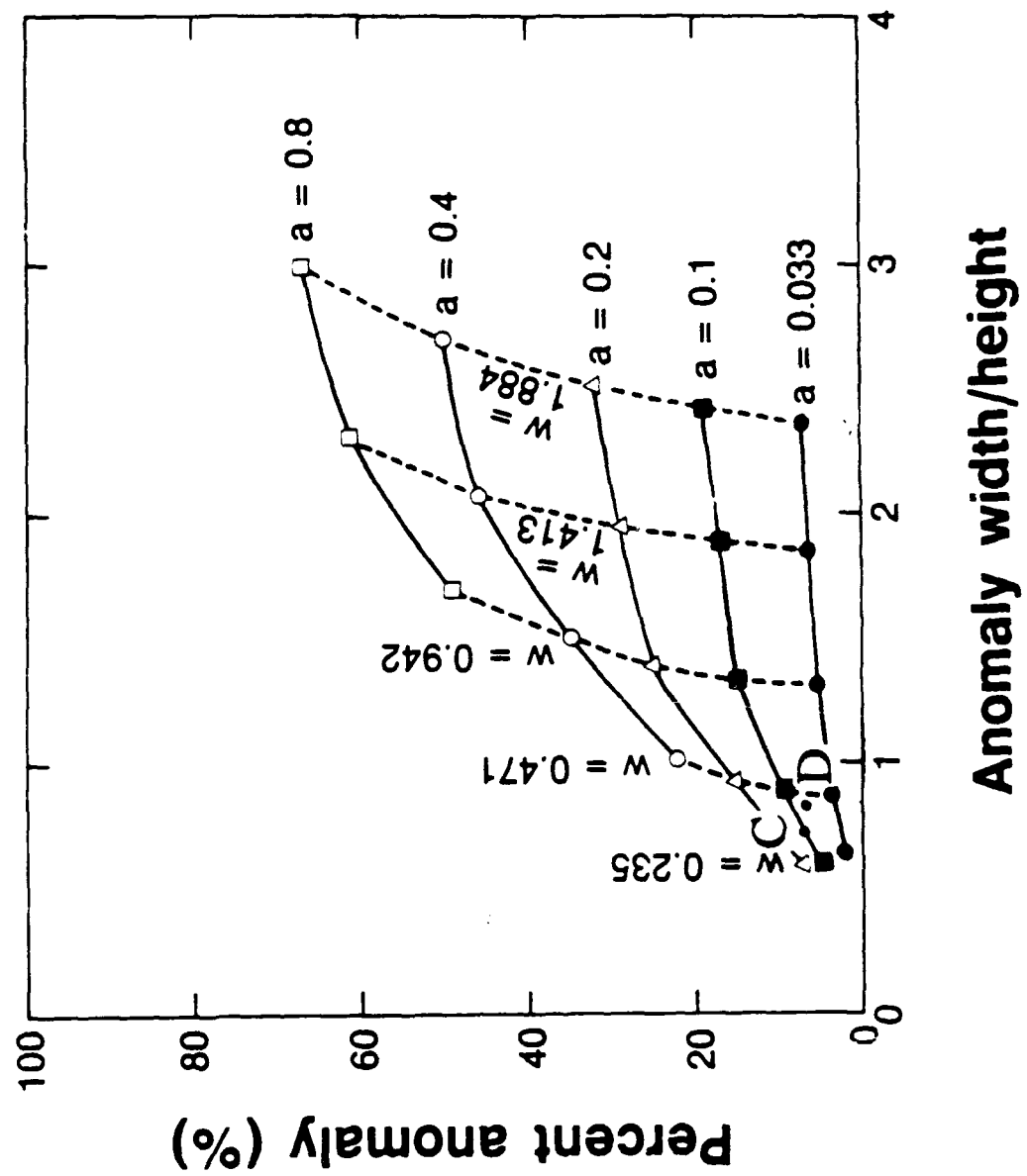


Fig.8 Interpretation Chart for HX System

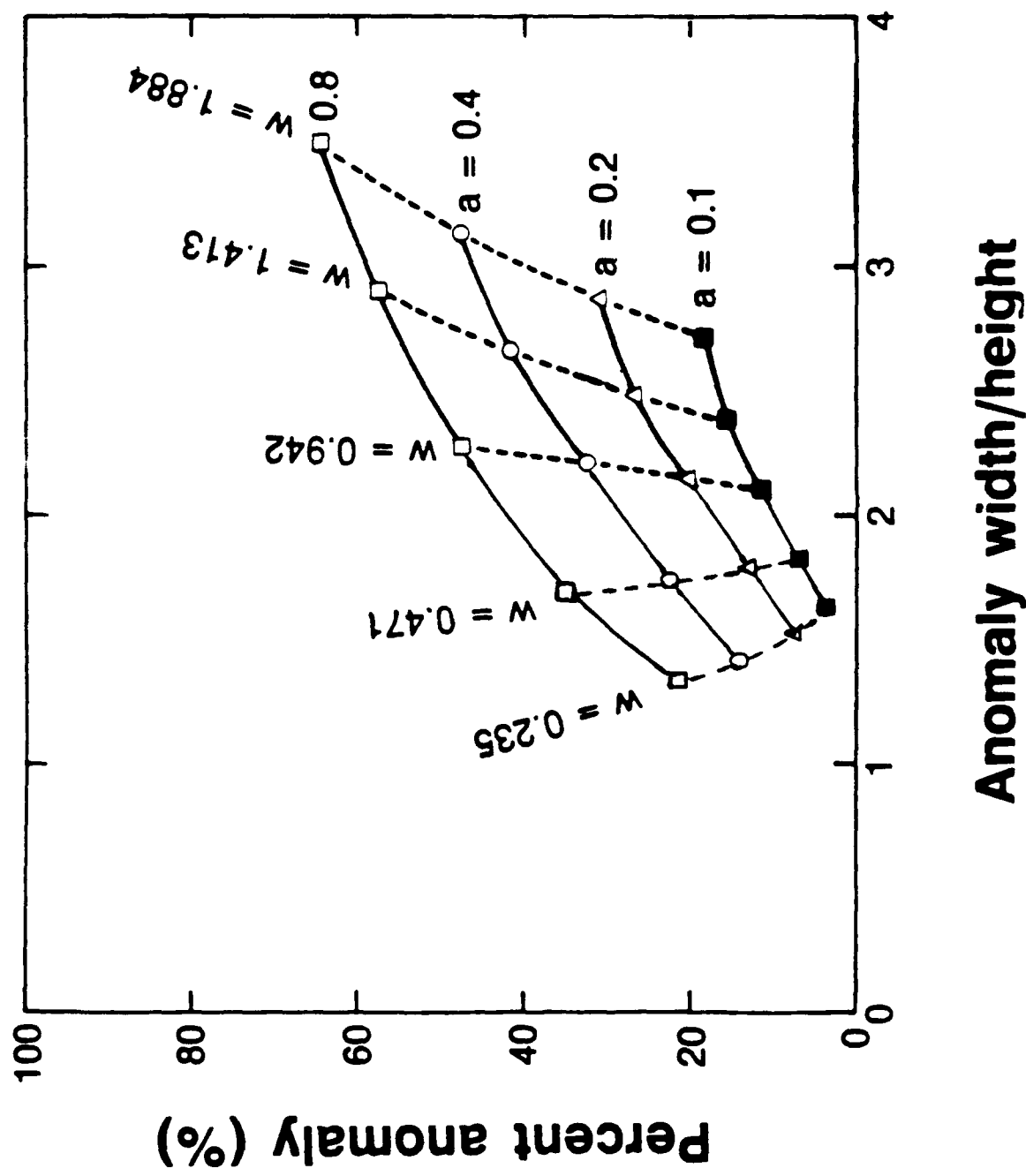


Fig.9 Interpretation Chart for HZ system

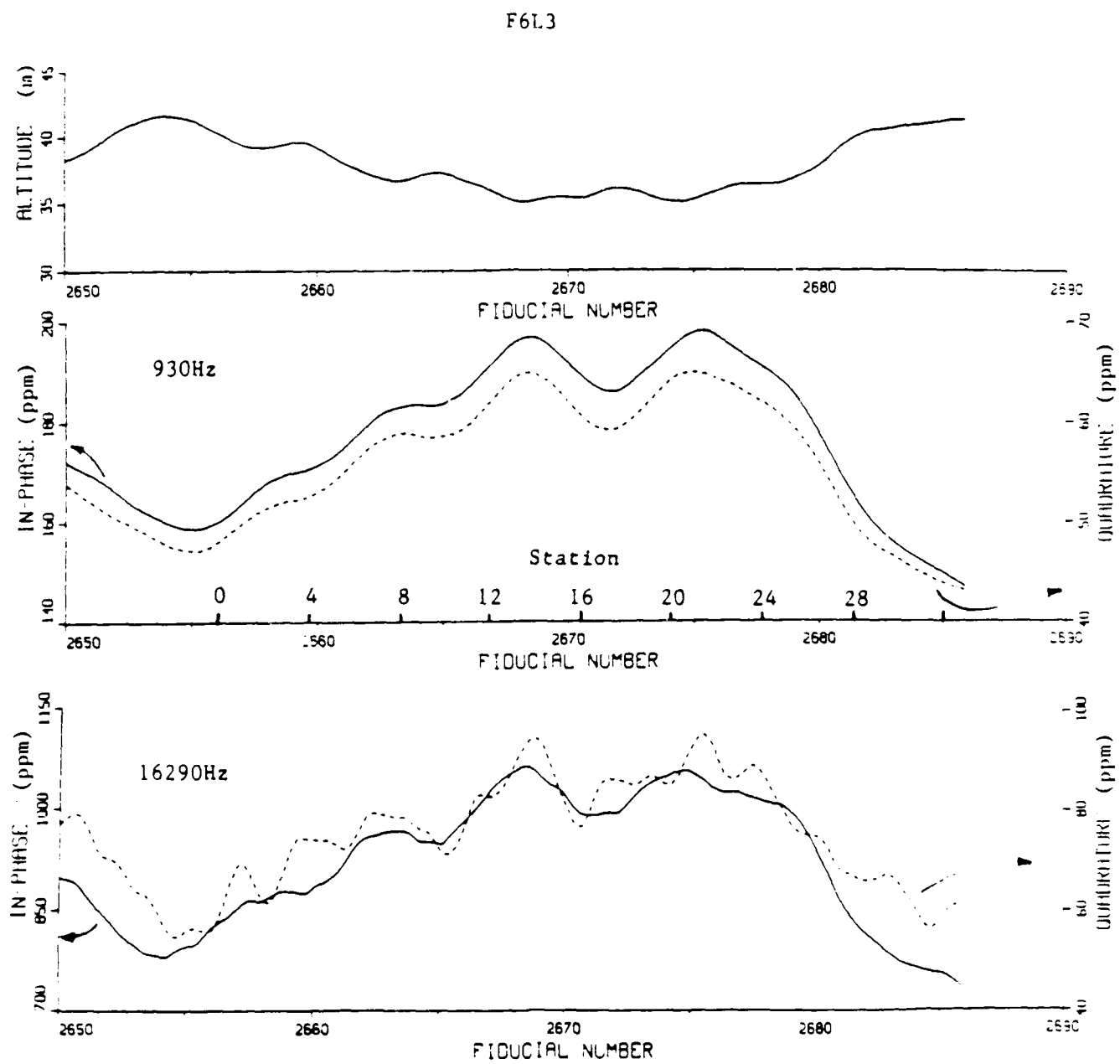


Fig.10 Field data. Line F6L3.

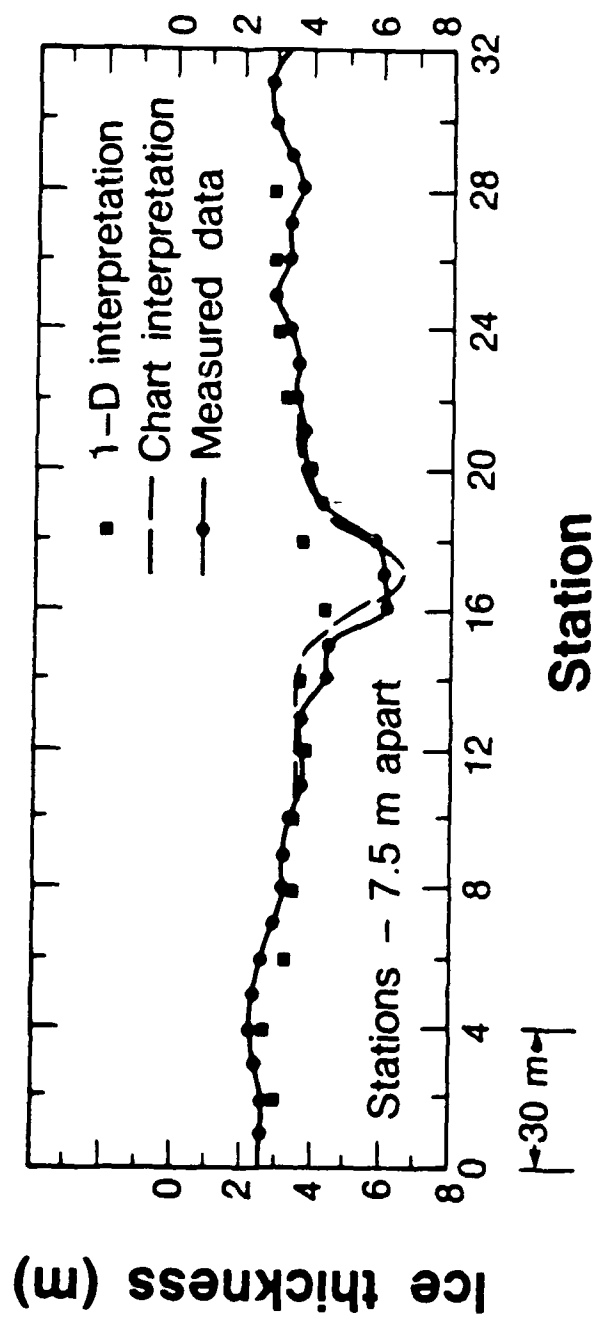


Fig.11 Interpretation of Field Data

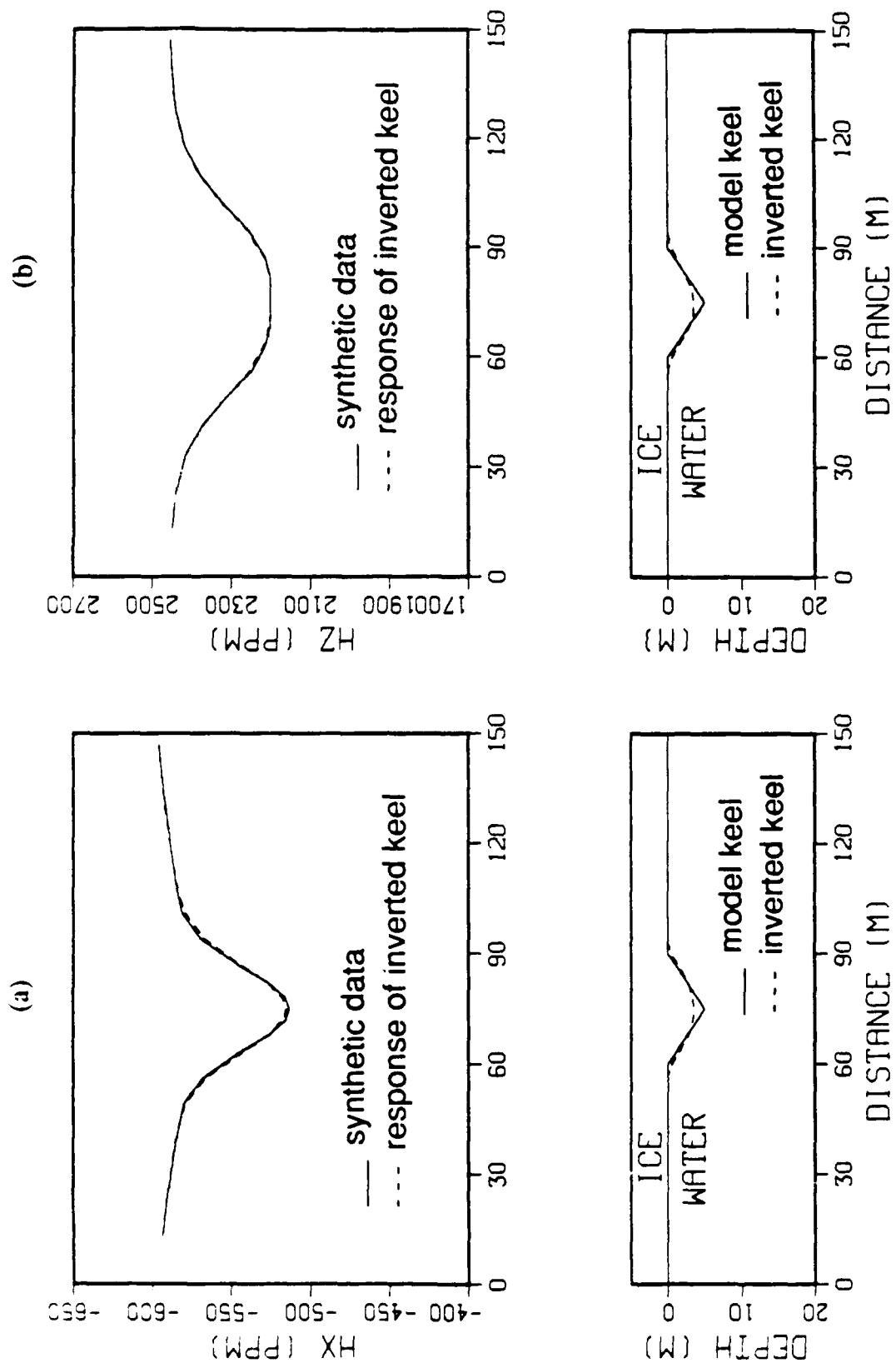


Figure 12 (a) Synthetic data for the HX system and inversion results, Model 1.  
 (b) Synthetic data for the Hz system and inversion results, Model 1.

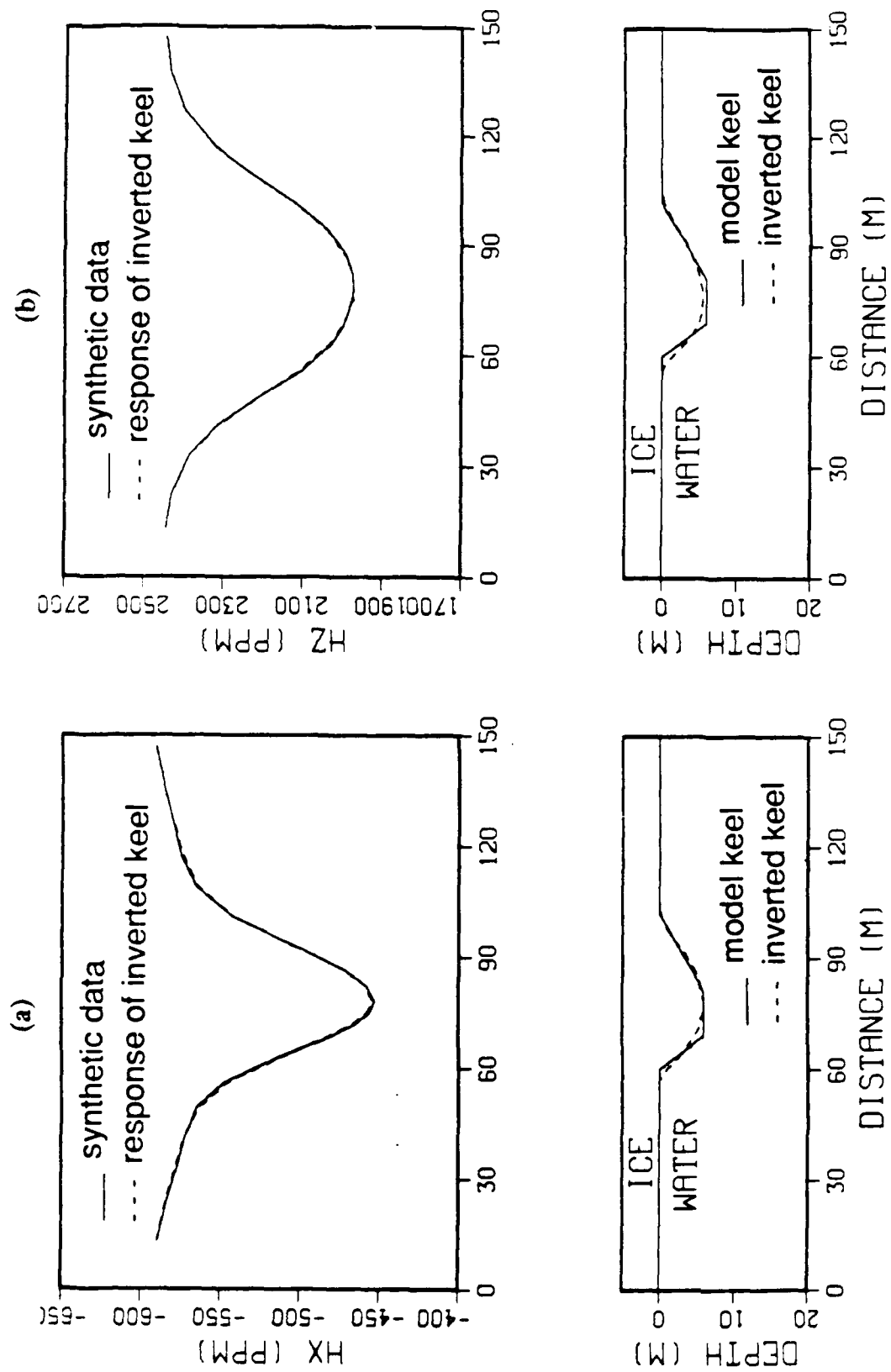


Figure 13 (a) Synthetic data for the HX system and inversion results, Model 2.  
 (b) Synthetic data for the Hz system and inversion results, Model 2.

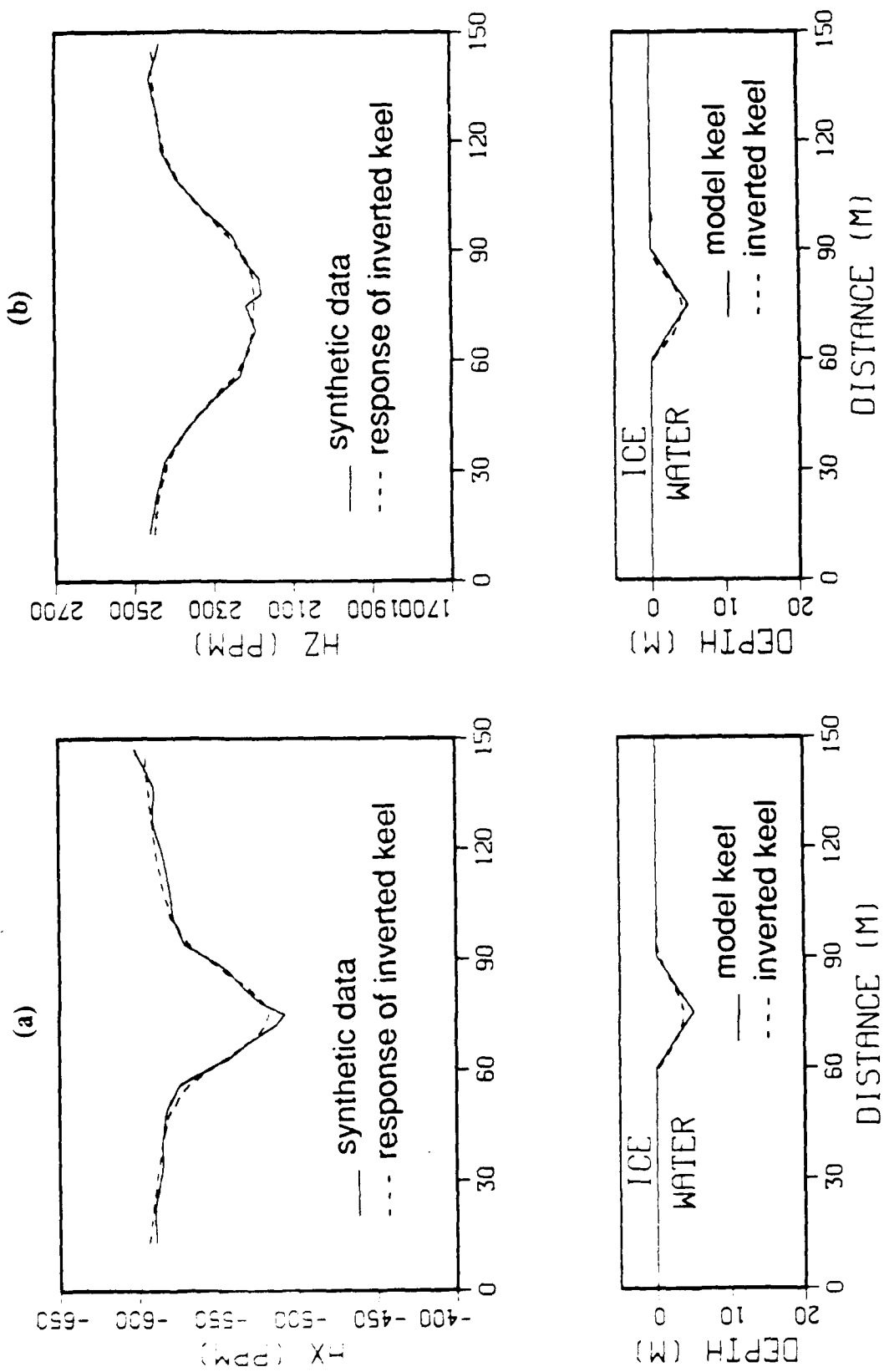


Figure 14 (a) Synthetic data with 5% added noise and inversion results for the HX system, Model 1.  
 (b) Synthetic data with 5% added noise and inversion results for the HZ system, Model 1.

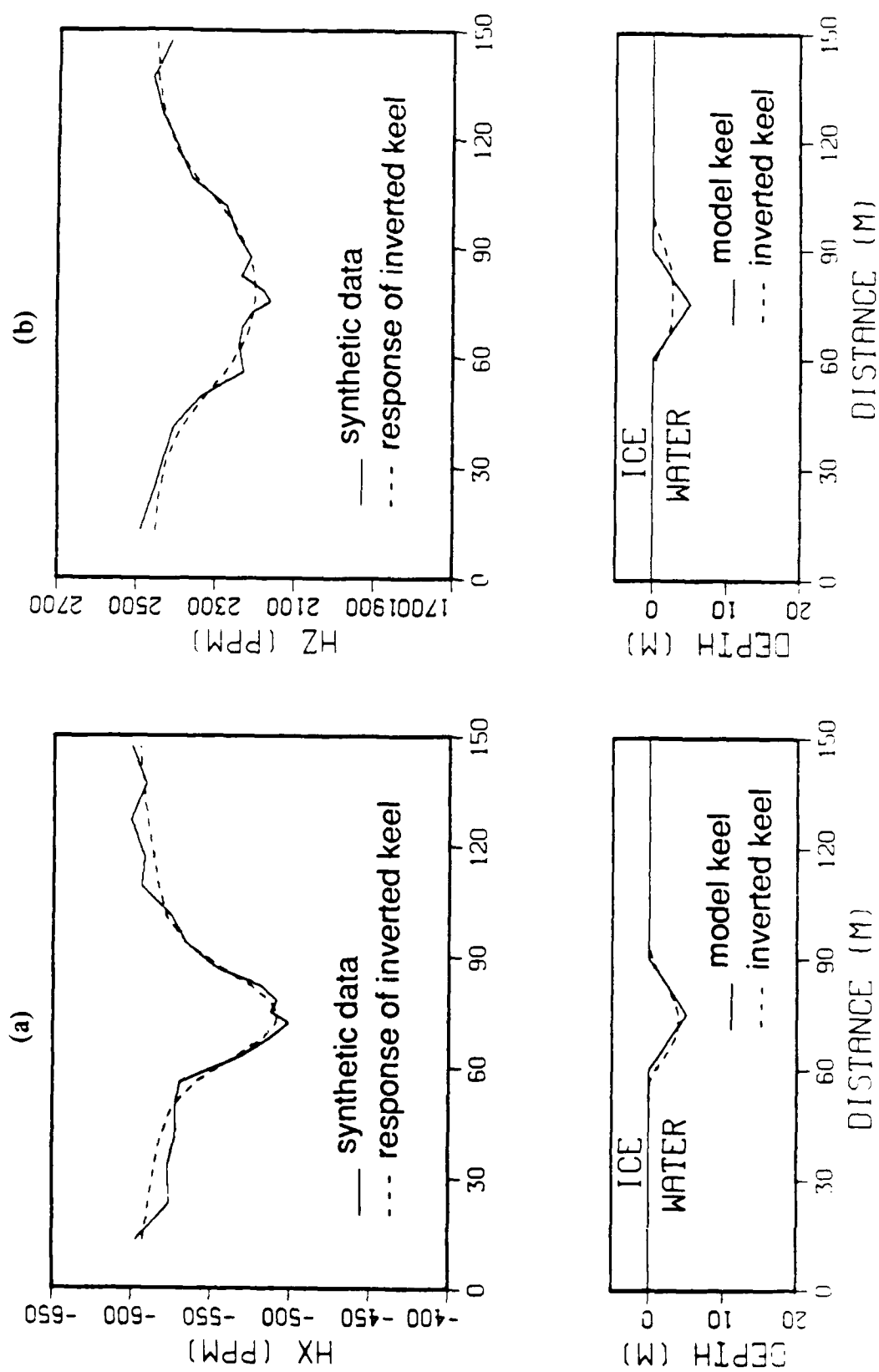


Figure 15 (a) Synthetic data with 10% added noise and inversion results for the HX system, Model 1. (b) Synthetic data with 10% added noise and inversion results for the Hz system, Model 1.

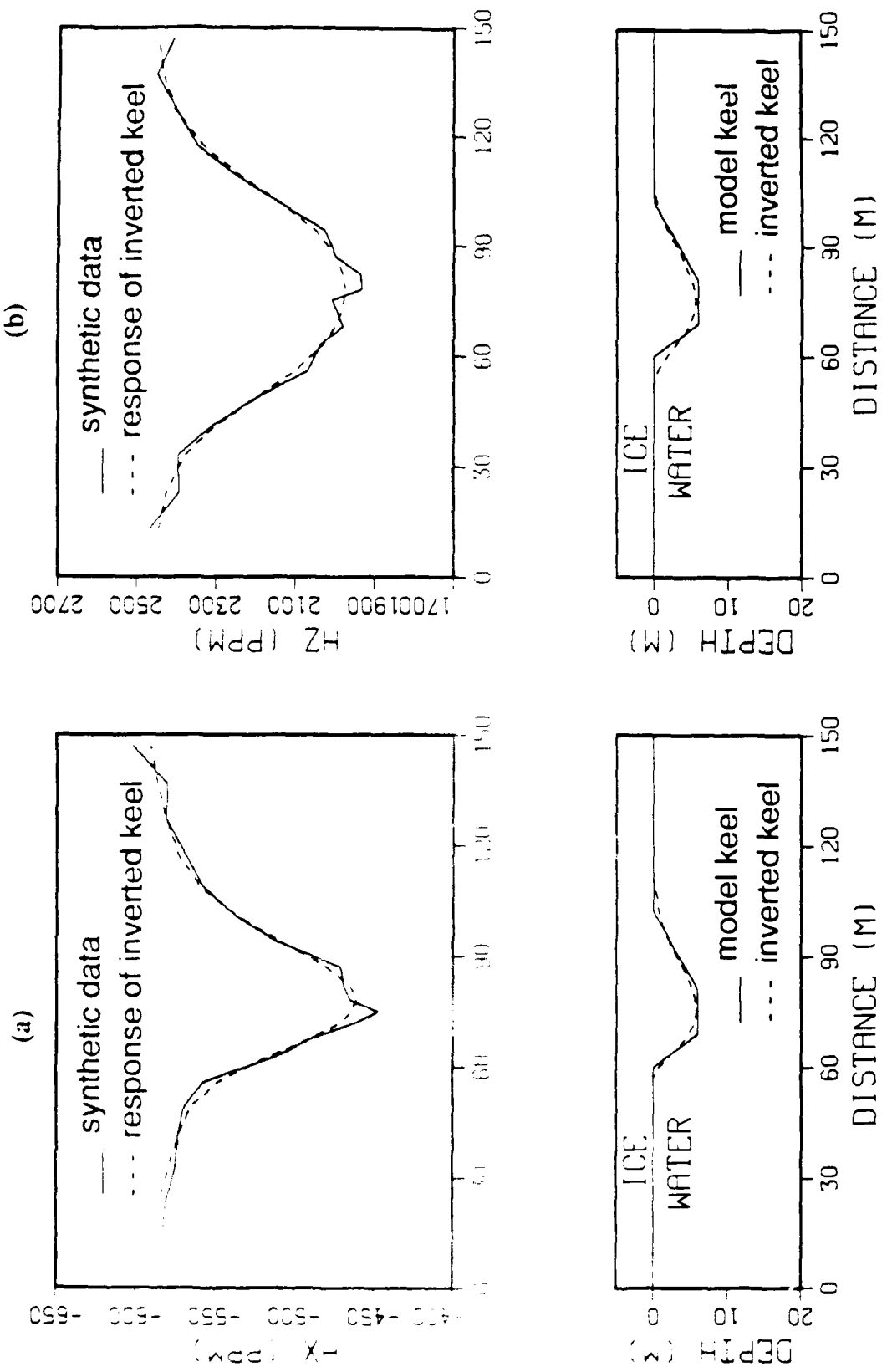


Figure 16 (a) Synthetic data with 5% added noise and inversion results for the HX system, Model 2. (b) Synthetic data with 5% added noise and inversion results for the HZ system, Model 2.

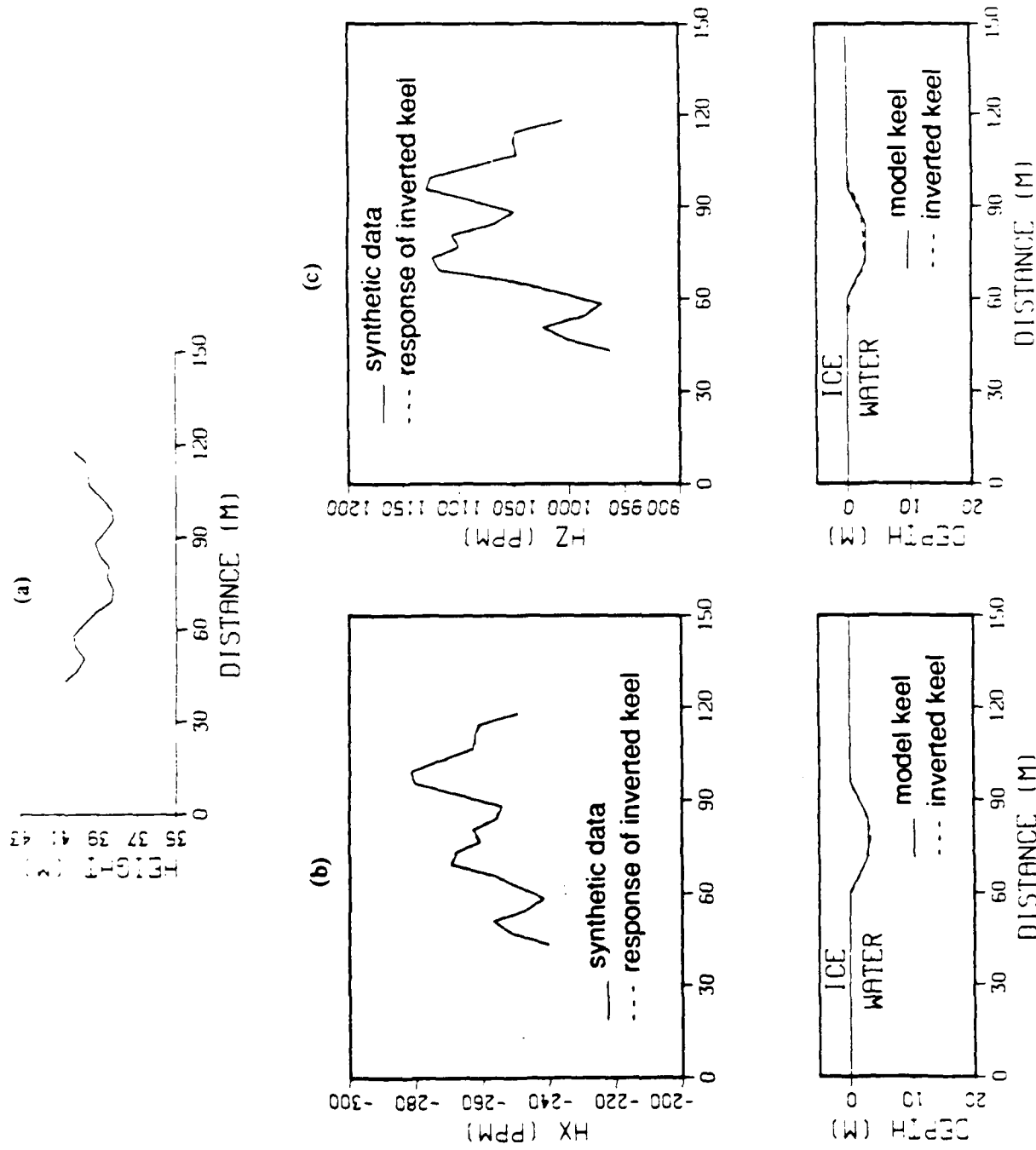


Figure 17 (a) Height of the system over the ice/water interface during the flight. (b) Synthetic data and inversion results for the HX system, Model 3. (c) Synthetic data and inversion results for the Hz system, Model 3.

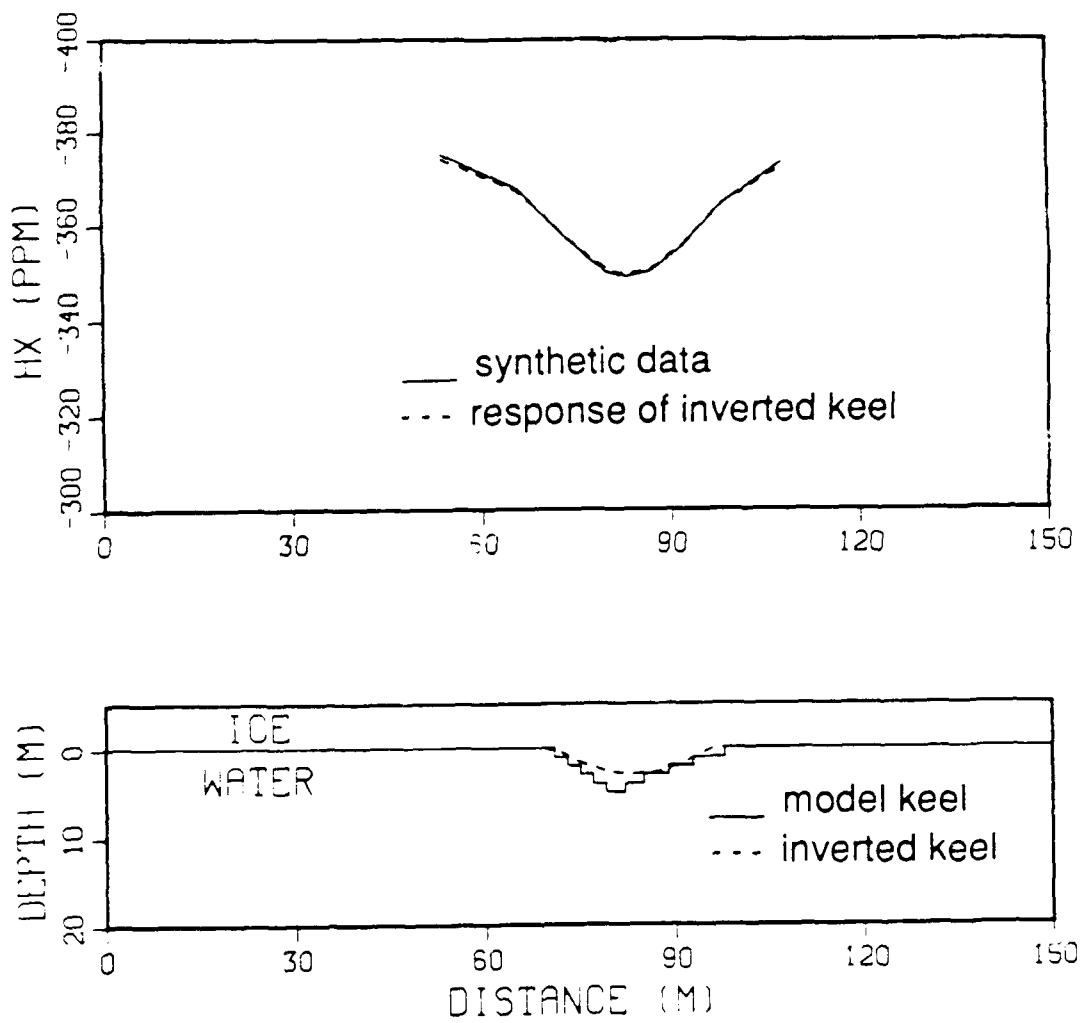


Figure 18 Synthetic data at 2500Hz and inversion results for the HX system, Model 4. The data shown are the scaled sum of the in-phase and quadrature components of the secondary magnetic field.

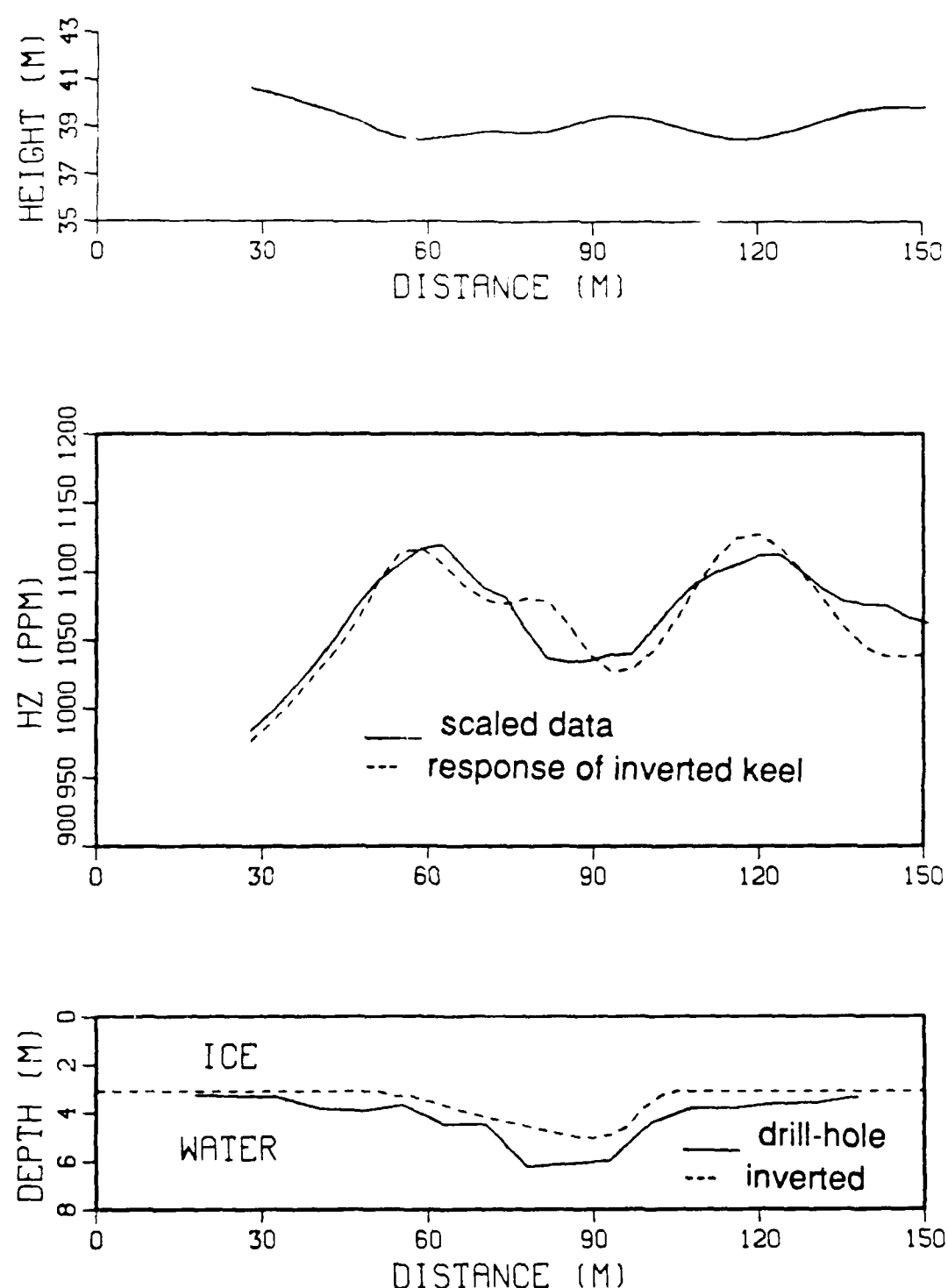
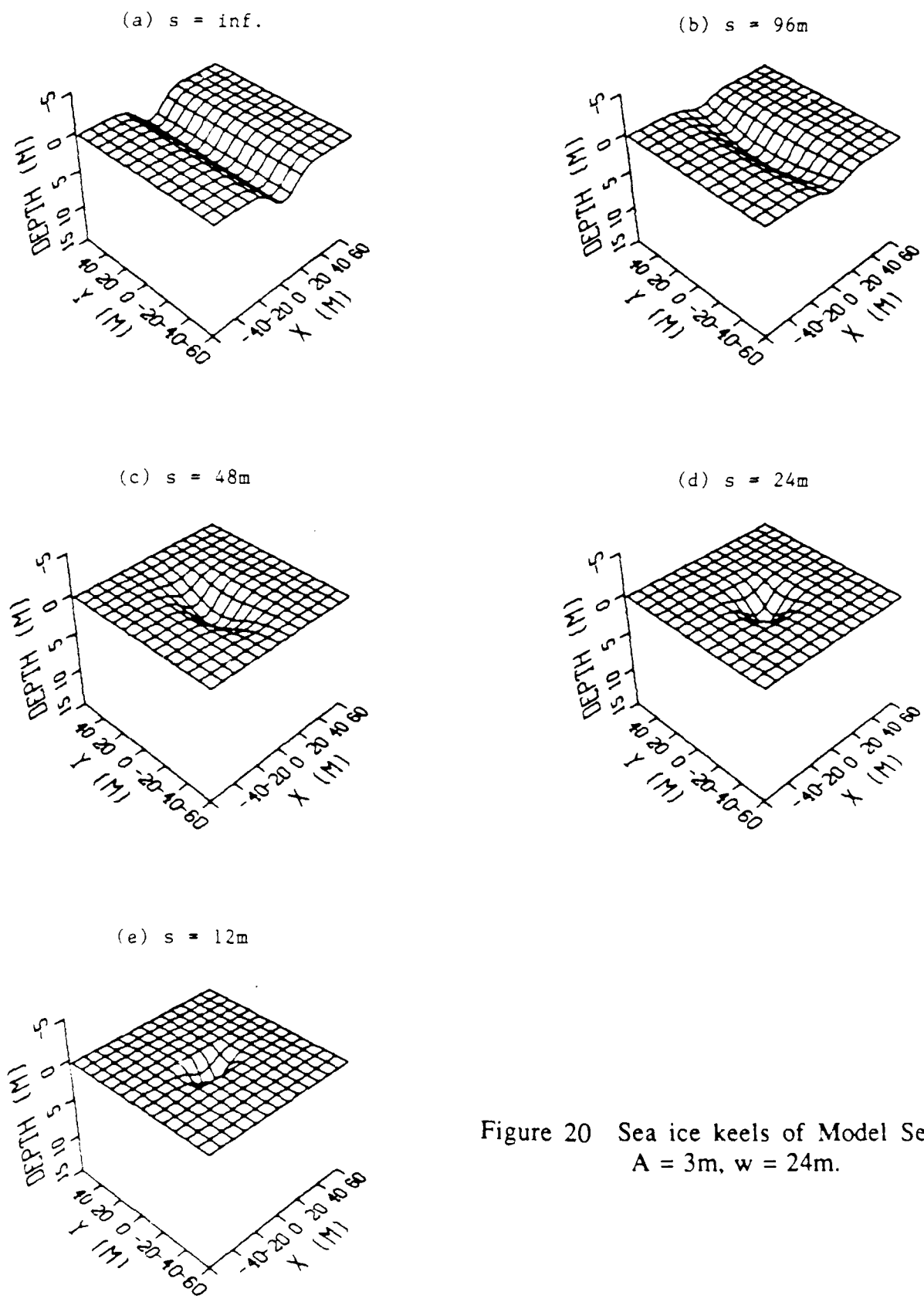


Figure 19 Scaled in-phase data at 16,290Hz and the inversion results for the HZ system. The data were collected at the Prudhoe Bay by Geotech Ltd. in 1985 on line F6L3.



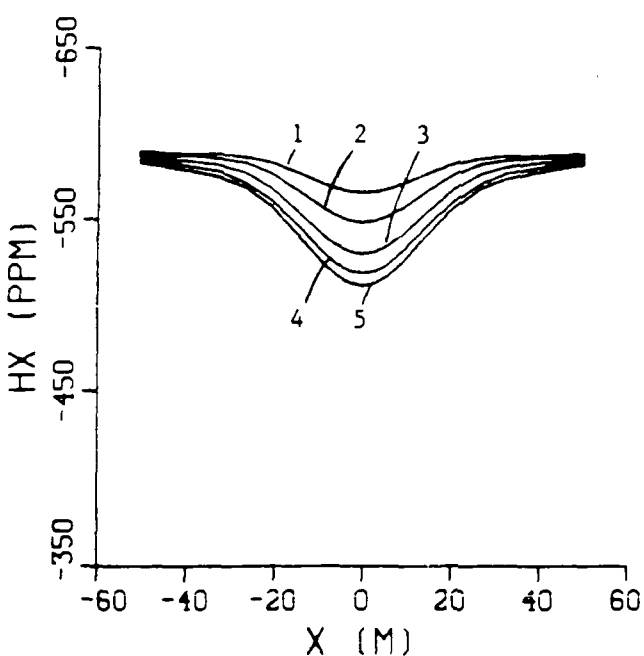


Figure 21(a) HX system response. Curves 1, 2, 3, 4, and 5 correspond to  $s = 12, 24, 48, 96$ , and inf meters respectively.

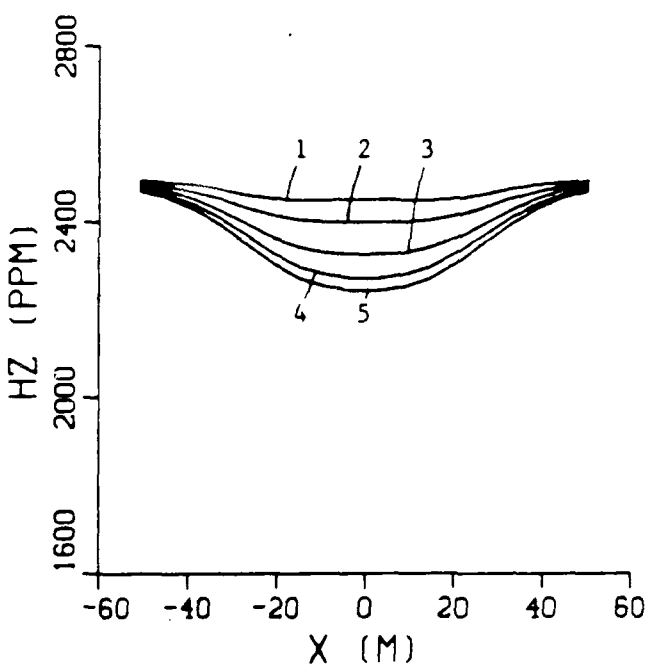


Figure 21(b) HZ system response. Curves 1, 2, 3, 4, and 5 correspond to  $s = 12, 24, 48, 96$ , and inf meters respectively.

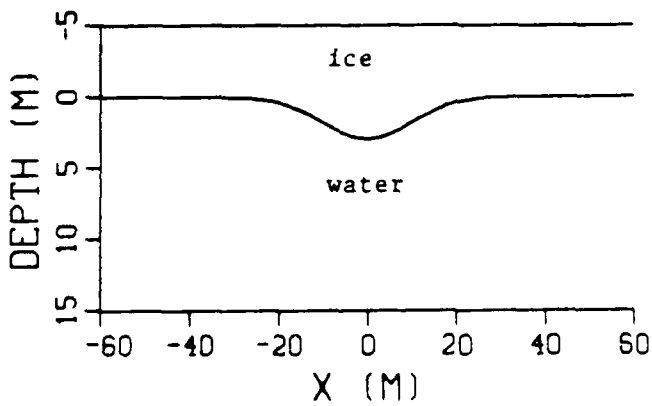


Figure 21(c) Cross section of the ice below the flight line.

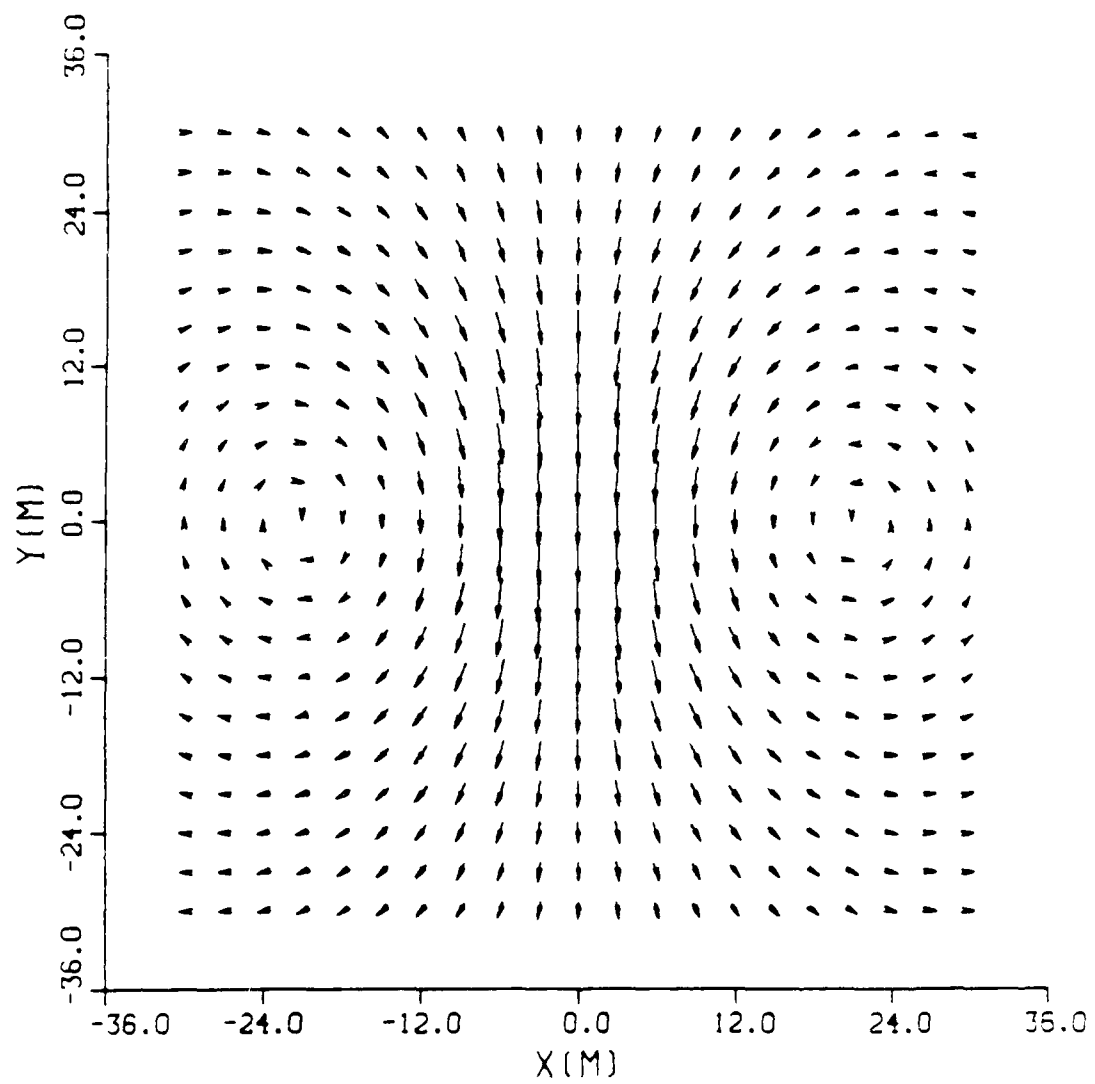


Figure 22 Surficial currents for a horizontal-axis transmitter,  
which is 30 meters above the center (0, 0).

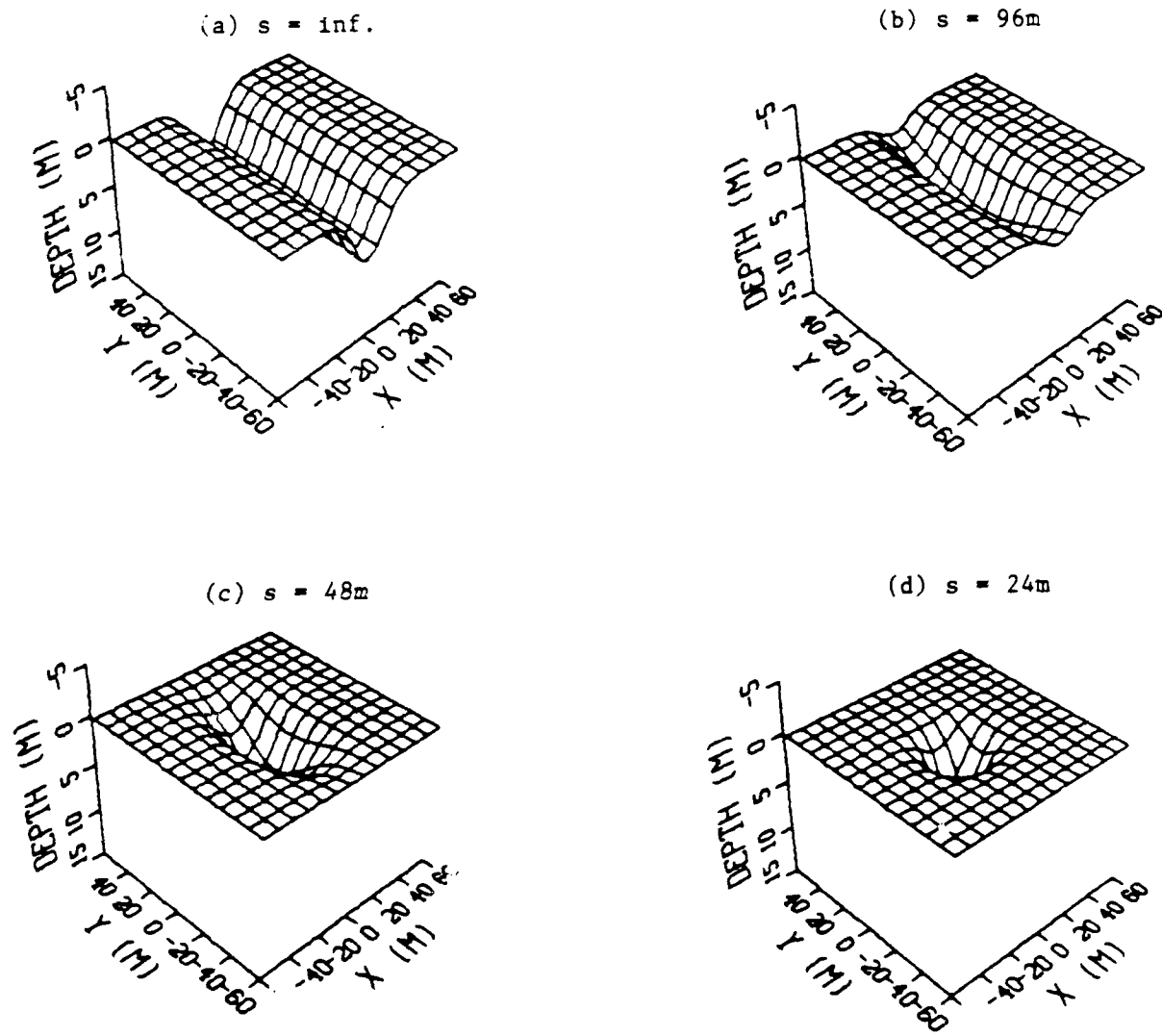


Figure 23 Sea ice keels of Model Set 2.  
 $A = 6\text{m}$ ,  $w = 24\text{m}$ .

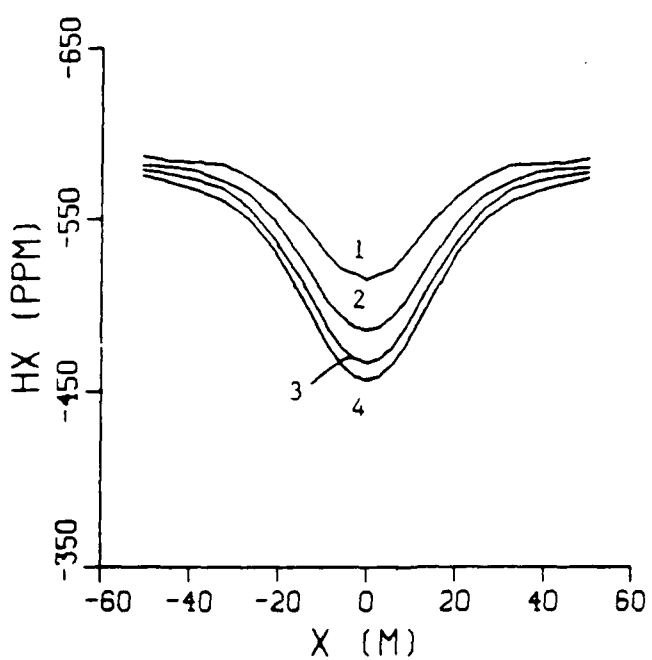


Figure 24(a) HX system response  
Curves 1, 2, 3, 4 correspond to  
 $s = 24, 48, 96$ , and inf. meters  
respectively.

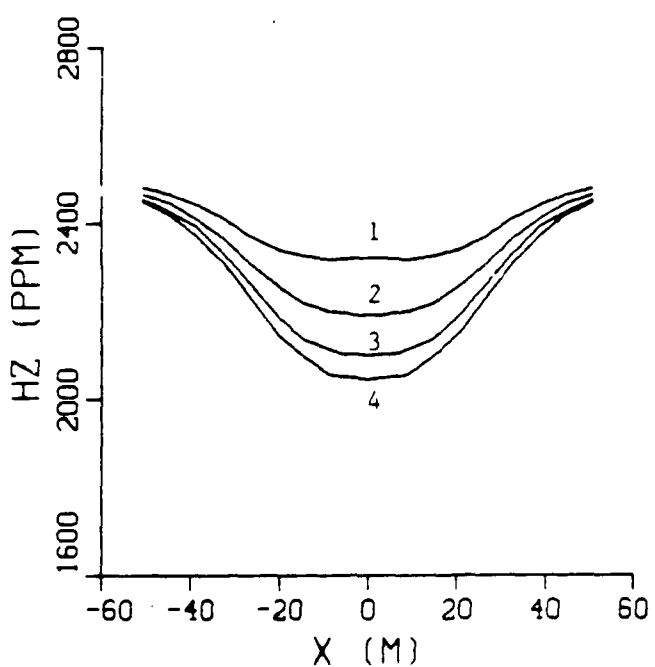


Figure 24(b) HZ system response  
Curves 1, 2, 3, 4 correspond to  
 $s = 24, 48, 96$ , and inf. meters  
respectively.

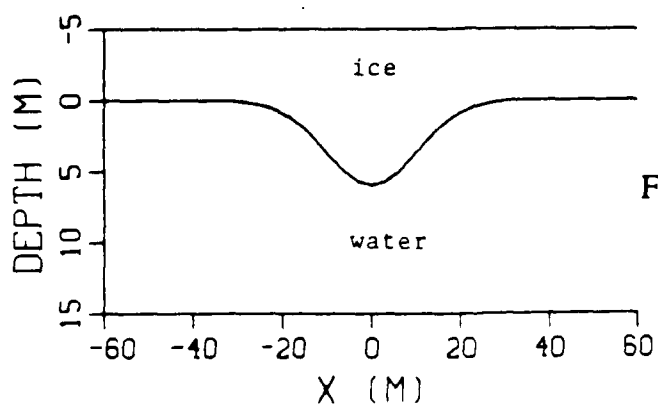


Figure 24(c) Cross section of the ice  
below the flight line.

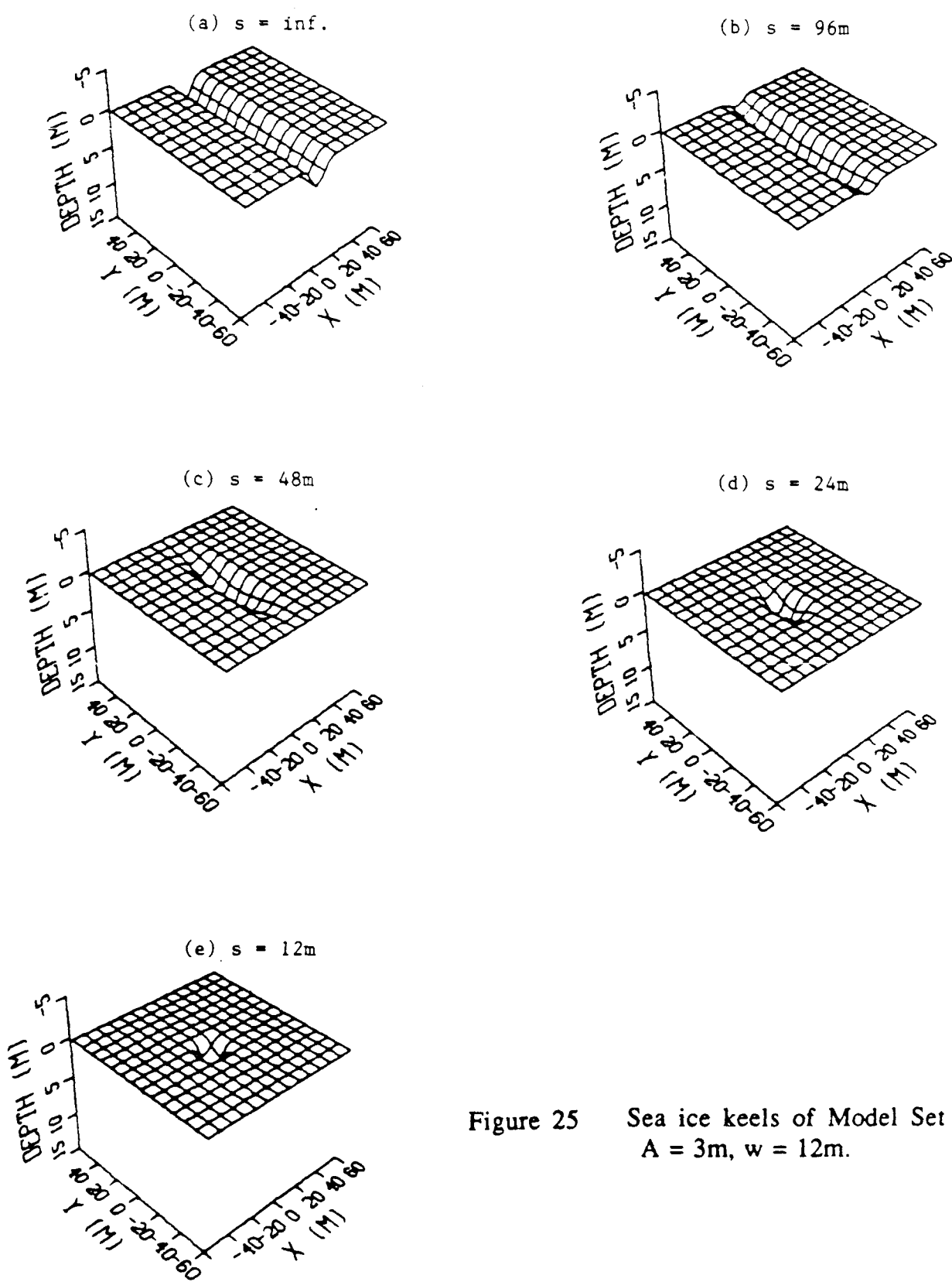


Figure 25 Sea ice keels of Model Set 3.  
 $A = 3\text{m}$ ,  $w = 12\text{m}$ .

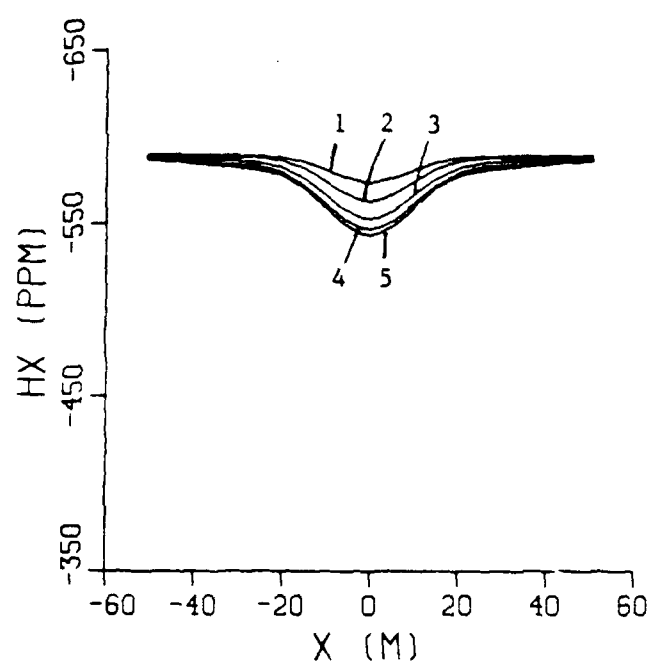


Figure 26(a) HX system respons  
Curves 1, 2, 3, 4 and 5 corres-  
pond to  $s = 12, 24, 48, 96$ , and in  
meters respectively.

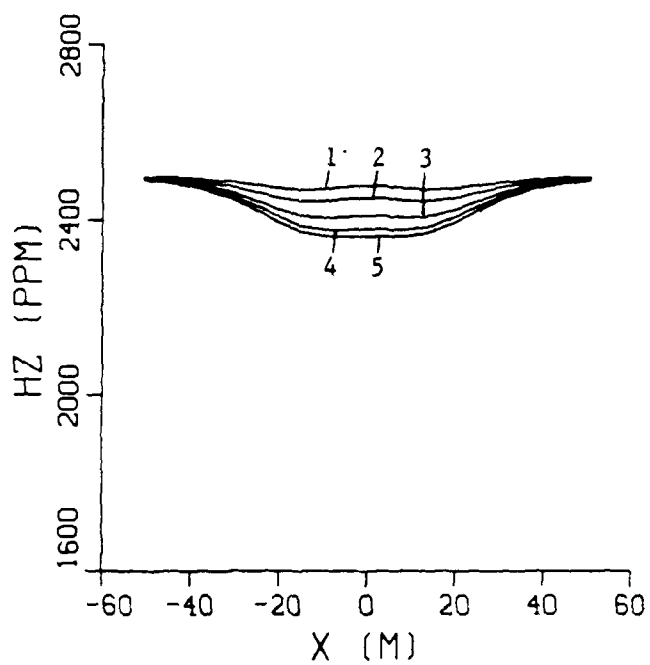


Figure 26(b) HZ system response  
Curves 1, 2, 3, 4 and 5 corres-  
pond to  $s = 12, 24, 48, 96$ , and in  
meters respectively.

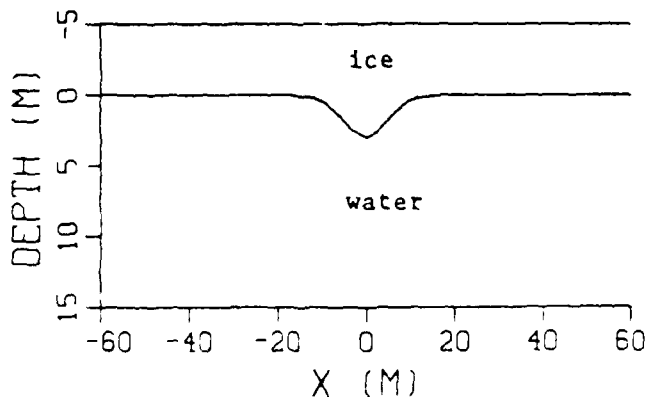


Figure 26(c) Cross section of the ice  
below the flight line.

## Appendix A

### Computational Methods

#### A.1 The General Case

Consider an alternating magnetic dipole ( current loop ) source T, located in free space as shown in Figure A1. Its orientation is arbitrary and it is positioned over a homogeneous, perfectly conductive medium with three-dimensional surface relief. Due to this source, electric currents are induced on the surface of the medium and they give rise to the secondary magnetic field  $\mathbf{H}_S$  in free space. It is our objective to calculate this quantity at any point above the surface S.

Here the height of the source above the medium is assumed to be small compared to the wavelength. The observation point is also assumed to be close to the source so that the electromagnetic field is quasi-static. In free space,  $\nabla \times \mathbf{H}_S = 0$ , and we may relate  $\mathbf{H}_S$  to a scalar magnetic potential  $\phi$

$$\mathbf{H}_S = -\nabla \times \phi \quad (1)$$

We also have  $\nabla \cdot \mathbf{H}_S = 0$  and correspondingly

$$\nabla^2 \phi = 0 \quad (2)$$

Since the lower medium is assumed to be infinitely conductive, the normal component of the total magnetic field must vanish on the surface S, i.e.

$$\mathbf{H}_{pn} + \mathbf{H}_{sn} = 0 \quad \text{on } S \quad (3)$$

Here,  $\mathbf{H}_{pn}$  and  $\mathbf{H}_{sn}$  are the normal components of the secondary and primary magnetic fields respectively. Hence,

$$\frac{\partial \phi}{\partial n} \Big|_S = -H_{sn} \Big|_S = H_{pn} \Big|_S \quad (4)$$

The Laplace equation (2) and the boundary condition (4) constitute the Neumann boundary value problem. That is, given the normal derivative of the potential on a surface S, we wish to calculate the potential itself in the free space. Once  $\phi$  is found,  $H_s$  may be calculated from equation (1).

The solution of the Neumann problem outside a closed surface can be expressed as the potential of a surface charge layer (Graham, 1980)

$$\phi(O) = \int_S \frac{\xi(p)}{r_{PO}} ds \quad (5)$$

where  $\xi(P)$  is a fictitious charge density function,  $r_{OP}$  is the distance between points P and O (see Figure 1). The charge density satisfies a Fredholm integral equation of the second kind

$$\xi(M) = -\frac{1}{2\pi} \frac{\partial \phi}{\partial n} \Big|_S - \frac{1}{2\pi} \int_S \xi(p) \frac{\cos(r_{PM}, N)}{r_{PM}^2} ds \quad \text{on } S \quad (6)$$

where  $(r_{PM}, N)$  is the angle between  $r_{PM}$  (the vector connecting P to M) and  $N$  (the unit normal vector at M). In our problem, the surface S extends to infinity and equations (5) and (6) are still valid.

To solve the integral equation (6), we use the successive approximation method (Mikhlin, 1964). The initial solution (first iteration) is assumed to be the first term on the right hand side of equation (6), i.e.

$$\xi(M) = -\frac{1}{2\pi} \frac{\partial \phi}{\partial n} \Big|_S = -\frac{1}{2\pi} H_{pn}$$

We then use this value in the integral in the equation to compute an improved value of  $\xi(M)$  and so on. Once the charge density is known,

the secondary magnetic field can be calculated from the following equation, which is obtained by combining equations (1) and (5)

$$\mathbf{H}_s = \int_S \frac{\xi(p)}{r_{po}^3} \mathbf{r}_{po} ds \quad (7)$$

Here  $\mathbf{r}_{po}$  is the vector connecting P to O.

In the above context, the electrodynamic problem is reduced to a potential problem under the quasi-static field assumption. The charge distribution on the surface of the conductive medium is computed first. The secondary magnetic field in the free space is then found by summing up the contributions from the individual charges. This is analogous to the integral equation approach for solving electromagnetic scattering problem (Parry and Ward, 1970), where the equivalent electric and magnetic currents are first sought; the electromagnetic field are then obtained by integrating the contributions from the current distribution.

In the special case where the surface S forms a plane, the solution given by equation (7) for an oscillating magnetic dipole source is identical to that obtained by the method of images (Jackson, 1975). To illustrate our computational method, we now show this to be true for a vertical magnetic dipole source. The coordinate system is chosen such that the z axis is pointing vertically downward. The XOY plane is on the surface of the conductor which occupies the half space  $z > 0$ . The dipole source is h meters above the plane on the z axis and points in the positive z direction.

Since  $\mathbf{r}_{pm}$  is perpendicular to N (cf. Figure 1), equation (6) reduces to

$$\xi(M) = -\frac{1}{2\pi} \frac{\partial \phi}{\partial n}|_S = -\frac{1}{2\pi} H_{pn} \quad (8)$$

On the conductor surface, the normal component of the primary magnetic field is

$$H_{pn} = -\frac{1}{4\pi} \frac{2h^2 - x^2 - y^2}{(x^2 + y^2 + h^2)^{5/2}} \quad (9)$$

Substituting equations (8) and (9) into (5), we obtain

$$\phi(x, y, z) = \int_{-\infty}^{+\infty} \int_{-\infty}^{+\infty} \frac{\xi(x', y', 0)}{[(x-x')^2 + (y-y')^2 + z^2]^{1/2}} dx' dy' \quad (z < 0)$$

$$\phi(0, 0, z) = \frac{1}{8\pi^2} \int_{-\infty}^{+\infty} \int_{-\infty}^{+\infty} \frac{2h^2 - x'^2 - y'^2}{(x'^2 + y'^2 + h^2)^{5/2}} \frac{dx' dy'}{(x'^2 + y'^2 + z^2)^{1/2}}$$

Let  $x' = R\cos\theta$ ,  $y' = R\sin\theta$ ,  $dx' dy' \approx Rd\theta dR$ , then

$$\phi(0, 0, z) = \frac{1}{8\pi^2} \int_0^{+\infty} \int_0^{2\pi} \frac{2h^2 - R^2}{(R^2 + h^2)^{5/2}} \frac{R d\theta dR}{(R^2 + z^2)^{1/2}}$$

Furthermore, let  $r^2 = R^2 + h^2$ ,  $RdR = r dr$ , then

$$\phi(0, 0, z) = \frac{1}{4\pi} \int_h^{+\infty} \frac{3h^2 - r^2}{r^4(r^2 - h^2 + z^2)^{1/2}} dr$$

The above integration can be carried out and the result is as follows

$$\phi(0, 0, z) = \frac{1}{4\pi} \frac{1}{(h-z)^2} \quad (z < 0)$$

The vertical component of the secondary magnetic field on z axis is

$$H_{sz}(0, 0, z) = -\frac{\partial \phi}{\partial z} = \frac{1}{2\pi} \frac{1}{(h-z)^3} \quad (10)$$

and as required is identical to the image field.

### A.2 The 2-D keel

In the 2-D case, the geometry of the ice-water interface does not change in the strike direction (  $y$ -direction here ). The relief of the interface is only a function of  $x$  , i.e.  $h(x,y) = h(x)$ . In this case, the potential of the scattered magnetic field is given by,

$$\phi(x, y, z) = \iint_{-\infty}^{+\infty} \frac{\xi(x', y') \sqrt{1 + [dh(x')/dx']^2}}{\sqrt{(x-x')^2 + (y-y')^2 + (z-h(x'))^2}} dx' dy' \quad (11)$$

and the surface charge density  $\xi(x, y)$  satisfies

$$\begin{aligned} \xi(x, y) = & -\frac{1}{2\pi} H_{pn}(x, y) - \frac{1}{2\pi} \iint_{-\infty}^{+\infty} \xi(x', y') \frac{(x-x') dh(x')/dx' - (h(x)-h(x'))}{[(x-x')^2 + (y-y')^2 + (h(x)-h(x'))^2]^{\frac{3}{2}}} \\ & \cdot \left[ \frac{1+(dh(x')/dx')^2}{1+(dh(x)/dx)^2} \right]^{\frac{1}{2}} dx' dy' \end{aligned} \quad (12)$$

Here  $H_{pn}(x, y)$  is the normal component of the primary magnetic field at the ice-water interface.

Notice that in equations 11 and 12 the integral with regard to  $y'$  is a convolution. Taking the Fourier transform of both sides we get

$$\begin{aligned} \phi(x, k_y, z) &= \int_{-\infty}^{+\infty} \phi(x, y, z) e^{-ik_y y} dy \\ &= 2 \int_{-\infty}^{+\infty} \xi(x', k_y) \sqrt{1 + [dh(x')/dx']^2} K_0(\rho |k_y|) dx' \end{aligned} \quad (13)$$

and

$$\xi(x, k_y) = -\frac{1}{2\pi} H_{pn}(x, k_y) - \frac{1}{2\pi} \int_{-\infty}^{+\infty} \xi(x', k_y) f(x, x', k_y) dx' \quad (14)$$

where the kernel of the integration is

$$f(x, x', k_y) = 2 \left[ \frac{1 + (dh(x')/dx')^2}{1 + (dh(x)/dx)^2} \right]_2^1 \frac{(x-x')dh(x')/dx' - (h(x)-h(x'))}{[(x-x')^2 + (h(x)-h(x'))^2]_2^1} \cdot |k_y| K_1(\rho' |k_y|) \quad (15)$$

In the above equations

$k_y$  = angular wave number in the y direction

$$\rho = \sqrt{(x-x')^2 + (z-h(x'))^2}$$

$$\rho' = \sqrt{(x-x')^2 + (h(x)-h(x'))^2}$$

$K_0()$  = modified Bessel function of the zeroth order. Second kind.

$K_1()$  = modified Bessel function of the first order. Second kind.

We have thus simplified the problem by decomposing a two dimensional integral equation into a number of integral equations in one dimension.

For the case where the source is a horizontal or vertical magnetic dipole, the normal component of the primary magnetic field can be analytically transformed into the wave-number domain (i.e.  $H_{pn}(x, k_y)$ ) as follows.

The normal component of the primary magnetic field at the ice-water interface is

$$H_{pn}(x, y) = \mathbf{H}_p(x, y) \cdot \mathbf{n}(x, y) \quad (16)$$

where  $\mathbf{n}(x, y)$  is the outward normal at point  $(x, y)$  on the interface. It is given by

$$\mathbf{n} = \left( \frac{h'(x)}{\sqrt{1 + [h'(x)]^2}}, 0, -\frac{1}{\sqrt{1 + [h'(x)]^2}} \right) \quad (17)$$

where  $h'(x) = dh(x)/dx$ . Thus

$$H_{pn}(x, y) = \frac{h'(x)}{\sqrt{1 + [h'(x)]^2}} H_{px} - \frac{1}{\sqrt{1 + [h'(x)]^2}} H_{pz} \quad (18)$$

(a) Horizontal magnetic dipole source located at  $(x_s, y_s=0, z_s)$

$$H_{px}(x, y) = \frac{2(x - x_s)^2 - y^2 - (h(x) - z_s)^2}{4\pi r^5}$$

$$H_{pz}(x, y) = \frac{3(x - x_s)(h(x) - z_s)}{4\pi r^5}$$

Here

$$r = \sqrt{(x - x_s)^2 + y^2 + (h(x) - z_s)^2}$$

Substituting the above equations into (18) and taking the Fourier transform give

$$H_{pn}(x, k_y) = \frac{1}{2\pi\rho^2 \sqrt{1 + [h'(x)]^2}} \left\{ [h'(x)(x - x_s)^2 - (x - x_s)(h(x) - z_s)] |k_y|^2 K_0(\rho|k_y|) - \{[(h(x) - z_s)^2 - (x - x_s)^2] h'(x) + 2(x - x_s)(h(x) - z_s)\} \frac{|k_y|}{\rho} K_1(\rho|k_y|) \right\} \quad (19)$$

where

$$\rho = \sqrt{(x - x_s)^2 + (h(x) - z_s)^2}$$

As  $k_y \rightarrow 0$ , the asymptotic forms of the modified Bessel functions are

$$K_0(\rho|k_y|) \rightarrow -\ln \rho|k_y|$$

$$K_1(\rho|k_y|) \rightarrow \frac{1}{\rho|k_y|}$$

Therefore

$$H_{pn}(x, k_y=0) = \frac{-1}{2\pi\rho^4 \sqrt{1 + [h'(x)]^2}} \{[(h(x) - z_s)^2 - (x - x_s)^2] h'(x) + 2(x - x_s)(h(x) - z_s)\} \quad (20)$$

(b) Vertical magnetic dipole source located at  $(x_s, y_s=0, z_s)$

$$H_{px}(x, y) = \frac{3(x - x_s)(h(x) - z_s)}{4\pi r^5}$$

$$H_{pz}(x, y) = \frac{2(h(x) - z_s)^2 - y^2 - (x - x_s)^2}{4\pi r^5}$$

$$H_{pn}(x, k_y) = \frac{1}{2\pi\rho^2 \sqrt{1 + [h'(x)]^2}} \left\{ \begin{aligned} & [-(h(x) - z_s)^2 + h'(x)(x - x_s)(h(x) - z_s)] |k_y|^2 K_0(\rho|k_y|) \\ & - [(h(x) - z_s)^2 - (x - x_s)^2 - 2h'(x)(x - x_s)(h(x) - z_s)] \frac{|k_y|}{\rho} K_1(\rho|k_y|) \end{aligned} \right\} \quad (21)$$

$$H_{pn}(x, k_y=0) = \frac{-1}{2\pi\rho^4 \sqrt{1 + [h'(x)]^2}} \{ (h(x) - z_s)^2 - (x - x_s)^2 - 2h'(x)(x - x_s)(h(x) - z_s) \} \quad (22)$$

Note here that the kernel  $f(x, x', k_y)$  is independent of the source and the receiver positions. Therefore it may be calculated once for each  $k_y$  value and stored for the computation of a complete profile of AEM system response. This is quite economical but impossible in the 3-D case where the matrix is too large to store. At  $x = x'$ , the kernel has a singularity. But this presents no difficulty for the numerical computation because it is integrable in the sense of Cauchy principal value.

The integral equation (14) can be solved for  $\xi(x, k_y)$  using successive approximation method identical to the one suggested above for the general case. This needs to be done at a number of positive  $k_y$  harmonics (including  $k_y = 0$ ). The values of  $\xi(x, k_y)$  at the negative  $k_y$  harmonics may be easily obtained by its property of symmetry. As usual, the sampling in the  $k_y$  space is done on a logarithmic scale.

Once the charge density is known, the x- and z- components of the scattered magnetic field may be directly computed from the following equations

$$\begin{aligned} H_{sx}(x, k_y, z) &= -\frac{\partial \phi(x, k_y, z)}{\partial x} \\ &= 2 \int_{-\infty}^{+\infty} (x - x') \xi(x', k_y) \sqrt{1 + [dh(x')/dx']^2} \frac{|k_y|}{\rho} K_1(\rho |k_y|) dx' \end{aligned} \quad (23)$$

and

$$\begin{aligned} H_{sz}(x, k_y, z) &= -\frac{\partial \phi(x, k_y, z)}{\partial z} \\ &= 2 \int_{-\infty}^{+\infty} (z - h(x')) \xi(x', k_y) \sqrt{1 + [dh(x')/dx']^2} \frac{|k_y|}{\rho} K_1(\rho |k_y|) dx' \end{aligned} \quad (24)$$

Now that the scattered magnetic field is obtained in the wave-number domain its inverse Fourier transform will yield the desired result in the space domain. But prior to performing the inverse Fourier transform, the field values at the logarithmically-spaced points in the  $k_y$  space need to be interpolated for uniformly spaced values. This is accomplished using cubic spline interpolation.

The above algorithm has been successfully implemented and its speed is more than 20 times faster than that of the general 3-D algorithm. The computation of a 20 point profile of the AEM system response takes about only 10 seconds CPU time on the IBM 3090.

### A.3 Computational Check

A scale model experiment was also performed to check the numerical solution. Aluminum was used to simulate the infinitely conductive medium at a scale of 1:250. A model airborne electromagnetic system was built at the same scale and was "flown" at a field height of 10m. The system consisted of a coplanar, vertical axis transmitter and receiver, which were operated at 6 kHz. Details of the model are shown in Figure A2 which also exhibits the traversed feature.

The cross section of the indented surface is a Gaussian curve that simulates a smooth ice keel. Its relief is given by

$$t(x) = A \exp\left(-\frac{x^2}{2\tau^2}\right) \quad (25)$$

and

$$\tau = 0.425W$$

Here

$x$  = distance from the keel center line

$t$  = keel thickness

$A$  = drawdown or maximum keel thickness

$W$  = keel width at half drawdown

The shape of the keel does not change along its strike direction. For this scale model,  $A$  and  $W$  were taken to be 3.4m and 21m respectively. We chose this type of surface because its simulation on the computer is simple as there are only two input parameters. Furthermore, it is easy to adjust these two parameters to simulate any real sea ice keel. The measurements and numerical calculation results (two iterations) for this model are displayed in Figure A3 , which shows an excellent agreement between the numerical and experimental data.

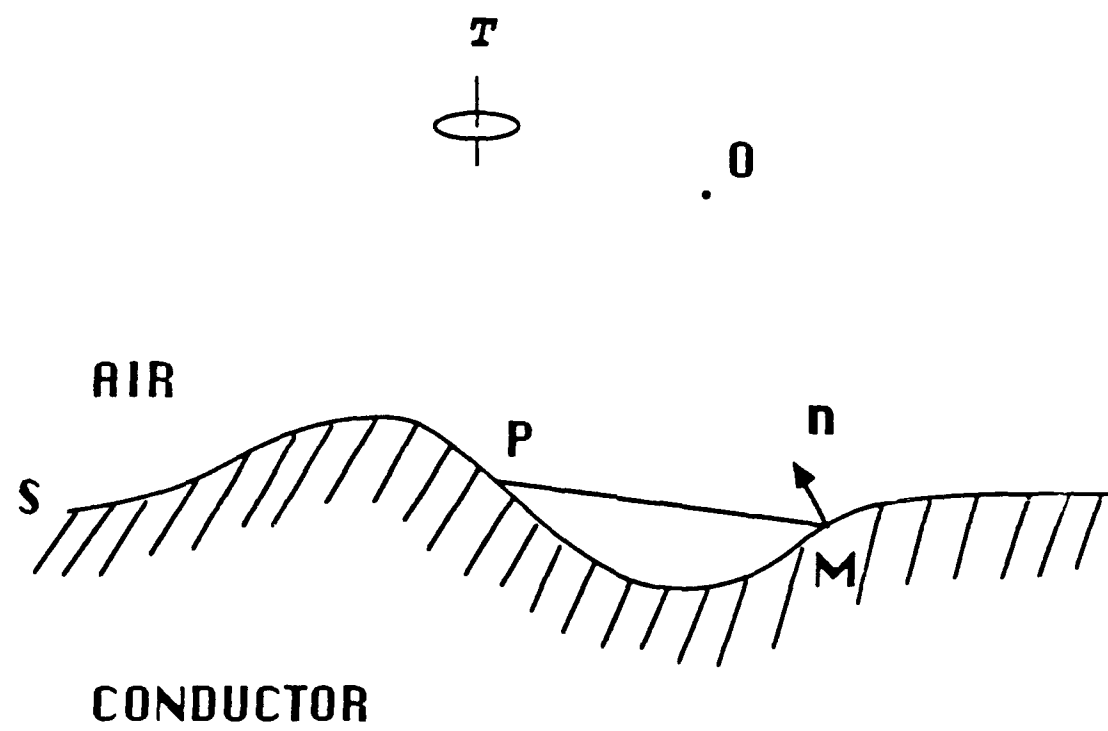


Fig.A1 The Neumann Problem

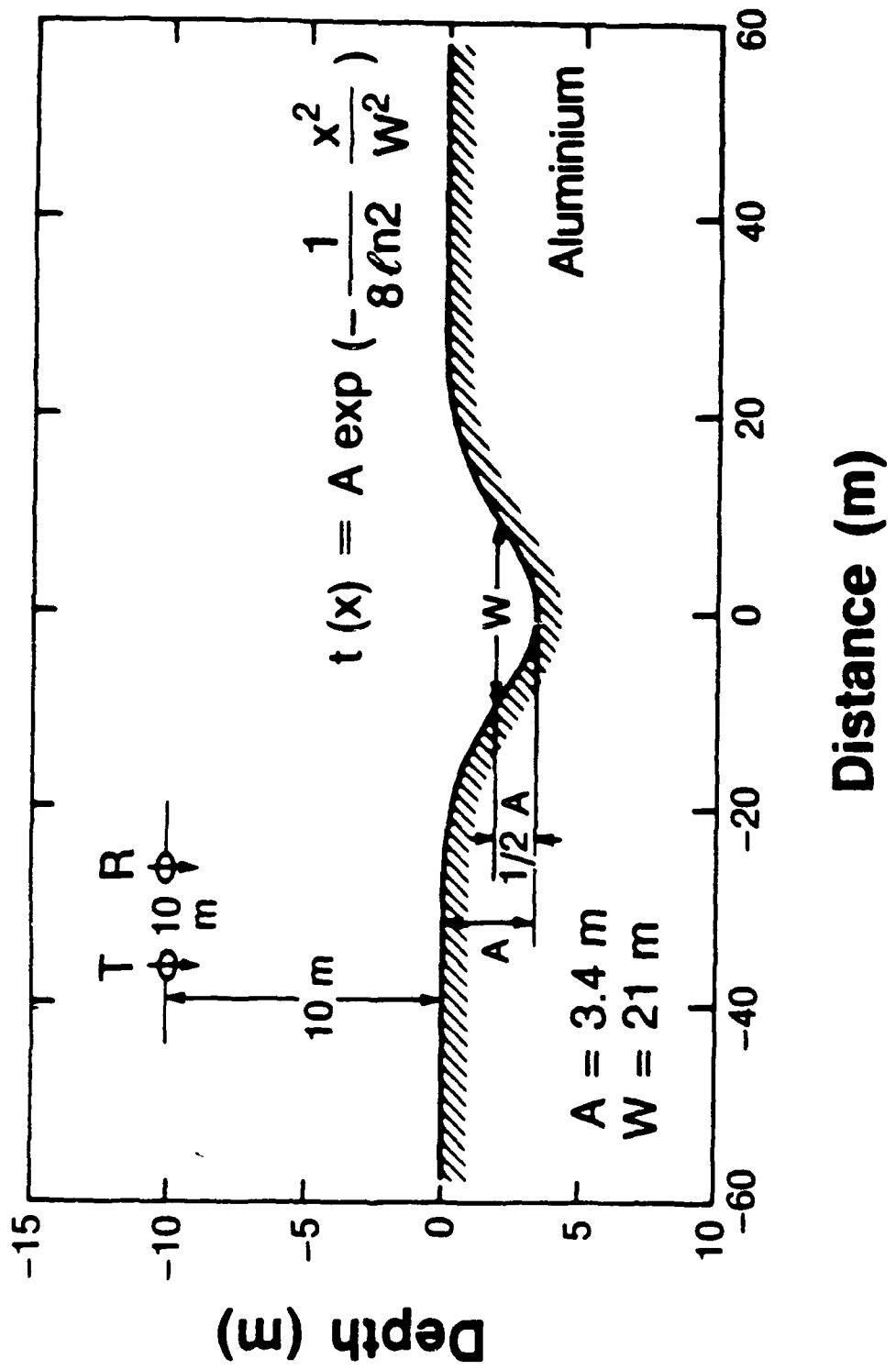


Fig.A2 Scale Model Geometry

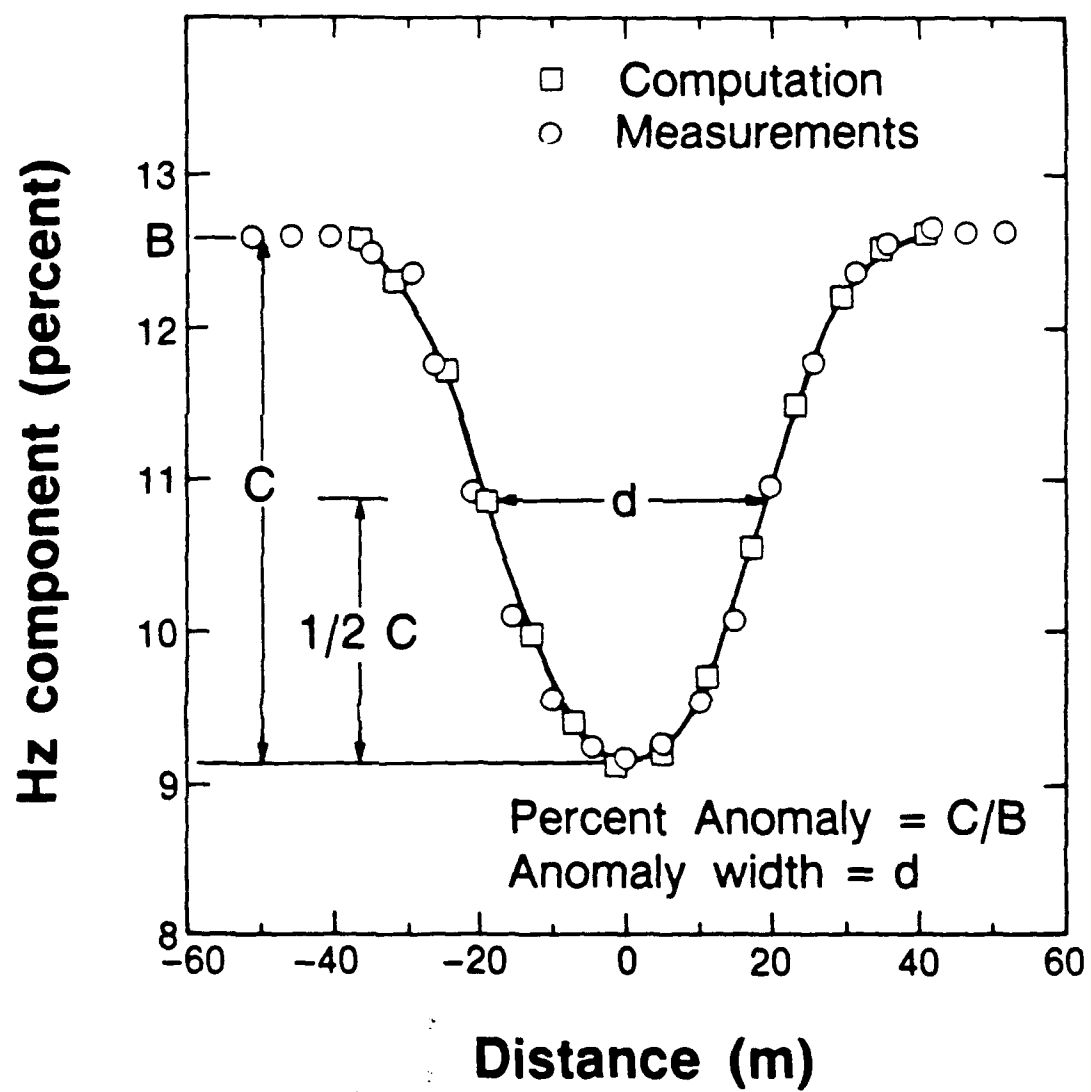


Fig.A3 Comparison of Measurements and Computation

## Appendix B

This Appendix includes a listing of three Fortran programs: SURF3D, ICE2D1, and INVSM.

SURF3D is a program for computing the AEM system response for a general three-dimensional ice keel. It may also be used to calculate the surface current distribution on the ice/water interface.

ICE2D1 is a fast modeling program for the computation of AEM system response over a two-dimensional (2-D) ice keel. It is generally more than 20 times faster than using SURF3D for an identical problem.

INVSM is an inversion program for obtaining a 2-D smooth ice keel from the AEM data. It uses ICE2D1 for modeling AEM system response. Here it is acknowledged that part of this program is adapted from program OCCAM1 by Constable.



## PROGRAM SURF3D

implicit real\*8 (a-h, o-z)

```

c * Purpose..... to compute the secondary electromagnetic response due to a magnetic dipole which sits above a perfectly conductive medium.
c * The secondary field is expressed in parts per million of the received primary field. The orientation of the dipole is arbitrary and the surface of the conductor is arbitrary. When ipattn = 1, the program outputs the total surface current density.
c * Program not optimized and can be further improved.
c * Program not documented.
c * Gaussian quadrature is used for the integration of the kernel.
c * For fast speed, ignore the Gaussian quadrature by setting theta in the IF statement.
c * Author ... Guimin Liu, Engineering Geoscience, U.C.Berkeley.
c * (415) 642-3809 . 1988
c * ***** DIMENSION ZH(121,121), XDER(121,121), YDER(121,121), HN(121,121),
c * . W2(121,121)
c * DIMENSION AMPDER(121,121)
c * COMMON /AA/ZH/BB/XDER/CC/YDER/DD/HN/EE/W/AMP/AMPDER
c * COMMON /TR/XS,YS,ZS,XR,YR,ZR
c * COMMON NX,NY,NX2,NY2,XDELTA,YDELTA
c * open (unit=3, file='surf3d.dat')
c * WHEN NPLOT=1 , THE OUTPUT IS ARRANGED FOR PLOTTING PURPOSE
c * READ(3,*),NPLOT,ipattn
c * ANGV = VERTICAL ANGLE. ANGH = HORIZONTAL ANGLE FROM X DIRECTION
c * INORM = NORMALIZATION COMPONENT. 1 = HX, 2 = HY, 3 = HZ
c * READ(3,*),ANGV, ANGH, INORM
c * READ IN NUMBER OF SOURCES
c * READ(3,*),NSOR
c * READ IN GRID NUMBER , MAXIMUM NUMBER OF ITERATIONS
c * READ(3,*),NX,NY,NLOOP
c * READ IN SURFACE PARAMETERS
c * GAUSSIAN DISTRIBUTION SHAPE
c * READ(3,*),HEIGHT,XWIDTH,YWIDTH
c * READ IN GRID SIZE
c * READ(3,*),XDELTA,YDELTA
c * NS=0
c * ANGV=ANGV/180.*3.14159
c * ANCH=ANGH/180.*3.14159
c * IF (INORM.EQ.1) WRITE(4,41)
c * IF (INORM.EQ.3) WRITE(4,42)
c * 41 FORMAT(4X,'HORIZONTAL MAGNETIC DIPOLE SOURCE')
c * 42 FORMAT(4X,'VERTICAL MAGNETIC DIPOLE SOURCE')
c * IF (NPLOT.EQ.1) GOTO 501
c * WRITE(4,112) ANGV, ANGH, INORM
c * WRITE(4,111) HEIGHT,XWIDTH,YWIDTH
c * WRITE(4,200) NX,NY,XDELTA,YDELTA,NLOOP
c * 112 FORMAT(7X,'ANGLE OF THE DIPOLE FROM VERTICAL =', F6.2,/
c *      + '7X,'ANGLE OF THE DIPOLE FROM X DIRECTION =', F6.2,/
c *      + '7X,'NORMALIZATION COMPONENT 1 = HX 2 = HY 3 = HZ ',16,/ )
c * 200 FORMAT(7X,'GRID NX = ',16,3X, 'NY = ',16,
c *      + '/7X,'ELEMENT SIZE DX = ',F10.6, 'DY = ',F10.6,
c *      + '/7X,'MAXIMUM ITERATION NUMBER', 18 ,//)
c * GOTO 666
c * 501 CONTINUE

```

```

C      WRITE(4,113) ANGV, ANGH, INORM
C      WRITE(4,101) HEIGHT, XWIDTH, YWIDTH
C      WRITE(4,201) NX, NY, XDELTA, YDELTA
101   FORMAT(5X,'HE =',F6.2,'X,', 'XW =',F6.2,'Y,', 'YW =',F6.2)
113   FORMAT(5X,2F18.2,1B)
201   FORMAT(5X,2I8,5X,2F18.2,/)
866   CONTINUE
C      READ IN NUMBER OF RECEIVERS
C      READ(3,*),NREC
C      READ IN SOURCE POSITION
C      READ(3,*),XS,YS,ZS
NR=0
C      FORMAT(7X,'SURFACE PARAMETER      HEIGHT = ',F7.1 ,1X,' XWIDTH = ',1X,SUR00610
        *      F7.1 ,1X,'YWIDTH = ',F7.1 ) SUR00620
C      GENERATING THE SURFACE OF THE WATER
C      CALL SURF(HEIGHT,XWIDTH,YWIDTH)

C      CALCULATE THE PRIMARY FIELD AT THE SURFACE. GENERATE THE BOUNDARY CO
C FOR NEUMANN PROBLEM.
C      CALL HNPRI(ANGV,ANGH) SUR00710
C      CALCULATE THE SURFACE CHARGE DENSITY BY SOLVING THE FREDHOLM INTEGRAL SUR00720
C EQUATION OF THE SECOND KIND. SUR00730
C      CALL SIGMA(NPLOT,NLOOP) SUR00740
C      compute the surface current pattern and then stop
C      if(ipattn.eq.1) call currnt(angs,angs) SUR00810
C      CALCULATE THE MAGNETIC FIELD AT A RECEIVER POINT.
C      CALL FIELD(NPLOT,ANGV,ANGH,INORM) SUR00820
C      CALC CONTINUE
C      READ IN RECEIVER POSITION
C      READ(3,*),XR,YR,ZR SUR00830
C      CALL FIELD(NPLOT,ANGV,ANGH,INORM) SUR00840
NR=NR+1
IF(NR.LT.NREC) GOTO 655
NS=N .1
IF(NS.LT.NSOR) GOTO 886
STOP
END

C      SUBROUTINE SURF(Z0,XW,YW)
implicit real*8 (a-h, o-z)
DIMENSION ZH(121,121),XDER(121,121),YDER(121,121),AMPER(121,121)
COMMON /AA/ZH/BB/XDER/CC/YDER/AMP/AMPER
COMMON /TR/XS,YS,ZS,XR,YR,ZR
COMMON NX,NY,NX2,NY2,XDELTA,YDELTA
NX2=(NX+1)/2
NY2=(NY+1)/2
TAUx=0 42468*XW
SUR00970
SUR00980
SUR00990
SUR01000
SUR01010
SUR01020
SUR01030
SUR01100
SUR01110

```

```

TAUY = 0 42468.YW
XDEV = TAUX - TAUX * 2.0
YDEV = TAU - TAU * TAU * 2.0
DO 10 I=1, NX
DO 20 J=1, NY
X = (I-NX2) * XDELT A + XS
Y = (J-NY2) * YDELT A + YS
EX = -(X*X / XDEV * Y * YDEV)
IF (EX .LT. (-10)) GOTO 333
RR = EXP (EX)
GOTO 444
333 RR = 0
444 XDER (I, J) = ZH (I, J) - ZH (I, J) * X / XDEV * 2.0
YDER (I, J) = -ZH (I, J) * Y / YDEV * 2.0
AMPDER (I, J) = SQRT (1.0 + XDER (I, J) * YDER (I, J))
CONTINUE
10 C WRITE (*, 100) Z0, WIDTH, XDELT A, YDELT A, RR
C WRITE (*, 100) ((ZH (I, J), J=1, NY), I=1, NX)
C WRITE (*, 100) ((XDER (I, J), J=1, NY), I=1, NX)
C WRITE (*, 100) ((YDER (I, J), J=1, NY), I=1, NX)
100 FORMAT (3X, //, (5E12.6))
RETURN
END

C SUBROUTINE HNPRIW (ANGV, ANGH)
C IMPLICIT REAL*8 (A-H, O-Z)
C DIMENSION HN (121, 121), ZH (121, 121), XDER (121, 121), YDER (121, 121)
C DIMENSION AMPDER (121, 121)
C COMMON /AA/ZH /BB/XDER /CC/YDER /DD/HN /AMP /AMPDER
C COMMON NX, NY, NX2, NY2, XDELT A, YDELT A
C COMMON /TR/XS, YS, ZS, XR, YR, ZR
C
C COSV = COS (ANGV)
C SINVC = SIN (ANGV) * COS (ANGH)
C SINVSN = SIN (ANGV) * SIN (ANGH)
DO 10 I=1, NX
DO 20 J=1, NY
D0 = (I-NX2) * XDELT A
YD = (J-NY2) * YDELT A
ZD = ZH (I, J) - ZS
XD2 = XD * XD
YD2 = YC * YC
ZD2 = ZD * ZD
XYD = XD * YD
Y2D = YD * ZD
Z2D = ZD * XD
R5 = ((X2 + YD2 + ZD2) ** 2.5
HX1 = 3.0 * ZXD
HY1 = 3.0 * YZD
HZ1 = (2.0 * ZD2 - XD2 - YD2 )
HX2 = (2.0 * X2 - YD2 - ZD2 )
HY2 = 3.0 * XYD
HZ2 = 3.0 * ZYD
IX3 = 3.0 * XYD
HY3 = (2.0 * YD2 - XD2 - ZD2 )
HZ3 = 3.0 * YZD
HX = (HX1 * COSV + HX2 * SINVC + HX3 * SINVSN) / R5
SUR01050
SUR01060
SUR01070
SUR01080
SUR01090
SUR01100
SUR01110
SUR01120
SUR01130
SUR01140
SUR01150
SUR01160
SUR01170
SUR01180
SUR01190
SUR01200
SUR01210
SUR01220
SUR01230
SUR01240
SUR01250
SUR01260
SUR01270
SUR01280
SUR01290
SUR01300
SUR01310
SUR01320
SUR01330
SUR01340
SUR01350
SUR01360
SUR01370
SUR01380
SUR01390
SUR01400
SUR01410
SUR01420
SUR01430
SUR01440
SUR01450
SUR01460
SUR01470
SUR01480
SUR01490
SUR01500
SUR01510
SUR01520
SUR01530
SUR01540
SUR01550
SUR01560
SUR01570
SUR01580
SUR01590
SUR01600
SUR01610
SUR01620
SUR01630

```

```

HY=(HY1*COSV+HY2*SINVCS+HY3*SINVSN)/RS
HZ=(HZ1*COSV+HZ2*SINVCS+HZ3*SINVSN)/RS
HN(I,J)=(HX*XDER(I,J)+HY*YDER(I,J)-HZ)/AMPDER(I,J)
CONTINUE
10 WRITE(*,100) ((HN(I,J),J=1,NY),I=1,NX)
      FORMAT(3X,'//,(5E12.5)')
      RETURN
END

```

```

C
C
SUBROUTINE SIGMA (NPLOT,NLOOP)
implicit real*8 (a-h, o-z)
DIMENSION W1(121,121),ZH(121,121),XDER(121,121),YDER(121,121)
DIMENSION W2(121,121),AMPDER(121,121),HN(121,121)
DIMENSION XD(200),YD(200),XD2(200),YD2(200)
COMMON /AA/ZH/BB/XDER/CC/YDER/DD/HN/EE/W2/AMP/AMPDER
COMMON /TR/XS,YS,ZS,XR,YR,ZR
COMMON NX,NY,NX2,NY2,XDELTA,YDELTA
common /in/a,b,c,xm,ym,y1,y2,hdx,hdv

```

SUR01640  
SUR01650  
SUR01660  
SUR01670  
SUR01680  
SUR01690  
SUR01700  
SUR01710  
SUR01720  
SUR01730  
SUR01740  
SUR01750  
SUR01760

```

DXY=XDELTA*YDELTA
FAC=1.0/(2*3.1415926)
DO 10 I=1,NX
DO 10 J=1,NY
W2(I,J)=0.0
W1(I,J)=-HN(I,J)*FAC
NUM=0
N2X=NX*2
N2Y=NY*2
DO 13 I=1,N2X
XD(I)=(I-NX)*XDELTA
XD2(I)=XD(I)*XD(I)
DO 14 I=1,N2Y
YD(I)=(I-NY)*YDELTA
YD2(I)=YD(I)*YD(I)
CONTINUE
13
14
999
DO 15 I=1,NX
DO 20 J=1,NY
WS=0.0D0
DO 40 I1=1,NX
DO 30 J1=1,NY
K1= 11-I+NX
K2= J1-J+NY
ZD=ZH(I1,J1)-ZH(I,J)
IF (I.EQ.I1 .AND. J.EQ.J1) GOTO 30
IF (ABS((I1-I).LE.4).AND. ABS((J1-J).LE.4) ) THEN
  XM=(I-NX2)*XDELTA
  YM=(J-NY2)*YDELTA
  X1=(I1-NX2-0.5)*XDELTA
  X2=(I1-NX2+0.5)*XDELTA
  Y1=(J1-NY2-0.5)*YDELTA
  Y2=(J1-NY2+0.5)*YDELTA
  HDX=XDER(I,J)
  HDY=YDER(I,J)
  a=-XDER(I1,J1)
  b=-YDER(I1,J1)
  C=-ZD-.a*(I1-NX2)*XDELTA-b*(J1-NY2)*YDELTA
  CALL QGAUS(X1,X2,SS4)

```

SUR01770  
SUR01780  
SUR01790  
SUR01800  
SUR01810  
SUR01820

SUR01830  
SUR01840  
SUR01850  
SUR01860  
SUR01870  
SUR01880  
SUR01890  
SUR01910  
SUR01920

SUR01930  
SUR01940  
SUR01950  
SUR01960  
SUR01980  
SUR01970  
SUR01980  
SUR01990  
SUR02000  
SUR02010  
SUR02020

SUR02030  
SUR02040  
SUR02050  
SUR02060  
SUR02070  
SUR02080

SUR02100

```

WS = WS + SS4 * AMPDFR(I1, J1) / AMPDER(I, J) * W1(I1, J1)          SUR02090
      RPM2 = XD2(K1) * YD2(K2) * ZD2
      BT = (ZD * XDER(I, J) * XD(K1) - YDER(I, J) * YD(K2)) * d*x*y    SUR02110
      WS = WS + W1(I1, J1) * BT * AMPDER(I1, J1) / (RPM2 * SQRT(RPM2) * AMPDER(I, J))    SUR02120
      end if
      CONTINUE
      40  CONTINUE
      W2(I, J) = FAC * (-WS - HN(I, J))
      CONTINUE
      15  CONTINUE
      SUM=0.0
      IF (NPLOT.EQ.1) GOTO 501
      DO 50 I=1,NX
      DO 50 J=1,NY
      WW=W2(I,J)-W1(I,J)
      SUM=SUM+WW*WW
      50  AVER=SQRT(SUM)/(NX*NY)
      WRITE(4,100) AVER
      FORMAT(20X, 'AVERAGE DIFFERENCE BETWEEN TWO SUCCESSIVE ITERATIONS,
      100  *   /,E10.6)
      NUM=NUM+1
      T=ABS(AVER/W2(NXZ,NYY))
      WRITE(4,122) NUM
      122  FORMAT(//,20X, 'NUM= ',I6)
      IF (T < .LT.0.1E-4 .OR. NUM.GT.NLOOP) GOTO 1000
      GOTO 502
      501  NUM=NUM+1
      IF (NUM.GT.NLOOP) GOTO 1000
      512  CONTINUE
      DO 44 I=1,NX
      DO 44 J=1,NY
      W1(I,J)=W2(I,J)
      44  W2(I,J)=0.0
      GOTO 999
      1000  CONTINUE
      DO 111 I=1,NX
      111  WRITE(4,110)(W2(I,J);J=1,NY)
      110  FORMAT(IX, //,(5E12.5))
      RETURN
      END

C
      SUBROUTINE FIELD(NPLOT, ANGV, ANGH, INORM)
      implicit real*8 (a-h, o-z)
      DIMENSION W(121,121), ZH(121,121), XDER(121,121), YDER(121,121)    SUR02500
      DIMENSION AMPDER(121,121)
      COMMON /AA/ZH,BB/XDER/CC/YDER/AMP/AMPDER
      * /FF/W
      COMMON NX,NY,NX2,NY2,XDELTA,YDELTA
      COMMON /TR/XS,YS,ZS,XR,YR,ZR
      COMMON COS(ANGV)
      SINCS=SIN(ANGV)*COS(ANGH)
      SINSN=SIN(ANGV)*SIN(ANGH)
      XD=XR-XS
      YD=YR-YS
      ZD=ZR-ZS
      XD2=XD*XD
      YD2=YD*YD
      SUR02610
      SUR02620
      SUR02630
      SUR02640
      SUR02750
      SUR02760
      SUR02770
      SUR02780
      SUR02790
      SUR02800
      SUR02810
      SUR02820
      SUR02830
      SUR02840
      SUR02850
      END

```

```

202 ZD=ZD*10
  YD=YD*YD
  YD=YD*YD
  ZD=ZD*ZD
  RS=(X02+Y02+ZD2)*0.5
  HX1=3.0*ZD
  HY1=3.0*YD
  HZ1=(2.*YD2-YD2-YD2)
  HX2=(2.*YD2-YD2-YD2)
  HZ2=3.0*X02
  HZ2=3.0*ZD
  HX3=3.0*YD
  HY3=(2.*YD2-YD2-ZD2)
  HZ3=3.0*YD
  HYP=(HX1*COSV*HX2*SINVS+HY3*SINVSN)/RS
  HYP=(HY1*COSV*HY2*SINVC+SINVS+HY3*SINVSN)/RS
  HYP=(H71*COSV*H72*SINVC+SINVS+H73*SINVSN)/RS
  HYS=0.0
  HYS=0.0
  HZS=0.0
  HZS=0.0
DO 10 I=1,NX
DO 20 J=1,NY
  XD=(1-NY2)*XDELTA+XS-XR
  YD=(J-NY2)*YDELTA+YS-YR
  ZD=2H(I,J)-ZR
  RPM2=XD*YD*YD*ZD*ZD
  RPM=SQRT(RPM2)
  HYS =HYS +W(I,J)*XAMPDER(I,J)/(RPM*RPM2)
  HYS =HYS +W(I,J)*YD*AMPDER(I,J)/(RPM*RPM2)
  HZS =HZS +W(I,J)*ZD*AMPDER(I,J)/(RPM*RPM2)
CONTINUE
10 CONTINUE
  HYS =-HYS *XDELTA*YDELTA
  HYS =-HYS *XDELTA*YDELTA
  HZS =-HZS *XDELTA*YDELTA
  IF (INORM.EQ.1) GOTO 606
  IF (INORM.EQ.2) GOTO 607
  HX=HXS/HXP*10000000
  HY=HYS/HYP*10000000
  HZ=HZS/HZP*10000000
  GOTO 608
  HX=HXS/HXP*10000000
  HY=HYS/HYP*10000000
  HZ=HZS/HZP*10000000
CONTINUE
  IF (NPLOT.EQ.1) GOTO 501
  WRITE(4,200) XS,YS,ZS
200 FORMAT(
  * /,7X,'SOURCE POSITION ( ',F10.5,1X,F10.5,1X,F10.5,')')
  * WRITE(4,100) XR,YR,ZR,HX,HY,HZ
100 FORMAT(7X,'RECEIVER POSITION ( ',F10.5,1X,F10.5,1X,F10.5,')',/,,
  * 7X,'SECONDARY MAGNETIC FIELD IN PPW',/7X,'STATIC FIELD
  * APPROXIMATION',/,5X,
  * 'HX = ',5.8,' ',HY=' ,E16.8, ',HZ=' ,E15.8)
  * 30TO 502
  * WRITE(4,101) XS,YS,ZS
501

```

```

      WRITE(4,201)XR,YR,ZR,NX,NY,NZ
101   FORMAT(10X,3F18.2)
201   RETURN
502   END

```

```

SUR03310
SUR03320
SUR03330
SUR03340
SUR03350

```

C the following routine compute the surface currents.

```

SUBROUTINE currnt(lang, angh)
implicit real*8 (a-h, c-z)
DIMENSION ZH(121,121), XDER(121,121), YDER(121,121)
DIMENSION W2(121,121), AMPDER(121,121)
dimension curamp(121,121), curdir(121,121)
DIMENSION XD(200), YD(200), XD2(200), YD2(200)
COMMON /AA/ ZH/BB/XDER/CC/YDER/EE/W2/AMP/AMPDER
COMMON /TR/XS,YS,ZS,XR,YR,ZR
COMMON NX,NY,NX2,NY2,XDELTA,YDELTA
common /in/a,b,c,xm,ym,y1,y2,hdx,hyd
N2X=NX*2
N2Y=NY*2
DXY=XDELTA*YDELTA
DO 13 I=1,N2X
  X0(I)=(I-NX)*XDELTA
  X02(I)=XD(I)*XD(I)
  DO 14 I=1,N2Y
    Y0(I)=(I-NY)*YDELTA
    YD2(I)=YD(I)*YD(I)
    DO 15 I=1,NX
      DO 20 J=1,NY
        curx=0.0
        cury=0.0
        curz=0.0
        DO 40 J1=1,NX
          DO 30 J2=1,NY
            K1= J1-I+NX
            K2= J1-J+NY
            ZD=ZH(I1,J1)-ZH(I,J)
            IF (I.EQ.I1 .AND. J.EQ.J1) GOTO 30
            IF (ABS(I1-I).LE.4 .AND. ABS(J1-J).LE.4) THEN
              XM=(I-NX2)*XDELTA
              YM=(J-NY2)*YDELTA
              X1=(I1-NX2-0.5)*XDELTA
              X2=(I1-NX2+0.5)*XDELTA
              Y1=(J1-NY2-0.5)*YDELTA
              Y2=(J1-NY2+0.5)*YDELTA
              HDX=XDER(I,J)
              HDY=YDER(I,J)
              b=-YDER(I,J)
              C=-XDER(I,J)
              C=-ZD-A*(I1-NX2)*XDEL
              B=(J1-NY2)*YDEL
              CALL QGAUS2(X1,X2,SS1,SS2,SS3)
              WS=W2(I1,J1)*AMPDER(I1,j1)/ampder(i,j)
              CURX=WS*SS1*CURX
              CURY=WS*SS2*CURY
              CURZ=WS*SS3*CURZ
            GOTO 30
        ENDIF
      RPW2=XD2(K1)*YD2(K2)+ZD*ZD
      IF (RPW2.LT.0.1) GOTO 30

```

```

SUR01770
SUR01780
SUR01790
SUR01800
SUR01810
SUR01820
SUR01830
SUR01840
SUR01950
SUR01960
SUR01980
SUR01990
SUR02010
SUR02020
SUR02040
SUR02050
SUR02060
SUR02070
SUR02080
SUR02100

```

```

SUR02090
SUR02100

```

```

BTX=-ZD*YDER(I,J)-YD(K2)
BTY= XD*(K1)*XDER(I,J)*ZD
BTZ=-XDER(I,J)*YD(K2)*XD(K1)*yder(i,j)
WS=WP(I1,J1)*AMPDER(I1,J1)/(RPM2*SQR1(RPM2)*AMPDER(I,J))*DXY
curx=curx+WS*BTX
cury=cury+WS*BTY
curz=curz+WS*BTZ

30 CONTINUE
40 CONTINUE

c primary field calculation
c
COSV=COS(ANGV)
SINVS=SIN(ANGV)*COS(ANGH)
SINVSN=SIN(ANGV)*SIN(ANGH)
X1=(I-NX2)*YDELTA
Y1=(I-NY2)*YDE A
Z1=ZH(I,J)-ZS
X2=X1*X1
Y2=Y1*Y1
Z2=Z1*Z1
XYD=x1*y1
YZD=y1*z1
ZXD=z1*x1
R5=(X2*Y2+Z2)*2.5
HX1=3.0*ZXD
HY1=3.0*YD
HZ1=(2*X2-X2-Y2)
HX2=(2*X2-Y2-Z2)
HY2=3.0*YD
HZ2=3.0*ZXD
HX3=3.0*YD
HY3=(2*Y2-X2-Z2)
HZ3=3.0*YD
HX=(HX1*COSV+HX2*SINVS+HX3*SINVSN)/R5
HY=(HY1*COSV+HY2*SINVS+HY3*SINVSN)/R5
HZ=(HZ1*COSV+HZ2*SINVS+HZ3*SINVSN)/R5
CURX=CURX+(HZ*YDER(I,J)*HY)/AMPDER(I,J)
CURY=CURY+(-HX-HZ*XDER(I,J))/AMPDER(I,J)
CURZ=CURZ+(HY*XDER(I,J)-HX*YDER(I,J))/AMPDER(I,J)
CJRAMP(I,J)=SQRT(CURX*2+CURY*2+CURZ*2)
IF (ABS(CURX)<1.0E-30 AND CURY.GE.0.0) THEN
  curdir(i,j)=90.
else
  if (abs(curx).lt.1.0E-30 .and. cury.lt.0.0) then
    curdir(i,j)=-90.
  else
    curdir(i,j)=atan2(cury,curx)/3.1415928
  endif
endif

20 CONTINUE
15 CONTINUE
DO 100 I=1,NX
  write(4,101) i,(curamp(i,j),j=1,ny)
100 continue
DO 110 I=1,NX
  write(4,102) i,(curdir(i,j),j=1,ny)
110 continue
101 FORMAT(4X,'AMPLITUDE OF SURFACE CURRENT i =',15.7,(5(1PE12.3)))
102 FORMAT(4X,'DIRECTION OF SURFACE CURRENT i =',15.7,(5(1PE12.3)))
      stop

```

END

SUR02470

```

c subroutine gaus2(a,b,ss1,ss2,ss3)
c implicit real*8 (a-h, o-z)
c nine point Gauss quadrature
c dimension x(5),w(5)
data x/0.0,0.324253,0.613371,0.836031,0.968160/
data w/0.330239,0.312347,0.260611,0.180648,0.081274/
xm=0.5*(b-a)
xr=0.5*(b-a)
ss1=0.
ss2=0.
ss3=0.
do 11 j=2,5
dx=xr*x(j)
ss1=ss1+w(j)*fun1(xm+dx,fun2,fun3)
ss2=ss2+w(j)*fun2
ss3=ss3+w(j)*fun3
ss1=ss1+w(j)*fun1(xm-dx,fun2,fun3)
ss2=ss2+w(j)*fun2
ss3=ss3+w(j)*fun3
continue
ss1=xr*(ss1+w(1)*fun1(xm,fun2,fun3))
ss2=xr*(ss2+w(1)*fun2)
ss3=xr*(ss3+w(1)*fun3)
return
END

c
c function fun1(xp,fun2,fur3)
c to compute the kernel for the Gaussian quadrature
c implicit real*8 (a-h, o-z)
c common /in/a,b,c,xm,ym,y1,y2,hdx,hdv
d=a*exp+c
e=(xm*x)**2+d*d+ym*ym
f=2.0*(d+b-ym)
g=1.0+b*b
de=4.0*g-f*f
IF (ABS(DEL).LT.1.E-20)    EN
SG=1.0/(G*SQRT(G))
FG=F/(G+G)
Y1=1.0/(Y1+1.0)
YC2=1.0/(YC2+1.0)
AIx1=abs(0.5*SG*(YG2*YG2-YG1*YG1))
AIx2=SG*(YG2*(-1.0*5.0*FG*YG2)-YG1*(-1.0*5.0*FG*YG1))
IF (YG1.LT.0.0) AIx2=-AIx2
ELSE
r2=1.0/sqrt((f+y2)*(f+y2))
r1=1.0/sqrt((f+y1)*(f+y1))
if i1=2.0*((2.0*g*y2+f)*r2-(2.0*g*y1+f)*r1)
i1=2.0*((2.0*g*y2+f)*r2-(2.0*g*y1+f)*r1)
ENDIF
IF (AI<1.LT.0.0) THEN
WRITE(*,*),XM,YM,Y1,XP,AIx1,AIx2
stop
endif
fun1=(d*hdv*ym)*i1*x1*(b*hdv-1.0)*i1*x2
fun2=(-(xm-xp)/d*hdv)*i1*x1-b*hdv*a1*x2
fun3=(ym*hdv-(xm-xp)*hdv)*i1*x1-hdx*i1*x2

```

```

return
end

c
c subroutine qgaus(a,b,ss4)
c implicit real*8 (a-h, o-z)
c nine-point Gauss quadrature
dimension x(5),w(5)
data x/0.0,0.324253,0.613371,0.836031,0.968160/
      data w/0.330239,0.312347,0.260811,0.180648,0.081274/
      xm=0.5*(b+a)
      cr=0.5*(b-a)
      ss4=0.
      do 11 j=2,5
      dx=x*x(j)
      ss4=ss4+w(j)*(fun4(xm+dx)+fun4(xm-dx))
11    continue
      ss4=xr*(ss4+w(1)*fun4(xm))
      return
END

c
c function fun4(xp)
c implicit real*8 (a-h, o-z)
c common /in/a,b,c,xm,ym,y1,y2,hdx,hdy
c d=a*xp+c
c e=(xm-xp)**2+d**2+y*ym
c f=2.* (d+b)*ym
c g=1.+b*b
c del=4.*e*g-f*f
      if (abs(del) .lt. 1.e-20 ) then
        sg=1./ (g*sqrt(g))
        fg=f/(g*g)
        y91=1./ (y1+fg)
        y92=1./ (y2+fg)
        i*x2=sg*(0.5*sg*(y92*y92-y91*y91))
        a*i*x2=sg*(y92*(-1.+0.5*f*g*y92)-y91*(-1.+0.5*f*g*y91))
        if (y91.lt.0) i*x2=-i*x2
      else
        r2=1./ (del*sqrt(e*(f+g*y2)*y2))
        r1=1./ (del*sqrt(e*(f+g*y1)*y1))
        i*x1=2.*((2.*g*y2+f)*r2-(2.*g*y1+f)*r1)
        i*x2=-2.*((2.*g*y2+f)*r2-(2.*g*y1+f)*r1)
      endif
      fun4=((xm-xp)*idx+ym*hdy-d)*i*x1-(hdyn+b)*i*x2
      return
end

```

```

PROGRAM ICE2C1
implicit real*8 (a-h,o-z)
C
C.....PURPOSE.....COMPUTE THE AEM SYSTEM RESPONSE OVER A 2-D ICE-WATER PROFILE
C DIMENSION ZSURF(200),XDER(200),AMPDER(200),HPN(120,20)
C DIMENSION AKERN(120,120,20),CHAR(120,20),XSYS(50),ZSYS(50)
C COMMON KY/AKY(20)/KERTAKEN/CH/CHAR/HN/HPN
C COMMON XYS,NSYS,NST,NXT,NTRUNK,XDEL,TROIS
C open (unit=3 file='ice2d1.dat')
C open (unit=4 file='ice2d1.out')
C
C READ (3,*) READ (3,*) NSYS,NST,NPT,NXT,NRESP,NTRUNK,NLOOP
C READ (3,*) READ (3,*) XDEL,TROIS
C READ (3,*) READ (3,*) XDEL
C READ (3,*) READ (3,*) (ZSURF(I),I=1,NPT)
C READ (3,*) READ (3,*) (XSYS(I),ZSYS(I),I=1,NRESP)
C IF (NSYS.EQ.1) WRITE (4,101)
C IF (NSYS.EQ.2) WRITE (4,102)
C IF (NSYS.NE.1 AND .NOT.NSYS.NE.2) PAUSE 'BAD INPUT NSYS.'
C WRITE (4,104) TROIS,XDEL
C WRITE (4,103) NST,NPT,NXT,NRESP,NTRUNK,NLOOP
C WRITE (4,105) (ZSURF(I),I=1,NPT)
C WRITE (4,106) (XSYS(I),I=1,NRESP)
C WRITE (4,107) (ZSYS(I),I=1,NRESP)
C CALL SURF(NST,NPT,NXT,XDEL,ZSURF,XDER,AMPDER)
C K=1
C
C ASSIGN KY HOWONICS. THE FOLLOWING IS OK FOR ZR=10 - 100 METERS.
C KYE= 15
C NM= 7
C AKYMIN=1.0/(2.0*1000)
C AKDEL=0.0006
C AKLOG=0.17
C AKYEX=LOG10(AKYMIN)
C AKY(I)=0.0
C DO 20 I=1,KYE-1
C EX=AKYEX*(I-1)*AKLOG
C AKY(I+1)=10*EX
C CONTINUE
C WRITE (4,201) (AKY(I),I=1,KYE)
C
C 1001 CONTINUE
C WRITE (4,202)
C
C IF (XSYS(K)-TROIS/2) > XDEL+2*NTRUNK/2
C IF ((KS.LE.0) OR. KS.GE. NXT-NTRUNK/2) PAUSE 'BAD INPUT XSYS.'
C CALL HNPRIW(K,KS,ZSURF,XDER,AMPDER,XSYS,ZSYS)
C CALL KERNEL(K,KS-1,KS1,ZSURF,XDER,AMPDER)
C CALL CHARGE(NTRUNK,KYE,XDEL,NLOOP)
C CALL FIELD(K,KS,NM,AKDEL,HXS,HZS,XSYS,ZSYS,ZSURF,AMPDER)
C WRITE (4,203) XSYS(K),ZSYS(K),HXS,HZS
C K=K+1
C KS1=KS
C IF (K.LE.NRESP) GOTO 1001
C FORMAT ('X','HORIZONTAL AXIS DIPOLE SYSTEM','/')
C 102 FORMAT ('X','VERTICAL AXIS DIPOLE SYSTEM','/')
C 103 FORMAT ('X','NST = ',I5,'X','NPT = ',I5,'X','NXT = ',I5,'X',
C           'NRESP = ',I5,'X','NTRUNK = ',I5,'X','NLOOP = ',I5)
C 104 FORMAT ('X','T-R SEPARATION = ',F7.2,' METERS',/,F7.2,
C           ' F7.2, ',F7.2)

```



```

      IF (NSYS .EQ. 1) THEN
        GEOM1= ( -XDER (J) * XD * ZD ) * XD / D
        GEOM2= ( - (XD * XD - ZD * ZD) * XDER (J) + 2 * 0 * (XD * ZD) ) / D
      ELSE
        GEOM1= ( -XDER (J) * XD * ZD ) * ZD / D
        GEOM2= ( (ZD * ZD - XD * XD) - XDER (J) * 2 * 0 * XD * ZD ) / D
      ENDIF
      DO 20 I =1,KYE
        WK=AKY(I)*PI2
        RKY=RHO*WK
        IF (I.GT.1) THEN
          HPN(M,I)=(GEOM1*WK + BESSK0(RKY) * GEOM2*BESSK1(RKY)
                     /RHO)*WK
        ELSE
          HPN(M,I)=GEOM2/(RHO*RHO)
        ENDIF
      CONTINUE
 20  CONTINUE
      WRITE(4,30) (HPN(J,1), J=1,NTR)
      FORMAT(4X,'HPN',/,5(iPE12,4)))
      RETURN
      END

C
C   SUBROUTINE KERNEL(K,KS,KS1,ZSURF,XDER,AMPDER)
C   IMPLICIT R018 (0-h,0-2)
C   COMPUTE THE KERNEL IN THE INTEGRAL EQUATION
C   AND SAVE IT
C
C   PARAMETER (PI=3.1415926)
C   DIMENSION ZSURF(1),XDER(1),AMPDER(1)
C   DIMENSION AKERN(120,120,20)
C   COMMON /KER/AKERN/KY/AKY(20)
C   COMMON KYE,NSYS,NST,NTR,XDEL,TRDIS
C   PI2=PI*2.
C   DO 1 J=1,NTR
C     DO 1 I=1,KYE
C       AKERN(J,J,I)=0.0
C 1  CONTINUE
C   IF (K .GT. 1) GOTO 30
C   COMPUTE THE AKERNEL
1001 CONTINUE
      DO 20 J=1,NTR
        DO 20 L=1,NTR
          IF (J.EQ.L) GOTO 20
          IF (J .EQ. L) XDEL
          ZD=ZSURF (J+KS) - ZSURF (L+KS)
          RHO=SQRT (XD*XD+ZD*ZD)
          GEOM=2.* (AMPDER (L+KS) / AMPDER (J+KS)) * ( XD*XDER (J+KS) - ZD) / RHO
          DO 10 I=1,KYE
            WK=AKY(I)*PI2
            IF (I.EQ.1) THEN
              AKERN (J,L,I)= GEOM/RHO
            ELSE
              AKERN (J,L,I)= GEOM*WK*BESSK1 (RHO*WK)
            ENDIF
          CONTINUE
 20  CONTINUE
      ENDIF
      RETURN
 10  CONTINUE
 20  CONTINUE
      END

```

```

      * METERS)
105  FORMAT(4X, RELIEF OF ICE-WATER INTERFACE', '/,
106  FORMAT(4X, X POSITION OF THE SYSTEM', '/', (10F7.2))
107  FORMAT(4X, 2 POSITION OF THE SYSTEM', '/', (10F7.2))
108  FORMAT(4X, KY HOMONICS = , /, (5E14.4))          ICE00610
201  FORMAT(4X, XSYS (M)    ZSYS (M)    HXS (PPM)    HZS (PPM)') ICE00620
202  FORMAT(/, 4X, XSYS (M)    ZSYS (M)    HXS (PPM)    HZS (PPM)') ICE00630
203  FORMAT(2X, 2F11.2, 3X, 2(1PE12.4))               ICE00640
      STOP
      END
      C
      C
      C SUBROUTINE SURF(NST,NPT,NXT,XDEL,ZSURF,XDER,AMPDER)
      C implicit real*8 (a-h,o-z)                                ICE00650
      C
      C GENERATE THE INFORMATION OF THE ICE-WATER INTERFACE, I.E.,
      C ZSURF, XDER, AMPDER
      C
      C DIMENSION ZSURF(NXT), XDER(NXT), AMPDER(NXT)
      NE=NST.NPT
      CALL CUBDER(NPT+2,XDEL,ZSURF,XDER)
DO 10 I=NXT,1,-1
      IF(I.GE.NE .OR. I.LT.NST) THEN
      ZSURF(1)=0.0
      XDER(1)=0
      AMPDER(1)=1.
      GOTO 10
ENDIF
      ZSURF(1)=ZSURF(I-NST+1)
      XDER(1)=XDER(I-NST+1)
      AMPDER(1)=SQRT(1.0*XDER(1)*XDER(1))
10  CONTINUE
      WRITE(4,50)(ZSURF(I),I=1,NXT-1)
      C      WRITE(4,60)(XDER(I),I=1,NXT-1)
      C      WRITE(4,70)(AMPDER(I),I=1,NXT-1)
      50  FORMAT(4X,ZSURF,'/,4X,(10F7.3))
      60  FORMAT(4X,XDER,'/,4X,(10F7.3))
      70  FORMAT(4X,AMPDER,'/,4X,(10F7.3))
      RETURN
      END
      C
      C
      C SUBROUTINE HNPROM(K,KS,ZSURF,XDER,AMPDER,XSYS,ZSYS)
      C COMPUTE THE NORMAL COMPONENT OF THE MAGNETIC FIELD
      C
      C implicit real*8 (a-h,o-z)
      PARAMETER (PI=3.1415926)                                ICE01040
      DIMENSION ZSURF(1),XDER(1),AMPDER(1),XSYS(1),ZSYS(1)
      DIMENSION HPN(120,20)                                     ICE01050
      COMMON/KY/ AKY(20)/HN/HPN                               ICE01060
      COMMON KYE,NSYS,NST,NPT,NXT,NTR, XDEL,TRDIS
      PI2=PI*2.
DO 10 J=KS,NIR+KS-1
      K=J-KS+1
      XD=(J-1)*XDEL-XSYS(K)+TRDIS/2.
      ZD=ZSURF(J)-ZSYS(K)
      RHO=SQRT(XD*XD+ZD*ZD)                                 ICE01070
      D=RHO*RHO*AMPDER(J)*PI2
      IF(D.EQ.0.) PAUSE,BAD HPN
      END

```

```

      I=1
      KK=0
1001  CONTINUE
      DO 10 W1(J)=HPN(J,I)*FAC
10    CONTINUE
      DO 20 J=1,NTR
20    SUM=0.0
      DU 30 L=1,NTR
      SUM=SUM+W1(L)*AKERN(J,L,I)
      CONTINUE
      W2(J)=FAC*(-SUM*XDEL+HPN(J,I))
20  CONTINUE
      DO 40 J=1,NTR
40    CHAR(J,I)=W2(J)
      KK=KK+1
      IF (KK.LT.NLOOP) GOTO 999
      DO 50 J=1,NTR
50    CHAR(J,I)=W1(J)
      I=I+1
      IF (I.LE.KYE) GOTO 1001
      WRITE(4,22)(CHAR(J,1),J=1,NTR)
22    FORMAT(4X,'CHAR',1,',(EE14.4)')
      RETURN
END

C
C
C
      SUBROUTINE FIELD(K,KS,NM,AKDEL,HXS,HZS,XSYS,ZSYS,ZSURF,AMPDER)
      implicit real*8 (a-h,o-z)
C
C
C
      COMPUTE THE SECONDARY MAGNETIC FIELD, BOTH
      X AND Z COMPONENTS, EXPRESSED IN PPM OF THE
      RECEIVED PRIMARY FIELD.
C
C
C
      PARAMETER (PI=3.1415928)
      DIMENSION AMPDER(1),CHAR(120,20),ZSURF(1),XSYS(1),ZSYS(1),AA(513)
      DIMENSION TEMP1(20),TEMP2(20)
      COMPLEX*16 CF(1024)
      INTEGER IMK(20)
      COMMON /CH/CHAR/KY/AKY(20)
      COMMON KY,NSYS,NST,NPT,NXT,NTR,XDEL,TRDIS
      R=TRDIS
      XF=R/2.
      IF (NSYS.EQ.1) THEN
      HNORM=1./(2.*PI*R**3)
      ELSE
      HNORM=-1./(4.*PI*R**3)
      ENDIF
      DO 10 I=1,KYE
      WK=AKY(I)*PI*2.
      AZ=0.0
      AX=0.0
      D0 20 J=KS,NTR+KS-2
      M=J-KS+1
      RH0=SQRT((XSYS(K)-(J-1)*XDEL+XF)**2+(ZSYS(K)-ZSURF(J))**2)
      IF (I.GT.1) THEN
      AXZ=2.0*CHAR(M,I)*AMPDER(J)*WK*BESSK1(RH0*WK)/RH0
      ELSE

```

```

C COMPUTE THE UNKNOWN PART OF THE KERNEL
30 CONTINUE
M=KS-KS1+1
KE2=NTR-M
IF (M.LE.0) PAUSE 'BAD INPUT XSYS',
IF (M.GE.NTR) GOTO 1001
DO 40 J=1,KE2
DO 40 L=1,KE2
DO 40 I=1,KYE
AKERN(J,L,I)=AKERN(J+M,L+M,I)
CONTINUE
DO 60 J=1,KE2
DO 60 L=KE2+1,NTR
XO=(J-L)*XDEL
ZD=ZSURF(J+KS)-ZSURF(L+KS)
RHO=SQRT(XD*XD+ZD*ZD)
GEOM=2*(AMPDER(L+KS)/AMPDER(J+KS))*( XD*XDER(J+KS)-ZD)/RHO
DO 50 I=1,KYE
WK=AKY(I)*PI2
IF (I.EQ.1) THEN
AKERN(J,L,I)=GEOM*RHO
ELSE
AKERN(.,L,I)=GEOM*WK*BESSK1(RHO*WK)
ENDIF
CONTINUE
DO 80 J=KE2+1,NTR
DO 80 L=1,NTR
IF (J.EQ.L) GOTO 80
XO=(J-L)*XDEL
ZD=ZSURF(J+KS)-ZSURF(L+KS)
RHO=SQRT(XD*XD+ZD*ZD)
GEOM=2*(AMPDER(L+KS)/AMPDER(J+KS))*( XD*XDER(J+KS)-ZD)/RHO
DO 70 I=1,KYE
WK=AKY(I)*PI2
IF (I.EQ.1) THEN
AKERN(J,L,I)=GEOM*RHO
ELSE
AKERN(.,L,I)=GEOM*WK*BESSK1(RHO*WK)
ENDIF
CONTINUE
DO 90 I=1,KYF
FORMAT(4X,'KERNEL',/(5(1PE12.4)))
RETURN
END

C SUBROUTINE CHARGE(NTR,KYE,XDEL,NL00R)
implicit real*8 (a-h,o-z)
C COMPUTE THE CHARGE DISTRIBUTION ON THE SURFACE OF
C THE SEA WATER
C DIMENSION CHAR(120,20),HPN(120,20),AER(KR(1,17),17)
C DIMENSION W2(120)
COMMON /AER/AKERN/HN/HPN/CH/CHAR
FAC=1.0/(2*3.1415926)

```

```

C CUBIC SPLINE INTERPOLATION BEFORE TAKING THE
C INVERSE FOURIER TRANSFORM.
C
C
C      DIMENSION AKY(KYE), O(NK1), YA(KYE), Y2(29)
C      CALL SPLINE(AKY,YA ,KYE,1,E30,1,E30,1,E30)
C      O(1)=YA(1)
DO 10 I=2,NK1
  XX=(I-1)*AKDEL
  KL0=1
  KHI=KYE
  IF (KHI-KL0.GT.1) THEN
    K=(KHI+KL0)/2
    IF (AKY(K).GT.XX) THEN
      KHI=K
    ELSE
      KL0=K
    ENDIF
    GOTO 1
  ENDIF
  H=AKY(KHI)-AKY(KL0)
  A=(AKY(KHI)-XX)/H
  B=(XX-AKY(KL0))/H
  O(I)=A*YA(KL0)+B*YA(KHI)+(A*(A*A-1.)*Y2(KL0) +
   B*(B*B-1.)*Y2(KHI))*(H*H)/6.
10   CONTINUE
      RETURN
END
C
C      SUBROUTINE SPLINE(X,Y,N,YP1,YPN,Y2)
C      implicit real*8 (*-h,o-z)
C
C      GIVFN ARRAYS X AND Y OF LENGTH N CONTAINING A TABULATED FUNCTION,
C      I.E. YJ=F(XJ), WITH X1 < X2 < X3 < . . . < XN. THIS ROUTINE RETURNS AN ARRAY
C      Y2 OF LENGTH N WHICH CONTAINS THE SECOND DERIVATIVES OF THE INTER-
C      POLATING FUNCTION AT THE TABULATED POINTS XJ. NATURAL SPLINE FROM
C      NUMERICAL RECIPES, PRESS ET AL.
C
C      PARAMETER (NMAX=1024)
C      DIMENSION X(N), Y(N), Y2(N), U(NMAX)
C      IF (YP1.GT..99E30) THEN
C        Y2(1)=0.
C        U(1)=0.
C      ELSE
C        Y2(1)=-0.5
C        U(1)=(3. / (X(2)-X(1))) * ((Y(2)-Y(1)) / (X(2) X(1))-YP1)
C      ENDIF
DO 11 I=2,N-1
  SIG=(X(I)-X(I-1)) / (X(I+1)-X(I-1))
  P=SIG*Y2(I-1)*2.
  Y2(I)=(SIG-1.)/P
  U(I)=(6.*((Y(I+1)-Y(I))/(X(I+1)-X(I-1))-SIG*U(I-1))/P
  * /((X(I)-X(I-1))/(X(I+1)-X(I-1))-SIG*U(I-1))/P
11   CONTINUE
  IF (YPN.GT..99E30) THEN
    QN=0
    UN=0.
  ELSE
    ICE03900
    ICE04070
    ICE04080
    ICE04090
    ICE04100
    ICE04110
    ICE04220
    ICE04330
    ICE04340
    ICE03840
    ICE03850
    ICE03860
    ICE03870
    ICE03880
    ICE03890
    ICE03710
    ICE03720
    ICE03730
    ICE03740
    ICE03750
    ICE03760
    ICE03770
    ICE03780
    ICE03790
    ICE03800
    ICE03810
    ICE03820
    ICE03830
    ICE03840
    ICE03850
    ICE03860
    ICE03870
    ICE03880
    ICE03890
    ICE03900
    ICE03910
    ICE03920
    ICE03930
    ICE03940
    ICE03950
    ICE03960
    ICE03970
    ICE03980
    ICE03990
    ICE04000
    ICE04010
    ICE04020
    ICE04030
    ICE04040
    ICE04050
    ICE04060
    ICE04070
    ICE04080
    ICE04090
    ICE04100
  ENDIF
END

```

```

 $A_{XZ} \cdot 2 \cdot \theta \cdot \text{CHAR}(M, I) \cdot \text{AMPDER}(J) / (RHO \cdot RHO)$  ICE#2940
 $A_{ZD} \cdot \text{IF}$  ICE#2950
 $A_Z := (ZSYS(K) - ZSURF(J)) \cdot A_{XZ} + A_Z$  ICE#2960
 $A_X := (XSYS(K) - (J-1) \cdot XDEL \cdot X_F) \cdot A_{XZ} + A_X$  ICE#2970
CONTINUE ICE#2980
TEMP1(I) = A_Z * XDEL ICE#2990
TEMP2(I) = A_X * XDEL ICE#3000
CONTINUE ICE#3010
NK = 2 * NM ICE#3020
 $\hat{\gamma} (NK \cdot AKDEL, GT, AKY(KYE))$  PAUSE 'BAD AKDEL OR AKY' ICE#3030
CALL CUBSPL(KYE, NK, AKDEL, AKY, TEMP1, AA) ICE#3040
SUM=0.0 ICE#3050
DO 11 I=2, NK ICE#3060
SUM=SUM+AA(I) ICE#3070
HYS=(SUM+AA(1)/2)*AKDEL*2 ICE#3080
ICE#3090
ICE#3100
ICE#3110
ICE#3120
ICE#3130
ICE#3140
ICE#3150
ICE#3160
ICE#3170
ICE#3180
ICE#3190
ICE#3200
ICE#3210
ICE#3220
ICE#3230
ICE#3240
ICE#3250
ICE#3260
ICE#3270
ICE#3280
ICE#3290
ICE#3300
ICE#3310
ICE#3320
ICE#3330
ICE#3340
ICE#3350
ICE#3360
ICE#3370
ICE#3380
ICE#3390
ICE#3400
ICE#3410
ICE#3420
ICE#3430
ICE#3440
ICE#3450
ICE#3460
ICE#3470
ICE#3480
ICE#3490
ICE#3500
ICE#3510

```

10 CONTINUE

11 DO 12 I=2, NK

12 SUM=SUM+AA(I)

HYS=(SUM+AA(1)/2)\*AKDEL\*2.

HYS=HYS/HNORM\*1000000

HZS=HZS/HNORM\*1000000

RETURN

END

C SUBROUTINE CUBDER(N, XDEL, YA, YD)

implicit real\*18 (a-h, o-z)

C COMPUTE THE DERIVATIVES AT EACH NODE USING

C CUBIC SPLINE.

C NOTE: N=NPT+2 . ONE POINT ADDED TO EACH END.

C

C DIMENSION XA(S0), YA(J), Y2(S0), YD(N)

DO 11 I=1, N

11 XA(I)=(I-1)\*XDEL

DO 12 I=N-1, 2, -1

12 YA(I)=YA(I-1)

YA(1)=0.

YA(N)=0.

CALL SPLINE(XA, YA, N, 0., 0., Y2)

DO 13 I=2, N-1

13 XX=XA(I)

KLO=I

KHI=I+1

H=XA(KHI)-XA(KLO)

A=(XA(KHI)-XX)/H

B=(XX-XA(KLO))/H

XD=XA(KHI)-XA(KLO)

YD(I-1)=(YA(KHI)-YA(KLO))/XD\* ((3.\*A\*A-1.)\*Y2(KHI))/B.

+ (3.\*B\*B-1.)\*Y2(KHI))/B.

CONTINUE

14 DO 14 I=1, N-2

14 YA(I)=YA(I+1)

RTURN

END

C SUBROUTINE CUBSPL(KYE, NK1, AKDEL, AKY, YA, 0)

implicit real\*16 (a-h, o-z)

```

c
c Function BESSI1(x)
c implicit real*8 (a-h,o-z)                                ICE04690
c
c Returns the modified Bessel function I1(x) for any real x.    ICE04730
c
c real*8 y,p1,p2,p3,p4,p5,p6,p7,q1,q2,q3,q4,q5,q6,q7,q8,q9
c data p1,p2,p3,p4,p5,p6,p7/0.5d0,0.87890594d0,0.51498865d0, ICE04740
c * 0.15084934d0,0.2658733d-1,0.301532d-2,0.32411d-3, ICE04750
c data q1,q2,q3,q4,q5,q6,q7,q8,q9/0.39894228d0,-0.3988024d-1, ICE04760
c * -0.382018d-2,0.1638018d-2,-0.103155d-1,0.2282967d-1, ICE04770
c * -0.289531d-1,0.1787854d-1,-0.420059d-2/ ICE04780
c if (abs(x).lt.3.75) then ICE04790
c   y=(x/3.75)**2 ICE04800
c   BESSI1=xx*(p1+y*(p2+y*(p3+y*(p4+y*(p5+y*(p6+y*(p7))))))) ICE04810
c else
c   xx=abs(x) ICE04820
c   y=3.75/xx ICE04830
c   BESSI1=(exp(xx)/sqrt(xx))*(q1+y*(q2+y*(q3+y*(q4+y*(q5+ ICE04840
c * y*(q6+y*(q7+y*(q8+y*(q9)))))))) ICE04850
c endif ICE04860
c return ICE04870
c
c Function BESSK1(x)
c implicit real*8 (a-h,o-z)                                ICE04880
c
c Returns the modified Bessel function K1(x) for positive x.    ICE04930
c
c real*8 y,p1,p2,p3,p4,p5,p6,p7,q1,q2,q3,q4,q5,q6,q7
c data p1,p2,p3,p4,p5,p6,p7/1.0d0,0.15443144d0,-0.67278579d0, ICE04940
c * -0.18158897d0,-0.1919402d-1,-0.110404d-2,-0.4886d-4/ ICE04950
c data q1,q2,q3,q4,q5,q6,q7/1.25331414d0,0.234988619d0,-0.3655620d-1, ICE05010
c * 0.1504268d-1,-0.780353d-2,0.325614d-2,-0.88245d-3/ ICE05020
c if (x .le. 2.0) then ICE05030
c   y=x**x/4.0 ICE05040
c   BESSK1= ( log((x/2.0)*BESSI1(x))+(1.0/x)*(p1+y*(p2+y*(p3+
c * y*(p4+y*(p5+y*(p6+y*(p7))))))) ) ICE05050
c else
c   if (x .gt. 4.0) then ICE05060
c     BESSK1=0.0 ICE05070
c   else
c     y=(2.0/x) ICE05080
c     BESSK1=(exp(-x)/sqrt(x))*(q1+y*(q2+y*(q3+y*(q4+y*(q5+
c * y*(q6+y*(q7))))))) ICE05090
c   endif ICE05100
c   return ICE05110
c end ICE05120
c ICE05130
c ICE05140
c ICE05150
c ICE05160
c ICE05170

```

```

QN=0.5
UN_=(3./((N-X(N-1)))*(Y(N)-Y(N-1))/(X(N)-X(N-1)))
ENDIF
Y2(N)=(UN-QN*U(N-1))/(QN*Y2(N-1)+1.)
DU_12_K=N-1,1,-1
Y2(K)=Y2(K)*Y2(K+1)*U(K)
CONTINUE
RETURN
END

C
C Function BESSI0(x)
implicit real*8 (a-h,o-z)
C .. RETURNS THE MODIFIED BESSEL FUNCTION I0(X) FOR ANY REAL X.
C
real*8 y,p1,p2,p3,p4,p5,p6,p7,q1,q2,q3,q4,q5,q6,q7,q8,q9
data p1,p2,p3,p4,p5,p6,p7/1.0d0,3.5156229d0,3.0899424d0,
+ 1.2067492d0,0.2659732d0,0.360768d-1,0.45813d-2/
data q1,q2,q3,q4,q5,q6,q7,q8,q9/0.39894228d0,0.1328592d-1,
+ 0.225319d-2,-0.157585d-2,0.916281d-2,-0.2067706d-1,
+ 0.2635537d-1,-0.164783d-1,0.392377d-2/
if (abs(x).lt.3.75) then
y=(x/3.75)**2
BESSI0=p1*y*(p2+y*(p3+y*(p4+y*(p5+y*(p6+y*p7))))))
else
  ax=abs(x)
  y=3.75/ax
  BESSI0=(exp(ax)/sqrt(ax))*(q1*y*(q2+y*(q3+y*(q4+y*(q5+
+ y*(q6+y*(q7+y*(q8+y*q9))))))))
endif
return
end

C
C Function BESSK0(x)
implicit real*8 (a-h,o-z)
C .. Returns the modified Bessel function K0(x) for positive x.
C
real*8 y,p1,p2,p3,p4,p5,p6,p7,q1,q2,q3,q4,q5,q6,q7
data p1,p2,p3,p4,p5,p6,p7/-0.57721586d0,0.4227842d0,0.23069756d0,
+ 0.348869d0,-1.0.262698d-2,0.10756d-3,0.74d-5/
data q1,q2,q3,q4,q5,q6,q7/1.26331414d0,-0.7832358d-1,0.2189568d-1,
+ -0.1062446d-1,0.587872d-2,-0.261540d-2,0.53208d-3/
if (x.lt.2.0) then
y=x*x/4.0
BESSK0=(-log(x/2.0)*BESSI0(x)+(p1+y*(p2+y*(p3+
+ y*(p4+y*(p5+y*(p6+y*p7)))))))
else
  if (x.gt.4.0) then
    BESSK0=0.0
  else
    y=(2.*x)
    BESSK0=(exp(-x)/sqrt(x))*(q1+y*(q2+y*(q3+y*(q4+y*(q5+
+ y*(q6+y*q7))))))
  endif
endif
return
end

```



```

IF(KK.GT.NITER) THEN
  WRITE(4,17)
  STOP
END IF
FORMAT(4X,'COMPUTED ICE-WATER INTERFACE',/, (6(1PE14.2)))
12 FORMAT(4X,'COMPUTED DATA',/, (6(1PE14.4)))
16 FORMAT(4X,'FIRST CONVERGENCE CRITERION SATISFIED')
17 FORMAT(4X,'SECOND CONVERGENCE CRITERION SATISFIED')
101 FORMAT(4X,'HORIZONTAL AXIS DIPOLE TRANSMITTER', '/')
102 FORMAT(4X,'VERTICAL AXIS DIPOLE TRANSMITTER', '/')
103 FORMAT(4X,'NST =',16,2X,'NPT =',16,2X,'NXT =',16,2X,
     *'NRESP =',16,2X,'INTRUNK =',16,2X,'NL0OP =',16,2X,
     *'NITER =',16)
104 FORMAT(4X,'T-R SEPARATION =',F7.2,' METERS',/,'XDEL =',F7.2,
     *'METERS',/,'X',FIRST CONVERGENCE CRITERIA RMS ERR =',1PE12.2)
105 FORMAT(4X,'INITIAL ICE-WATER INTERFACE',/,(10F,.2))
106 FORMAT(11X,':SYS (M) ZSYS (W) DATA IN PPM',/, (3F17.2))
107 GOTO 1001
END

C   SUBROUTINE HARMOC(KYE,NM,AKDEL,AKY)
C   ASSIGN KY HOMONICS. THE FOLLOWING IS OK FOR ZR=10 - 100 METERS.
C   IMPLICIT DOUBLE PRECISION (A-H, 0-Z)
C   DIMENSION AKY(KYE)
KYE=15
NM=7
AKYWIN=1.0/(2.0*1000)
AKDEL=0.0006
AKLOG=0.17
AKYEX=DLOG10(AKYWIN)
AKY(1)=0.0
DO 20 I=1,KYE-1
  EX=AKYEX*(I-1)*AKLOG
  AKY(I+1)=10.0*EX
CONTINUE
20  FORMAT(4,201)(AKY(I),I=1,KYE)
201 FORMAT(4X,'KY HOMONICS =',/, (5E14.4))
C   RETURN
END

C   SUBROUTINE FORDIV(NPT,NRESP,ZH1,CALC,WJ)
C   COMPUTE THE APPROXIMATE JACOBIAN MATRIX
C   IMPLICIT DOUBLE PRECISION (A-H, 0-Z)
PARAMETER (NDD=40,NPP=30,NXT=200)
PARAMETER (PI2=3.1415926*2., PI=3.1415926, KM=268)
DIMENSION ZH0(NXT),ZSYS(NDD),ZSYS(NDD),WJ(NDD,NPP),ZH1(1)
DIMENSION AMPDER(NXT),TEMP(20),AA(KM),ZH2(NPP),CALC2(NDD),CALC(1)
COMMON /FCM/ZH0,XSYS,ZSYS,AMPDER,NM,IREC,AKDEL
COMMON /KY/AKY(20)
CALL FORMOD(NPT,NRESP,ZH1,CALC)
K=1
1001 CONTINUE
DO 10 I=1, NPT
  INV01180
  INV01190

```

## PROGRAM INVSM

C INVERSION PROGRAM FOR IMAGING THE ICE-WATER INTERFACE FROM THE  
 C AIRBORNE ELECTROMAGNETIC DATA.  
 C QUADRATIC PROGRAMMING APPROACH.  
 C SMOOTH INVERSION

```

C IMPLICIT DOUBLE PRECISION (A-H, 0-Z)
PARAMETER (NXT=200, NTRUNK=100, NL0DP=R, NOD=40, NPP=30)           INV00010
DIMENSION FKERN(NOD,NPP), DEL2H(NDD), AMPDER(NXT), ZH0(NXT)          INV00020
DIMENSION XSYS(NDD), ZSYS(NDD), CALC(NDD), CALC(NDD)                  INV00030
COMMON /DATA/NRESP, DAT(NOD), SD(NDD)                                     INV00040
COMMON /MODEL/NPT, ZH1(NPP), DM(NDD), LJMP(NPP)                         INV00050
COMMON /KY/AKY(20)                                                       INV00060
COMMON /FCM/ZH0, XSYS, ZSYS, AMPDER, NM, IREC, AKDEL                   INV00070
COMMON KYE, NSYS, NST, XDEL, TRDIS                                       INV00080
OPEN (UNIT=3, FILE='invhz.dat')                                           INV00090
OPEN (UNIT=4, FILE='invhz.out')                                         INV00090
READ (3,*), NSYS, IREC, NST, NPT, NRESP, NITER                          INV00100
READ (3,*), XDEL, TRDIS, ERR, PMU                                       INV00110
READ (3,*), NST, XDEL, TRDIS, ERR, PMU                                   INV00120
READ (3,*), (ZH1(I), I=1, NPT)                                         INV00130
READ (3,*), (XSYS(I), ZSYS(I), DAT(I), CALC(I)), I=1, NRESP            INV00140
READ (3,*), (SD(I), I=1, NRESP)                                         INV00150
READ (3,*), (DAT(I), I=1, NPT)                                         INV00160
READ (3,*), (LJMP(I), I=1, NPT)                                         INV00170
IF (IREC.EQ.2) THEN
  DO 3 I=1, NRESP
    DAT(I)=CALC(I)
  ENDIF
3
C OUTPUT THE INPUT DATA
C
IF (NSYS.EQ.1) WRITE(4,101)
IF (NSYS.EQ.2) WRITE(4,102)
IF (NSYS.NE.1 .AND. NSYS.NE.2) PAUSE 'BAD INPUT NSYS'
IF (IREC.NE.1 .AND. IREC.NE.2) PAUSE 'BAD INPUT IREC'
WRITE(4,104) TRDIS, XDEL, ERR
WRITE(4,103) NST, NPT, NXT, NRESP, NTRUNK, NL0DP, IREC, NITER
WRITE(4,105) (ZH1(I), I=1, NPT)
WRITE(4,106) (ZSYS(I), I=1, NPT)
WRITE(4,107) (NM(I), I=1, NRESP)
3
C ASSIGN THE KY HARMONICS
C
CALL HARMDC(KYE, NM, AKDEL, AKY)                                         INV00180
KK=KK+1
CONTINUE
1001
C CALL THE SMOOTH INVERSION ROUTINE
CALL OCCAM1(1,ERR,TOBT,0,NIT,STEPSZ,KONV,4,PMU)                         INV00190
WRITE(4,11) (ZH1(I), I=1, NPT)
WRITE(4,12) (NM(I), I=1, NRESP)
IF (TOBT.LT.ERR) THEN
  WRITE(4,13)
STOP
ELSE
  INV00200
  INV00210
  INV00220
  INV00230
  INV00240
  INV00250
  INV00260
  INV00270
  INV00280
  INV00290
  INV00300
  INV00310
  INV00320
  INV00330
  INV00340
  INV00350
  INV00360
  INV00370
  INV00380
  INV00390
  INV00400
  INV00410
  INV00420
  INV00430
  INV00440
  INV00450
  INV00460
  INV00470
  INV00480
  INV00490
  INV00500
  INV00510
  INV00520
  INV00530
  INV00540
  INV00550
  INV00560
  INV00570
  INV00580
  INV00590
END

```

```

C TOBT = RMS MISFIT OF NEW MODEL RESPONSE.                                INV01800
C NIT = NUMBER OF PREVIOUS CALLS TO OCCAM1 DURING THIS INVERSION      INV01810
C STEPSZ = SUM OF SQUARES OF THE CHANGES IN THE MODEL PARAMETERS       INV01820
C KONV = STATUS FLAG:                                                 INV01830
C   0 = NORMAL EXIT FOR A SUCCESSFUL ITERATION,                         INV01840
C     1 = A PERFECTLY SMOOTH MODEL HAS BEEN FOUND, FOR THE REQUIRED TOLERANCE INV01850
C     2 = CONVERGENCE PROBLEMS. UNABLE TO FIND A MODEL WITH AN R.M.S. MISFIT INV01860
C       LESS THAN OR EQUAL TO THAT OF THE INITIAL MODEL.                  INV01870
C UM = THE MU VALUE USED AT THE MINIMUM OF THE MISFIT IN THIS ITERATION INV01880
C
C SUBROUTINES REQUIRED AND SUPPLIED:                                     INV01890
C
C MAKDEL, A SUBROUTINE WHICH CREATES THE ROUGHENING MATRIX             INV01900
C TOFMU(AMU), A FUNCTION WHICH RETURNS THE RMS MISFIT OF THE RESPONSE    INV01910
C OF THE MODEL CONSTRUCTED USING THE LAGRANGE MULTIPLIER AMU.           INV01920
C CALLS CHOLIN, CHOLSL, FORMOD, ANORM.                                 INV01930
C
C INITM, TRMULT, MULT AND ANORM, SUBROUTINES FOR SIMPLE MATRIX OPERATIONS INV01940
C FMIN, A SUBROUTINE WHICH MINIMISES A UNIVARIATE FUNCTION            INV01950
C FRONT, A SUBROUTINE WHICH FINDS THE ROOT OF A UNIVARIATE FUNCTION    INV01960
C MIN, RM, A SUBROUTINE WHICH BRACKETS A UNIVARIATE MINIMUM            INV01970
C
C SUBROUTINES WHICH MUST BE SUPPLIED BY THE USER:                      INV01980
C FORMOD(NP,ND,PW,DP,DW) COMPUTES THE FORWARD FUNCTION FOR MODEL PM()    INV01990
C THE DATA PARAMETERS DP() AND RETURNS IT IN DM().                     INV02000
C FORDIV(NP,ND,PW,DP,DW,WJ), COMPUTES THE FORWARD FUNCTION AS DOES FORMIN INV02010
C BUT ALSO RETURNS THE MATRIX OF PARTIALS, WJ(ND,NP).                  INV02020
C
C PARAMETERS ND AND NPP SHOULD BE SET TO THE MAXIMUM DIMENSIONS OF THE INV02030
C DATA AND PARAMETER VECTORS, RESPECTFULLY. DON'T FORGET TO ADJUST INV02040
C THEM IN TOFMU, MAKDEL, BLOCKDATA AND ANY I/O SUBROUTINES.           INV02050
C
C NOTE THAT DOUBLE PRECISION IS USED THROUGHOUT. SOME COMPILERS WILL REINV02060
C EXTERNAL TOFMU TO BE DECLARED IN OCCAM1'S CALLING PROGRAM.          INV02070
C
C IMPLICIT DOUBLE PRECISION (A-H, O-Z)
C PARAMETER (ND = 40, NPP = 30)
C COMMON /DATA/ ND,D(ND),SD(ND)
C COMMON /MODEL/ NP,PW(NPP),DM(ND),LJMP(NPP)
C /RESULT/ IS USED TO CARRY INFO IN AND OUT OF TOFMU AND STORE LAST INV02110
C VALUE OF MU USED.
C COMMON /RESULT/ PTP(NPP,NPP),WJTWJ(NPP,NPP),WJTWD(NPP),PM2(NPP),
C • PM1, NFOR, NITER, RLAST, IFFTOL INV02120
C DIMENSION WJ(ND,ND),RLST(ND,ND),DHAT(ND),WK(NPP)                   INV02130
C EXTERNAL TOFMU                                         INV02140
C
C ON FIRST ENTRY CREATE TRANS(P).P', WHERE P IS THE ROUGHENING MATRIX OR INV02150
C ROUGHENING MATRIX SQUARED, AND SET MU TO AN ARBITRARY (LARGE) VALUE. INV02160
C
C IF (NITER .EQ. 0) THEN                                           INV02170
C   CALL MAKDEL(1TRUF)                                              INV02180
C   PWU = 10000.                                                       INV02190
C   PMU=UM
C   RLAST = 10000.
C   KONV = 0
C END IF
C
C FRAC CONTROLS THE STEP SIZE; NORMALLY WILL REMAIN AT 1.0 UNLESS WE HAVE INV02200
C CONVERGENCE PROBLEMS
C   FRAC = 1.0
C CALCULATE THE MATRIX OF PARTIALS AND MODEL RESPONSE                INV02210
C   CALL FORDIV(NP,ND,PW,DM,WJ)                                         INV02220
C   WRITE(IOUT,11) (DM(I),I=1,ND)                                         INV02230
C

```

```

10      ZH2(I) = ZH1(I)
      ZH2(K) = ZH1(K)*0.2
      CALL FORMOD(NPNT,NRESP,ZH2,CALC2)
      DO 30 I=1,NRESP
      WJ(I,K) = (CALC2(I)-CALC(I))/0.2
30      CONTINUE
      K=K+1
      IF (K.LE.NPT) GOTO 1001
      DO 61 I=1,NRESP
      C       WRITE(*,60) (WJ(I,J), J=1,NPT)
      C61     CONTINUE
      60     FORMAT(4X,'INVERSION KERNEL',/(6(1PE14.4)))
      RETURN
      END
C***** SUBROUTINE OCCAM1(IRUF,TOLREQ,T0BT,IBUG,NIT,STEPSZ,KONV,IOUT,UM)
C
C MODIFIED VERSION OF OCCAM1
C OCCAM1 EXECUTES ONE ITERATION OF A ONE DIMENSIONAL SMOOTH MODEL FINDFRINV01380
C REFERENCE: CONSTABLE, PARKER & CONSTABLE, 1987: GEOPHYSICS 52, 289-300 INV01390
C S. CONSTABLE, MARCH 1986, S.I.O., LA JOLLA, CA 92093, U.S.A. (VERSION INV01400
C OCTOBER 1987, (VERSION INV01420
C
C IF YOU OBTAIN THIS CODE FROM A THIRD PERSON, PLEASE SEND YOUR NAME AND INV01440
C TO S. CONSTABLE. YOU WILL THEN RECEIVE UPDATES, NEWS ON BUGS, ETC. INV01460
C
C ON INPUT:
C /DATA/ CONTAINS
C   ND = NUMBER OF DATA
C   D(ND) = VECTOR OF DATA VALUES
C   SD(ND) = VECTOR OF ABSOLUTE STANDARD ERRORS IN THE DATA
C   DP(ND,4) = MATRIX CONTAINING UP TO FOUR PARAMETERS ASSOCIATED WITH INV01530
C   EACH DATUM (RANGE, FREQUENCY, DATA TYPE ETC)
C   NPD = NUMBER OF PARAMETERS ASSOCIATED WITH EACH DATUM (E.G. FOR FRINV01560
C   THUS LJMP = 4,10,0
C   NPD = 1, FOR FREQ. AND RANGE ND = 2)
C
C /MODEL/ CONTAINS
C   NP = NUMBER OF MODEL PARAMETERS, USUALLY THE NUMBER OF LAYERS INV01490
C   PM(NP) = VECTOR OF INITIAL MODEL PARAMETERS, USUALLY LOG10(LAYER INV01500
C   LJMP(NP) = A VECTOR DESCRIBING PLACES WITHIN THE MODEL TO RELAX TIME INV01510
C   SMOOTHNESS CONSTRAINT, IN MONOTONIC ORDER FOLLOWED BY A ZERO. INV01520
C   INV01530
C   INV01540
C   INV01550
C   INV01560
C   INV01570
C   INV01580
C   INV01590
C   INV01600
C   INV01610
C   INV01620
C   INV01630
C   INV01640
C   INV01650
C   INV01660
C   INV01670
C   INV01680
C   INV01690
C   INV01700
C   INV01710
C   INV01720
C   INV01730
C   INV01740
C   INV01750
C   INV01760
C   INV01770
C   INV01780
C   INV01790
C
C ON OUTPUT:
C /MODEL/ CONTAINS
C   PM(NP) = VECTOR OF UPDATED MODEL PARAMETERS
C   DM(ND) = VECTOR CONTAINING RESPONSE OF NEW MODEL

```

```

165      WK(I) = PM2((I) - PM2(I-1))
      ELSE
      DO 170 I = 2,N'-1
         WK(I) = PM2((I+1) - 2.*PM2(I) + PM2(I-1))
      170     WK(NP) = 0.0
      END IF
C REMOVE ENTRIES IN ROUGHNESS VECTOR WHERE JUMPS ARE ALLOWED
      I = 1
      IF (LJMP(I).NE.0) THEN
         WK(LJMP(I)) = 0.0
      176     GOTO 176
      END IF
      RUF = ANORM(NP,WK)
C IF WE HAVE ATTAINED THE INTERCEPT BUT THE MODEL IS GETTING ROUGHER
C WE HAVE PROBLEMS WITH CONVERGENCE.
C SAVE NEW MODEL AND COMPUTE STEP SIZE
      DO 180 I = 1,NP
         WK(I) = PM2(I) - PM(I)
         PM(I) = PM2(I)
180     STEPSZ = ANORM(NP,WK)
         STEPSZ = SQRT(STEPSZ/NP)
         WRITE(IOUT,'(A)') 'STEPSIZE IS = ',STEPSZ
         WRITE(IOUT,'(A)') 'ROUGHNESS IS = ',RUF
         NITER = NITER + 1
         RETURN
      END

C*****SUBROUTINE MAKDEL(IRUF)
C*****MAKDEL CONSTRUCTS TRANS(DEL).DEL FOR 1ST OR 2ND DERIVATIVE ROUGHNESS
C ON INPUT:
C   IRUF = 1 FOR 1ST DERIVATIVE ROUGHNESS
C   2 FOR 2ND DERIVATIVE ROUGHNESS
C /MODEL/ CONTAINS
C   LJMP = ARRAY OF LAYER LOCATIONS WHERE A JUMP IN RESISTIVITY IS ALLOWED
C   TERMINATED BY A ZERO
C IMPLICIT DOUBLE PRECISION (A-H, O-Z)
PARAMETER (NDD = 40, NPP = 30)
COMMON /MODEL/ NP,PM(NPP),DM(NDD),LJMP(NPP)
COMMON /RESULT/ PTP(NPP,NPP),WTWJ(NPP,NPP),WTWD(NPP),PM2(NPP),
• PMU,NFOR,NITER,FRAC,RLAST,IFFTOL
DIMENSION DEL(NPP,NPP)

C MAKE PARTIALS MATRIX
CALL INITW(NPP,NP,NP,DEL)
DO 180 I = 2,NP
      DEL(I,I-1) = -1.
      DEL(I,I) = 1.
180     C REMOVE ANY ENTRIES WHERE MODEL IS ALLOWED TO JUMP
      I = 0
      I = I+1
      N = LJMP(I)
C CANNOT REMOVE AIR/ EARTH INTERFACE (N=1):
      IF (N .EQ. 1) GOTO 20
      IF (I.NE.NP+1 .AND. N.NE.0) THEN

```

```

11 FORMAT(4X,'COMPUTED DATA',/,5(1PE14.4))
C CALC MISFIT VECTOR AND MISFIT
DO 80 I = 1,ND
  DD(I) = (D(I) - DM(I))/SD(I)
80  CHI0 = ANORM(ND,DD)
  TOL0 = SQRT(CHI0/ND)
  IF (NITER .EQ. 0) THEN
    WRITE (IOUT,*) 'STARTING R.M.S. = ',TOL0
  END IF
C #EIGHT THE PARTIALS MATRIX
  DO 70 I = 1,ND
    DO 70 J = 1,NP
      WJ(I,J) = WJ(I,J)/SD(I)
70  C FORM W.J.TRANS(W.J)
    CALL TRMULT(ND,ND,NPP,NP,WJ,WJTW)
C FORM THE WEIGHTED, TRANSLATED DATA AND PREMULTIPLY BY TRANS (W.J)
    CALL MULT(ND,ND,NPP,NP,WJ,PW,DHAT)
  DO 80 I = 1,ND
    DHAT(I) = DD(I) + DHAT(I)
    CALL TRMULT(ND,ND,NPP,NP,WJ,DHAT,WJTW)
C PRODUCE THE MISFIT FUNCTION IF REQUIRED
    IF (TIBUG .EQ. 1) THEN
      WRITE (IOUT,*) 'MISFIT AS A FUNCTION OF MU'
      DO 100 K = 18,1,-1
        AMU = 10.0*(FLOAT(K)/2. - 1.)
        T = TOFMU(AMU)
        IF (T .GE. 1.0E+09) GOTO 110
        WRITE (IOUT,*) AMU,T
      END IF
      CONTINUE
100   WRITE (IOUT,*) ''
      WRITE (IOUT,*) '** ITERATION ',NITER+1,' *'
C THE NEXT BLOCK OF CODE CONTROLS THE SELECTION OF THE LAGRANGE MULTIPLIER
C PMU
110   IF(TOL = 0)
120   FIND MINIMUM
    CALL MINBRK(AMU1,AMU2,AMU3,TAMU1,TAMU2,TAMU3,TOFMU)
    WRITE (IOUT,*) 'AMU1',AMU1,'MISFIT',TAMU1
    WRITE (IOUT,*) 'AMU2',AMU2,'MISFIT',TAMU2
    WRITE (IOUT,*) 'AMU3',AMU3,'MISFIT',TAMU3
    TOBT = FMIN(AMU1,AMU2,AMU3,TAMU2,TOFMU,PMU)
    PMU = AMU2
    TOBT = TAMU2
C COMPUTE THE MODEL PARAMETERS (AGAIN) AT WHICH MINIMUM MISFIT WAS
OBTAINED. TORDUM IS DUMMY
    TORDUM=TOFMU(PMU)
    WRITE (IOUT,*) 'MINIMUM TOL IS AT MU = ',PMU
    WRITE (IOUT,*) 'AND IS = ',TOBT
    WRITE (IOUT,*) 'USING ',NFOR, 'EVALUATIONS OF FUNCTION'
C IF THE NEW MINIMUM TOLERANCE IS GREATER THAN THE TOLERANCE FROM THE
C PREVIOUS MODEL, WE ARE HAVING CONVERGENCE PROBLEMS.
C ••FIND LAGRANGE MULTIPLIER SELECTION
    C COMPUTE ROUGHNESS
    WK(1) = 0.0
    IF (TIRUF .EQ. 1) THEN
      DO 186 I = 2,NP

```

```

PD (I) = PM(I)
CVEC(I) = WJTWD(I)
CONTINUE
10 CALL QUAD(PD ,NPP , NPP , NPP , HESS ,CVEC)
DO 16 I=1,NP
16 PM2(I) = PD(I)
C CUR STEP SIZE IF NECESSARY
IF (FRAC .LT. 0.999) THEN
DO 30 I = 1,NP
30 PM2(I) = PM(I) + FRAC*(PM2(I)-PM(I))
END IF
C CALC. MODEL RESPONSE AND MISFIT
CALL FORMOD(NP,ND,PM2,DM)
DO 40 I = 1,ND
40 WK(I) = (D(I) - DM(I))/SD(I)
CHI = ANORM(ND,WK)
TOFMU = SQRT(CHI/ND)
RETURN
C
SUBROUTINE QUAD(PD ,NRWHL,NCOLH,N,HESS,CVEC)
IMPLICIT REAL*8 (A-H,0-Z)
PARAMETER (ITMAX=60, MSGVL=1, NROWA=1,
           NCLIN=0, NPP=50)
1. BIGBND=1.E+10, LWORK=60, LWORK=1980, NCLIN=0, NPP=50
REAL*8 A(1,NPP), BL(NPP), BU(NPP), CVEC(N),
1 HESS(NRWHL,NCOLH), CLAMDA(NPP), WORK(LWORK), IWORK(LWORK),
2 ISTATE(NPP), PD(N)
LOGICAL COLD, LP, ORTHOG
EXTERNAL QPHESS
DATA NOUT/7/
CALL X04ABF(1,NOUT)
COLD=.TRUE.
LP=.FALSE.
ORTHOG=.FALSE.
NCTOTL=N+NCLIN
DO 10 I=1,N
10 BL(I)=0.
BL(I)=20.
BU(I)=20.
FEATOL(I)=0.02
1A CONTINUE
1A BU(1)=0.
BU(N)=0.
IFAIL=0.
IFAIL=0.
C QUADRATIC PROGRAMMING
C CALL E04NAF(ITMAX,MSGVL,N,NCLIN,NCTOTL,NRWHL,NCOLH,
C 1. BIGBND,A,BL,BU,CVEC,FEATOL,HESS,QPHESS,
C 2. COLD,LP,ORTHOG,PD,ISTATE,ITER,OUT,J,
C . CLAMDA,IWORK,LWORK,WORK,LWORK,ITAIL)
C . CALL VE04A(N,HESS,NRWHL,CVEC,BL,BU,PD,Q,IWORK,K,WORK)
IF (IFAIL.GT.0) THEN
  WRITE(4,20) IFAIL
  STOP
ENDIF
20 FORMAT('E04NAF TERMINATED WITH IFAIL :: ', I3)
END
SUBROUTINE QPHESS(N, NRWHL, NCOLH, JTHCOL, HESS, X, HX)
IMPLICIT REAL*8 (A-H,0-Z)
INTEGER JTHCOL,N,NCOLH,NRWH
REAL*8 HESS(NRWHL,NCOLH), HX(N), X(N)

```

```

      DEL(N,N-1) = 0.          INV03600
      DEL(N,N) = 0.           INV03610
      GOTO 20                 INV03620
END IF
IF (LRFU .EQ. 2) THEN     INV03630
  CALL MULT(NPP,NP,NPP,NP,NP,DEL,DEL,PTP)
  DO 30 I = 1,NP          INV03640
    DO 30 J = 1,NP          INV03650
      DEL(J,I) = PTP(J,I)  INV03660
    END IF
  C FORM TRANS(DEL), DEL           INV03670
  CALL TRMULT(NPP,NP,NPP,NP,NP,DEL,DEL,PTP)
  RETURN                   INV03680
END

C BLOCKDATA BLOCK           INV03740
IMPLICIT DOUBLE PRECISION (A-H, 0-Z)   INV03750
PARAMETER (NDD = 40, NPP = 30)           INV03760
COMMON /RESULT/ PTP(NPP,NPP),WJTWJ(NPP,NPP),WJTWD(NPP),PM2(NPP),
  • PMU,NFOR,NITER,FRAC,RLAST,IFFTOL   INV03770
  DATA NITER /0/                  INV03780
END

C FUNCTION TOFMU(AMU)           INV03840
FUNCTION TOFMU(AMU)                  INV03850
*****                                         INV03860
C FUNCTION TOFMU RETURNED THE RMS MISFIT OF THE RESPONSE OF A MODEL CONSTINV03880
C USING THE GIVEN VALUE OF LAGRANGE MULTIPLIER           INV03870
C S. CONSTABLE, MARCH 1988, S.I.O., LA JOLLA, CA 92093, U.S.A.   INV03890
C
C ON INPUT:          INV03910
C AMU = LAGRANGE MULTIPLIER          INV03920
C THE MODEL IS ALSO A FUNCTION OF THE ARRAYS PASSED IN COMMON BLOCK /RESINV03940
C ON OUTPUT          INV03950
C TOFMU = R.M.S. MISFIT OR 1.0E+10 IF CHOLESKY DECOMPOSITION FAILED   INV03960
C /MODEL/ CONTAINS THE MODEL WHICH PRODUCES THE MISFIT TOFMU, AS WELL INV03970
C AS ITS RESPONSE          INV03980
C SUBROUTINES USED:          INV03990
C CHOLIN, CHOLSL ARE R.L. PARKER'S SUBROUTINES TO PERFORM CHOLESKY DEINV04010
C AND THEN SOLVE A LINEAR SYSTEM BY BACK SUBSTITUTION.          INV04020
C ANORM, FORMOD ARE EXPLAINED IN OCCAM1          INV04030
C
C IMPLICIT DOUBLE PRECISION (A-H, 0-Z)          INV04040
PARAMETER (NDD = 40, NPP = 30)          INV04050
COMMON /DATA/ ND, D(NDD), SD(NDD)        INV04060
COMMON /MODEL/ NP, PM(NPP), DM(NDD), LJMP(NPP)          INV04070
COMMON /RESULT/ PTP(NPP,NPP), WJTW(NPP,NPP), WJTWD(NPP), PM2(NPP),          INV04080
  • PMU,NFOR,NITER,FRAC,RLAST,IFFTOL          INV04090
  DIMENSION WK(NDD)          INV04100
  REAL•8 PD(NPP), HESS(NPP,NPP), CVEC(NPP)          INV04110
  INV04120
  INV04130
  INV04140
  INV04150
  INV04160
  INV04170
  INV04180
  INV04190

C NFOR = NFOR + 1
C ADD AMU,TRANS(PARTIAL).PARTIAL TO TRANS(W,J).W,J
DO 20 I = 1,NP
  DO 20 J = 1,NP
    HESS(I,J) = AMU•PTP(I,J) + WJTWJ(I,J)
  DO 10 I = 1,NP

```

```

12  CONTINUE
      RETURN
END

C
C   SUBROUTINE TRMULT(MAD,MA,NAD,NA,NB,A,B,C)
C   MULTIPLIES THE TRANSPOSE OF A 2D MATRIX BY ANOTHER MATRIX
C   IMPLICIT DOUBLE PRECISION (A-H, 0-Z)
C   DIMENSION A(MAD,NA),B(MAD,NB),C(NAD,NB)
DO 12 I = 1, NA
DO 12 J = 1, NB
  CIJ = 0.0
  DO 10 K = 1, MA
    CIJ = A(K,I)*B(K,J) + CIJ
  10  C(I,J) = CIJ
  12  RETURN
END

C
C   SUBROUTINE MINBRK(AX,BX,CX,FA,FB,FC,FUNC)
C   MINBRK BRACKETS A UNIVARIATE MINIMUM OF A FUNCTION. TO BE USED PRIOR
C   TO BE USED PRIOR TINY=1.E-21
C   ON INPUT:
C   AX, BX = TWO DISTINCT ESTIMATES OF THE MINIMUM'S WHEREABOUTS
C   FUNC = THE FUNCTION IN QUESTION
C   ON OUTPUT:
C   AX,BX,CX = THREE NEW POINTS WHICH BRACKET THE MINIMUM
C   FA,FB,FC = FUNC(AX), FUNC(BX) ETC.
C
C   IMPLICIT DOUBLE PRECISION (A - H, 0 - Z)
C   PARAMETER (GOLD=1.618034, GLIMIT=100., TINY=1.E-21)
C
      DUM = AX
      AX = BX
      BX = DUM
      DUM = FB
      FB = FA
      FA = DUM
  ENDIF
      CX = BX + GOLD*(BX - AX)
      FC = FUNC(CX)
      IF (FB.GE.FC) THEN
        R = (BX - AX)*(FB - FC)
        Q = (BX - CX)*(FB - FA)
        U = BX - ((BX-CX)*Q-(BX-AX)*R)/(2.*SIGN(MAX(ABS(Q-R), TINY), Q-R))
        ULIM = BX + GLIMIT*(CX - BX)
        IF ((BX - U)*(U - CX) .GT. 0.) THEN
          FU = FUNC(U)
          IF (FU.LT.FC) THEN
            AX = BX
            FA = FB
            BX = U
          ENDIF
        ENDIF
      ENDIF
    ENDIF
    IF (FU.LT.FC) THEN
      AX = BX
      FA = FB
      BX = U
    ENDIF
  ENDIF
END

```

```
      INTEGER I,J
      DU B0 1:1,N
      HX(I) = B0
      DO 100 J=1,N
        DU B0 I=1,N
        HX(I)=HX(I)+MESS(I,J)*X(J)
 100  CONTINUE
      END
C
C
C      FUNCTION ANORM(N,D)
C      RETURNS THE SQUARE OF THE EUCLIDEAN NORM OF A VECTOR
C      IMPLICIT DOUBLE PRECISION (A-H, 0-Z)
      DIMENSION D(N)
      ANORM = B0
      DO 10 I = 1,N
        ANORM = ANORM + D(I)*D(I)
 10   CONTINUE
      RETURN
      END
C
C      SUBROUTINE INITM(MD,M,N,A)
C      ZEROS A 2D MATRIX
      IMPLICIT DOUBLE PRECISION (A-H, 0-Z)
      DIMENSION A(MD,N)
      DO 10 I = 1,M
        DO 10 J = 1,N
          A(I,J) = B0
 10   RETURN
      END
C
C      SUBROUTINE MULT(MAD,MA,NAD,NA,NB,A,B,C)
C      MULTIPLIES TWO 2D MATRICES
      IMPLICIT DOUBLE PRECISION (A-H, 0-Z)
      DIMENSION A(MAD,NA),B(NAD,NB),C(MAD,NB)
      DO 12 I = 1,MA
        DO 12 J = 1,NB
          C(IJ) = B0
 12   DO 10 K = 1,NA
    C(IJ) = A(I,K)*B(K,J) + C(IJ)
 10   RETURN
      END
C
C      SUBROUTINE DMULT(MAD,MA,NA,DIAG,A,B)
C      MULTIPLIES A 2D MATRIX BY A DIAGONAL MATRIX
      IMPLICIT DOUBLE PRECISION (A-H, 0-Z)
      DIMENSION DIAG(MA),A(MAD,NA),B(MAD,NA)
      DO 12 J = 1,NA
        DO 11 I = 1,WA
          B(I,J) = DIAG(I)*A(I,J)
 11   CONTINUE
 12   RETURN
      END
C
C      SUBROUTINE DMULTD(MA,NA,DIAG,A,B)
C      MULTIPLIES A 2D MATRIX BY A DIAGONAL MATRIX
      IMPLICIT DOUBLE PRECISION (A-H, 0-Z)
      DIMENSION DIAG(MA),A(MAD,NA),B(MAD,NA)
      DO 12 J = 1,NA
        DO 11 I = 1,WA
          B(I,J) = DIAG(I)*A(I,J)
 11   CONTINUE
 12   RETURN
      END
```

```

Y = BX
W = V
X = V
E = 0.
FX = FBX
FV = FX
FW = FX
DO 11 ITER = 1, ITMAX
  XM = 0.5*(A + B)
  TOL1 = TOL*ABS(X) + ZEPS
  TOL2 = 2.*TOL1
  IF (ABS(X - XM).LE. (TOL2 - .5*(B - A))) GOTO 3
  IF (ABS(E).GT. TOL1) THEN
    R = (X - W)*(FX - FV)
    Q = (X - V)*(FX - FW)
    P = (X - V)*Q - (X - W)*R
    Q = 2.*(Q - R)
    IF (Q.GT.0.) P = -P
    Q = ABS(Q)
    ETEMP = E
    E = D
    IF (ABS(P).GE. ABS(.5*Q*ETEMP).OR.P.LE.Q*(A - X)).OR.
      P.GE.Q*(B - X)) GOTO 1
    D = P/Q
    U = X + D
    IF (U - A.LT.TOL2 .OR. B - U.LT.TOL2) D = SIGN(TOL1,XM - X)
    GOTO 2
  ENDIF
  1   IF (X.GE.XM) THEN
    E = A - X
    ELSE
    E = B - X
    ENDIF
    D = CGOLD*E
    IF (ABS(D).GE. TOL1) THEN
      U = X + D
    ELSE
      U = X + SIGN(TOL1,D)
    ENDIF
    FU = F(U)
    IF (FU.LE.FX) THEN
      IF (U.GE.X) THEN
        A = X
      ELSE
        B = X
      ENDIF
      ENDIF
      V = W
      FV = FW
      W = X
      FW = FX
      X = U
      FX = FU
    ELSE
      IF (U.LT.X) THEN
        A = U
      ELSE
        B = U
      ENDIF
      IF (FU.LE.FW .OR. W.EQ.X) THEN
        Y = W
      ENDIF
    ENDIF
  ENDIF
  2

```

```

FB = FU
GO TO 1
ELSE IF (FU.GT.FB) THEN
CX = U
FC = FU
GO TO 1
ENDIF
U = CX + GOLD*(CX - BX)
FU = FUNC(U)
FU = FUNC(U)
IF (FU.LT.FC) THEN
BX = CX
CX = U
U = CX + GOLD*(CX - BX)
FB = FC
FC = FU
FU = FUNC(U)
ENDIF
ELSE IF ((U - ULIM)*(ULIM - CX) .GE. 0.) THEN
U = ULIM
FU = FUNC(U)
ELSE
U = CX + GOLD*(CX - BX)
FU = FUNC(U)
ENDIF
AX = BX
BX = CX
CX = U
FA = FB
FB = FC
FC = FU
GO TO 1
ENDIF
IF (AX.LT.0.) AX=0.
IF (CX.LT.0.) CX=0.
RETURN
END

C     FUNCTION FMIN(AX,BX,CX,F,BX,F,TOL,XMIN)
C     FMIN RETURNS THE MINIMUM VALUE OF A FUNCTION
C     ON INPUT:
C     AX,BX,CX = INDEPENDENT VARIABLE WHICH BRACKET THE MINIMUM
C     FUNCTION (USUALLY AVAILABLE FROM THE BRACKETING PROCEDURE)
C     F = FUNCTION IN QUESTION
C     TOL = FRACTIONAL TOLERANCE REQUIRED IN THE INDEPENDENT VARIABLE
C     ON OUTPUT:
C     XMIN = ABSISSA OF MINIMUM
C     FMIN = F(XMIN)
C
C     IMPLICIT DOUBLE PRECISION (A - H, 0 - I)
C     PARAMETER (ITMAX=100,CGOLD=.3819880,ZEPS=1.0E - 10)
C     A = MIN(AX,CX)
C     B = MAX(AX,CX)

```

```

CALL CUBDER(NPT+2,XDEL,ZSURF,XDER)
DO 10 I=NXT,1,-1
  IF (I.GE.NE.'OR. I.LT.NST) THEN
    ZSURF(I)=0.0
    XDER(I)=0.
    AMPDER(I)=1.
    GOTO 10
  END IF
  ZSURF(I)=ZSURF(I-NST+1)
  XDER(I)=XDER(I-NST+1)
  AMPDER(I)=SQRT(1.0*XDER(I)*XDER(I))
  CONTINUE
  WRITE(4,50) (ZSURF(I), I=1,NXT)
  WRITE(4,60) (XDER(I), I=1,NXT)
  WRITE(4,70) (AMPDER(I), I=1,NXT)
  FORMAT(4X,'ZSURF: ',/,'4X,(10F7.3)')
  FORMAT(4X,'XDER: ',/,'4X,(10F7.3)')
  FORMAT(4X,'AMPDER: ',/,'4X,(10F7.3)')
  RETURN
END

C
C SUBROUTINE HNPRIM(K,KS,ZSURF,XDER,AMPDER,XSYS,ZSYS,NTR)
C COMPUTE THE NORMAL COMPONENT OF THE MAGNETIC FIELD
C
C      IMPLICIT DOUBLE PRECISION (A-H, 0-Z)
C      PARAMETER (PI=3.1415926)
C      DIMENSION ZSURF(1),XDER(1),AMPDER(1),XSYS(1),ZSYS(1)
C      DIMENSION HPN(120,20)
C      COMMON /KY/AKY(20)/HN/HPN
C      COMMON KY,NSYS,NST,XDEL,TRDIS
C      P12=PI*2.
C      DO 10 J=KS,NTR+KS-1
C        M=J-KS+1
C        XD=(J-1)*XDEL-XSYS(K)+TRDIS/2.
C        ZD=ZSURF(J)-ZSYS(K)
C        RHO=SQRT(XD*XD+ZD*ZD)
C        D=RHO*RHO*AMPDER(J)*PI2
C        IF (D.EQ.0.) PAUSE 'BAD HPN'
C        IF (NSYS.EQ.1) THEN
C          GEOM1=(-XDER(J)*XD+ZD)*XD/D
C          GEOM2=(-(XD*XD-ZD*ZD)*XDER(J)+2.0*(XD*ZD))/D
C        ELSE
C          GEOM1=(-XDER(J)*XD+ZD)*ZD/D
C          GEOM2=((ZD*ZD-XD*XD)-XDER(J)*2.0*XD*ZD)/D
C        ENDIF
C        D0 20 I=1,KYE
C        WK=AKY(I)*PI2
C        RKY=RHO*WK
C        IF (I.GT.1) THEN
C          HPN(M,I)=(GEOM1*WK+BESSK0(RKY)+GEOM2*BESSK1(RKY))/RHO*WK
C        ELSE
C          HPN(M,I)=GEOM2/(RHO*RHO)
C        ENDIF
C        CONTINUE
C        WRITE(4,30)(HPN(J,1),J=1,NTR)
C        FORMAT(4X,'HPN: ',/,(5(1PE12.4)))
  END

```

```

FV = FW          INV07190
W = U           INV07200
FW = FU          INV07210
ELSE IF (FU.LE.FV .OR. V.EQ.X .OR. V.EQ.W) THEN
  V = U           INV07220
  FW = FX          INV07230
ENDIF           INV07240
FV = FU          INV07250
RETURN          INV07260
ENDIF           INV07270
INV07280
INV07290
INV07300
INV07310
INV07320
INV07330
INV07340
INV07350
INV07360
INV07370
INV07380
INV07390
INV07400
INV07410
INV07420
INV07430
INV07440
INV07450
INV07460
INV07470
INV07480
INV07490
INV07500
INV07510
INV07520
INV07530
INV07540
INV07550
INV07560
INV07570
INV07580
INV07590
INV07600
INV07610
INV07620
INV07630
INV07640
CONTINUE        INV07650
KS=(XSYS(K)-TRDIS/2.)/XDEL+2.-NTRUNK/2    PAUSE 'BAD INPUT XSYS'
IF (KS.LE.0 .OR. KS.GE.NXT-NTRUNK/2)         CALL HNPROM(K,KS,ZSURF,XDER,AMPER,XSYS,ZSYS,NTRUNK)
CALL HNPROM(K,KS,ZSURF,XDER,AMPER,XSYS,ZSYS,NTRUNK)
CALL KERNEL(K,KS-1,KS1,ZSURF,XDER,AMPER,NTRUNK)
CALL CHARGE(NTRUNK,KYE,XDEL,NLOOP)
CALL FIELD(K,KS,NM,AKDEL,HXS,HZS,XSYS,ZSYS,ZSURF,AMPER,NTRUNK)
IF (IREC.EQ.1) CALC(K)=HXS
IF (IREC.EQ.2) CALC(K)=HZS
KS=1
KS1=KS
IF (K.LE.NRESP) GOTO 1001
RETURN
END

1001
CONTINUE
KS=(XSYS(K)-TRDIS/2.)/XDEL+2.-NTRUNK/2
IF (KS.LE.0 .OR. KS.GE.NXT-NTRUNK/2) PAUSE 'BAD INPUT XSYS'
CALL HNPROM(K,KS,ZSURF,XDER,AMPER,XSYS,ZSYS,NTRUNK)
CALL KERNEL(K,KS-1,KS1,ZSURF,XDER,AMPER,NTRUNK)
CALL CHARGE(NTRUNK,KYE,XDEL,NLOOP)
CALL FIELD(K,KS,NM,AKDEL,HXS,HZS,XSYS,ZSYS,ZSURF,AMPER,NTRUNK)
IF (IREC.EQ.1) CALC(K)=HXS
IF (IREC.EQ.2) CALC(K)=HZS
KS=1
KS1=KS
IF (K.LE.NRESP) GOTO 1001
RETURN
END

SUBROUTINE SURF (NST,NPT,NXT,XDEL,ZSURF,XDER,AMPER)
C   GENERATE THE INFORMATION OF THE ICE-WATER INTERFACE, I.E.,
C   ZSURF, XDER, AMPER
C   IMPLICIT DOUBLE PRECISION (A-H, 0-Z)
C   DIMENSION ZSURF (NXT), XDER (NXT), AMPER (NXT)
NE = NST+NPT
INV07780
INV07790
INV07710
INV07720
INV07730
INV07740
INV07750
INV07760
INV07770
INV07780

```

```

WK=AKY(I)*PI2
IF (I.EQ.1) THEN
  AKERN(J,L,I)= GEOM/RHO
ELSE
  AKERN(J,L,I)= GEOM*WK*BESSK1 (RHO*WK)
ENDIF
CONTINUE
DO 80 J=KE2+1,NTR
  DO 80 L=1,NTR
    IF (J.EQ.L) GOTO 80
    XD=(J-L)*XDEL
    ZD=ZSURF (J+KS)-ZSURF (L+KS)
    RHO=SQRT (XD*XD+ZD*ZD)
    GEM=2.* (AMPDER (L+KS)/AMPDER (J+KS))* ( XD*XDER (J+KS)-ZD) /RHO
    DO 70 I=1,KYE
      WK=AKY(I)*PI2
      IF (I.EQ.1) THEN
        AKERN(J,L,I)= GEOM/RHO
      ELSE
        AKERN(J,L,I)= GEOM*WK*BESSK1 (RHO*WK)
      ENDIF
    CONTINUE
    WRITE(4,90) ( AKERN(40,10,I) , I=1,KYE)
    FORMAT(4X,'KERNEL ,/, (6(1PE12.4)))
    RETURN
  END

C   SUBROUTINE CHARGE (NTR, KYE, XDEL, NL00P)
C   COMPUTE THE CHARGE DISTRIBUTION ON THE SURFACE OF
C   THE SEA WATER
C   IMPLICIT DOUBLE PRECISION (A-H, 0-2)
C   DIMENSION CHAR(120,20),HPN(120,20),AKERN(120,120,20),W1 (120)
C   DIMENSION W2(120)
C   COMMON /KER/AKERN/HN/HPN/CH/CHAR
C   FAC=1.0/(2*3.1415928)
C   I=1
  KK=0
1001 CONTINUE
  DO 10 J=1,NTR
    W1(J)=MPN(J,I)*FAC
  CONTINUE
  DO 20 J=1,NTR
    SUM=0.0
    DO 30 L=1,NTR
      SUM=SUM+W1(L) *AKERN (J,L,I)
    CONTINUE
    W2(J)=FAC* (-SUM*XDEL+MPN(J,I))
  CONTINUE
  DO 40 J=1,NTR
    W1(J)=W2(J)
  KK=KK+1
  IF (KK.LT.NL00P) GOTO 999
  DO 50 J=1,NTR
    CHAR(J,I)=W1(J)
  I=I+1

```

```

RETURN
END

C   SUBROUTINE KERNEL(K,KS,KS1,ZSURF,XDER,AMPDER,NTR)
C   COMPUTE THE KERNEL IN THE INTEGRAL EQUATION
C   AND SAVE IT
C   IMPLICIT DOUBLE PRECISION (A-H, 0-Z)
PARAMETER (PI=3.1415926)
DIMENSION ZSURF(1),XDER(1),AMPDER(1)
DIMENSION AKERN(120,120,120)
COMMON /KER/AKERN/KY/AKY(20)
COMMON KYE,NSYS,NST,XDEL,TRDIS
PI2=PI*2.

DO 1 J=1,NTR
  DO 1 I=1,KYE
    AKERN(J,J,I)=0.0
1 CONTINUE
  IF (K.GT.1) GOTO 30
C COMPUTE THE AKERNEL
1001 CONTINUE
DO 20 J=1,NTR
  DO 20 L=1,NTR
    IF (J.EQ.L) GOTO 20
    XD=(J-L)*XDEL
    ZD=ZSURF(J+KS)-ZSURF(L+KS)
    RHO=SQRT(XD*XD+ZD*ZD)
    GEOM=2.* (AMPDER(L+KS)/AMPDER(J+KS))*( XD*XDER(J+KS)-ZD)/RHO
    DO 10 I=1,KYE
      WK=A KY(I)*PI2
      IF (I.EQ.1) THEN
        AKERN(J,L,I)= GEOM/RHO
      ELSE
        AKERN(J,L,I)= GEOM*WK*BESSK1(RHO*WK)
      ENDIF
    CONTINUE
20 CONTINUE
  RETURN

C   COMPUTE THE UNKNOWN PART OF THE KERNEL
30 CONTINUE
M=KS-KS1+1
KE2=NTR-M
IF (M.LE.0) PAUSE 'BAD INPUT XSYS'
IF (M.GE.NTR) GOTO 1001
DO 40 J=1,KE2
  DO 40 L=1,KE2
    DO 40 I=1,KYE
      AKERN(J,L,I)=AKERN(J+M,L+M,I)
40 CONTINUE
  DO 60 J=1,KE2
    DO 60 L=KE2+1,NTR
      XD=(J-L)*XDEL
      ZD=ZSURF(J+KS)-ZSURF(L+KS)
      RHO=SQRT(XD*XD+ZD*ZD)
      GEOM=2.* (AMPDER(L+KS)/AMPDER(J+KS))*( XD*XDER(J+KS)-ZD)/RHO
      DO 50 I=1,KYE

```

```

RETURN
END

C   SUBROUTINE CUBDER(N,XDEL,YA,YD)
C   COMPUTE THE DERIVATIVES AT EACH NODE USING
C   CUBIC SPLINE.
C   NOTE: N=NPT+2 . ONE POINT ADDED TO EACH END.
C

C   IMPLICIT DOUBLE PRECISION (A-H, 0-Z)
C   DIMENSION XA(60), YA(N), Y2(60), YD(N)
DO 11 I=1,N
  XA(I) = (I-1)*XDEL
  DO 12 I=N-1,2,-1
    YA(I) = YA(I-1)
  1.  YA(I) = 0.
  YA(N) = 0.
CALL SPLINE(XA,YA,N,0.,0.,Y2)
DO 10 I=2,N-1
  XX=XA(I)
  KLO=I
  KHI=I+1
  H=XA(KHI)-XA(KLO)
  A=(XA(KHI)-XX)/H
  B=(XX-XA(KLO))/H
  XD=XA(KHI)-XA(KLO)
  YD(I-1)=(YA(KHI)-YA(KLO))/XD-XD*((3.*A*A-1.)*Y2(KLO)
  *-(3.*B*B-1.)*Y2(KHI))/6.
  * CONTINUE
  DO 14 I=1,N-2
    YA(I)=YA(I+1)
  14  RETURN
END

C   SUBROUTINE CUBSPL(KYE,NK1,AKDEL,AKY,YA,0)
C   CUBIC SPLINE INTERPOLATION BEFORE TAKING THE
C   INVERSE FOURIER TRANSFORM.
C

C   IMPLICIT DOUBLE PRECISION (A-H, 0-Z)
C   DIMENSION AKY(KYE), O(NK1), YA(KYE), Y2(2E)
CALL SPLINE(AKY,YA,KYE,1.E30,1.E30,Y2)
O(1)=YA(1)
DO 10 I=2,NK1
  XX=(I-1)*AKDEL
  KLO=1
  KHI=KYE
  IF (KHI-KLO.GT.1) THEN
    K=(KHI+KLO)/2
    IF (AKY(K).GT.XX) THEN
      KHI=K
    ELSE
      KLO=K
    ENDIF
    GOTO 1
  ENDIF
  H=AKY(KHI)-AKY(KLO)

```

```

C IF (I.L.E.KYE) GOTO 1001
C WRITE(4,22)(CHAR(J,1),J=1,NTR)
C FORMAT(4X,'CHARGE',/(5E14.4))
C RETURN
C END

C SUBROUTINE FIELD(K,KS,NM,AKDEL,HXS,HZS,XSYS,ZSYS,ZSURF,AMPDER,NTR)
C
C COMPUTE THE SECONDARY MAGNETIC FIELD, BOTH
C X AND Z COMPONENTS, EXPRESSED IN PPM OF THE
C RECEIVED PRIMARY FIELD.
C
C IMPLICIT DOUBLE PRECISION (A-H, 0-Z)
C PARAMETER (PI=3.141592)
C DIMENSION AMPDER(1),CHAR(120,20),ZSURF(1),XSYS(1),ZSYS(1),AA(613)
C DIMENSION TEMP1(20),TEMP2(20)
C COMMON /CH/CHAR/KY/AKY(20)
C COMMON KYE,NSYS,NST,XDEL,TRDIS
C R = TRDIS
C XF=R/2
C IF (NSYS.EQ.1) THEN
C   HNORM=1./(2.*PI*R**3)
C ELSE
C   HNORM=-1./(4.*PI*R**3)
C ENDIF
C DO 10 I=1,KYE
C   WK=AKY(I)*PI**2.
C   AZ=0.0
C   AX=0.0
C   DO 20 J=KS,NTR+KS-2
C     M=J-KS+1
C     RH0=SQRT((XSYS(K)-(J-1)*XDEL+XF)**2*(ZSYS(K)-ZSURF(J))**2)
C     IF (I.GT.1) THEN
C       AXZ=2.*0.0*CHAR(M,I)*AMPDER(J)*WK*BESSK1(RH0*WK)/RH0
C     ELSE
C       AXZ=2.*0.0*CHAR(M,I)*AMPDER(J)/(RH0*RH0)
C     ENDIF
C     AZ=(ZSYS(K)-ZSURF(J))*AXZ+AZ
C     AX=(XSYS(K)-(J-1)*XDEL+XF)*AXZ+AX
C 20  CONTINUE
C     TEMP1(I)=AZ*XDEL
C     TEMP2(I)=AX*XDEL
C 10  CONTINUE
C     NK =2.*N'
C     IF (NK*AKDEL .GT. AKY(KYE)) PAUSE 'BAD AKDEL OR AKY'
C     CALL CUB.PL(KYE,NK,AKDEL,AKY,TEMP1,AA)
C     SUM=0.0
C     DO 11 I=2,NK
C       SUM=SUM+AA(I)
C     HZS=(SUM*AA(1)/2.)*AKDEL**2.
C     CALL CUB.PL(KYE,NK,AKDEL,AKY,TEMP2,AA)
C     SUM=0.0
C     DO 12 I=2,NK
C       SUM=SUM+AA(I)
C     HXS=(SUM*AA(1)/2.)*AKDEL**2.
C     HXS=HXS/HNORM*1000000
C     HZS=HZS/HNORM*1000000

```

```

if (abs(x).lt.3.76) then
y=(x/3.76)**2
BESSI0=p1*y*(p3+y*(p4*y*(p5+y*(p6+y*p7)))))
else
ax=abs(x)
y=3.76/ax
BESSI0=(exp(ax)/sqrt(ax))*(q1+y*(q2+y*(q3+y*(q4+y*(q5+
+ y*(q6+y*(q7+y*(q8+y*q9))))))))
endif
return
end

c
c   Function BESSK0(x)
c   ... Returns the modified Bessel function K0(x) for positive x.
c
c   IMPLICIT DOUBLE PRECISION (A-H, 0-Z)
real,y,p1,p2,p3,p4,p5,p6,p7,q1,q3,q4,q5,q6,q7
data p1,p2,p3,p4,p5,p6,p7/.0,57721568d0,.0,42278420d0,.0,23069766d0,
+.0,3488596d-1,.0,262898d-2,.0,1076d-3,.0,74d-6/
data q1,q2,q3,q4,q5,q6,q7/.1,2633141d0,-0,7832358d-1,.0,21895588d-1,
-.0,1032416d-1,.0,587872d-2,-0,261540d-2,.0,53208d-3/
if (x .le. 2.) then
y=x*x/4.0
BESSK0=(-log(x/2.0)*BESSI0(x)+(p1+y*(p2+y*(p3+
+ y*(p4+y*(p5+y*(p6+y*p7)))))))
else
if (x .gt. 4.0) then
BESSK0=0.0
else
y=(2.0/x)
BESSK0=(exp(-x)/sqrt(x))*(q1+y*(q2+y*(q3+y*(q4+y*(q5+
+ y*(q6+y*q7))))))
endif
endif
return
end

c
c   Function BESSI1(x)
c   ... Returns the modified Bessel function I1(x) for any real x.
c
c   IMPLICIT DOUBLE PRECISION (A-H, 0-Z)
real,y,p1,p2,p3,p4,p5,p6,p7,q1,q2,q3,q4,q5,q6,q7,q8,q9
data p1,p2,p3,p4,p5,p6,p7/.0,87890594d0,.0,.61498869d0,
+.0,16084934d0,.0,266873d-1,.0,301632d-2,.0,32411d-3/
data q1,q2,q3,q4,q5,q6,q7,q8,q9/.0,39894228d0,-0,3988024d-1,
-.0,382018d-2,.0,163801d-2,-0,1031555d-1,.0,2282967d-1,
+.0,289531d-1,.0,1787354d-1,-0,420059d-2/
if (abs(x).lt.3.76) then
y=(x/3.76)**2
BESSI1=x*(p1+y*(p2+y*(p3+y*(p4+y*(p5+y*(p6+y*p7)))))))
else
ax=abs(x)
y=3.76/ax
BESSI1=(exp(ax)/sqrt(ax))*(q1+y*(q2+y*(q3+y*(q4+y*(q5+
+ y*(q6+y*(q7+y*(q8+y*q9))))))))
endif

```

```

A=(AKY(KHI)-XX)/H
B=(XX-AKY(KLO))/H
O(1)=A•YA(KLO)+B•YA(KHI)+(A•(A•A-1.)•Y2(KLO)•
   B•(B•B-1.)•Y2(KHI))•(H•H)/8.
   * CONTINUE
   RETURN
END

C   SUBROUTINE SPLINE(X,Y,N,YP1,YPN,Y2)
C   GIVEN ARRAYS X AND Y OF LENGTH N CONTAINING A TABULATED FUNCTION,
C   I.E., YJ=F(XJ), WITH X1<X2<X3...<XN, THIS ROUTINE RETURNS AN ARRAY
C   OF LENGTH N WHICH CONTAINS THE SECOND DERIVATIVES OF THE INTER-
C   POLATING FUNCTION AT THE TABULATED POINTS XJ. NATURAL SPLINE FROM
C   NUMERICAL RECIPES, PRESS ET AL.
C   IMPLICIT DOUBLE PRECISION (A-H, 0-Z)
C   PARAMETER (NMAX=1024)
C   DIMENSION X(N),Y(N),Y2(N),U(NMAX)
C   IF (Y1.GT..99E30) THEN
C     Y2(1)=0.
C     U(1)=0.
C   ELSE
C     Y2(1)=-0.6
C     U(1)=(3./((X(2)-X(1))•((Y(2)-Y(1))/(X(2)-X(1))-YP1))
C   END IF
DO 11 I=2,N-1
  SIG=(X(I)-X(I-1))/(X(I+1)-X(I-1))
  P=SIG•Y2(I-1)+2.
  Y2(I)=(SIG-1.)/P
  U(I)=(8.*((Y(I-1)-Y(I))/((X(I+1)-X(I))-
    /((X(I)-X(I-1)))/(X(I+1)-X(I-1))-SIG•U(I-1)))/P
  * CONTINUE
11 IF (YPN.GT..99E30) THEN
  QN=0.
  UN=0.
ELSE
  QN=0.6
  UN=(3./((X(N)-X(N-1))•(YPN-(Y(N)-Y(N-1))/(X(N)-X(N-1))))
ENDIF
Y2(N)=(UN-QN•U(N-1))/(QN•Y2(N-1)+1.)
DO 12 K=N-1,1,-1
  Y2(K)=Y2(K)•Y2(K+1)+U(K)
  * CONTINUE
12 CONTINUE
RETURN
END

C   Function BESSIO(x)
C   RETURNS THE MODIFIED BESSEL FUNCTION 10(X) FOR ANY REAL X.
C   IMPLICIT DOUBLE PRECISION (A-H, 0-Z)
C   r=0.8 Y,P1,P2,P3,P4,P5,P6,P7,Q1,Q2,Q3,Q4,Q5,Q6,Q7,Q8,Q9
C   d=.0007492d0,0 2.659732d0,0 3.880788d-1,0 .4B813d-2/
C   d=.021,q1,q2,q3,q4,q5,q6,q7,q8,q9,q0 3.9894728d0,0 1.3286592d-1,
C   * .0.226319d-2,-0.167586d-2,0 .916281d-2,-0 .2065700d-1,
C   * .0.2836537d-1,-0 .1647633d-1,0 .392377d-2/
C

```

```

IOUT=0
DEL=0.
DO 21 I=K1,N
LI=L(T(I))
IF(X(LI).EQ.BL(LI).AND.G(I).GE.0.)GOTO21
IF(X(LI).EQ.BU(LI).AND.G(I).LE.0.)GOTO21
IF(G(I).LT.0.)GOTO22
Z=X(LI)-BL(LI)
J=1
GOTO23
22 CONTINUE
Z=BU(LI)-X(LI)
J=0
23 CONTINUE
IF(G(ICAC+I).LE.0.)GOTO24
BETA=ABS(G(I))/G(ICAC+I)
TF(BETA.GE.Z)GOTO24
Z=BETA
D=.6*Z*ABS(G(I))
J=-1
GOTO26
24 CONTINUE
D=.6*(ABS(G(I))-.6*Z*C(TCAC+I))
26 CONTINUE
IF(D.LT.DEL) GOTO21
DEL=D
ALPHA=Z
IOUT=I
LIN=I
IF(J.LT.0) LIN=0
LB=J
21 CONTINUE
IF(IOUT.NE.0) GOTO29
27 CONTINUE
Q=0.
DO 28 I=1,N
LI=L(T(I))
Q=Q+X(LI)*(G(I)-B(LI))
LIN=LIN+Q
RETURN
29 CONTINUE
SIG=1.
IF(G(IOUT).GT.0.)SIG=-1.
SAS=G(ICAC+IOUT)
LIDOUT=L(T(IOUT))
LINN=LINOUT
26 CONTINUE
DO 30 I=1,K
G(1S+I)=G(1D+I)*A(IOUT,I)
31 CONTINUE
I=L(T(I))
DO 37 I=K1,N
IF(LI-LIOUT)32,37,33
Z=A(LI,LIDOUT)
GOTO34
33 Z=A(LI,LIDOUT)
34 CONTINUE
IF(K.EQ.0)GOTO36
DO 36 J=1,K
INV12690
INV12690
INV12619
INV12629
INV12830
INV12840
INV12850
INV12860
INV12870
INV12880
INV12890
INV12760
INV12710
INV12720
INV12730
INV12740
INV12750
INV12760
INV12770
INV12780
INV12790
INV12800
INV12810
INV12820
INV12830
INV12840
INV12850
INV12860
INV12870
INV12880
INV12890
INV12900
INV12910
INV12920
INV12930
INV12940
INV12950
INV12960
INV12970
INV12980
INV12990
INV13000
INV13050
INV13010
INV13020
INV13060
INV13080
INV13090
INV13100
INV13110
INV13120
INV13130
INV13140
INV13150
INV13160
INV13160
INV13170
INV13180

```

```

      return
      end

      c   Function BESSK1(x)
      c   Returns the modified Bessel function K1(x) for positive x.
      c
      IMPLICIT DOUBLE PRECISION (A-H, 0-Z)
      real*8 y, p1,p2,p3,p4,p5,p6,p7,q1,q2,q3,q4,q5,q6,q7
      data p1,p2,p3,p4,p5,p6,p7/1.0d0,0,-0.87278679d0,
      *-0.18168897d0,-0.181940d1,-0.119494d2,-0.4888d-4/
      data q1,q2,q3,q4,q5,q6,q7/1.-633141d0,0.23498819d0,-0.36566820d-1,INV1211d0
      *0.15042688d-1,-0.780363d-2,0.325614d-2,-0.88246d-3/
      INV1212d0
      if (x .le. 1.0) then
      y=x*x/4.0
      BESSK1= (log(x/2.0)*BESSI1(x))+(1.0/x)*(p1+y*(p2+y*(p3+
      *y*(p4+y*(p5+y*(p6+y*(p7)))))))
      else
      if (x .gt. 4.0) then
      BESSK1=0.0
      else
      y=(2.0/x)
      BESSK1=(exp(-x)/sqrt(x))*(q1+y*(q2+y*(q3+y*(q4+y*(q5+
      *y*(q6+y*q7))))))
      endif
      endif
      return
      end

      SUBROUTINE VEB4(N,A,IA,B,BL,BU,X,Q,LT,K,G)
      IMPLICIT REAL*8 (A-H,0-Z)

      c   QUADRATIC PROGRAMMING FROM HARWELL LIBRARY.
      c   SIMPLE BOUND CONSTRAINTS.

      DIMENSION A(IA,1),B(1),BL(1),BU(1),X(1),LT(1),G(1)
      IS=N
      IAS=N
      IV=N
      ICAC=N*N
      ID=ICAC
      D0 9  I=1,N
      9  G(I)=-B(I)
      D0 10  I=1,N
      X(I)=0
      LT(I)=I
      G(ICAC+I)=A(I,I)
      IF (0 .GE. BL(I) .AND. 0 .LE. BU(I)) GOTO10
      IF (0 .LT. BL(I)) X(I)=BL(I)
      IF (0 .GT. BU(I)) X(I)=BU(I)
      D0 12  J=1,I
      12  G(J)=G(J)+A(J,I)*X(I)
      I=I+1
      D0 11  J=II,N
      11  G(J)=G(J)+A(I,J)*X(I)
      10  CONTINUE
      K=0
      K1=1
      20  CONTINUE

```

```

VD=V/G(ID+I1)
S1=S0+N*VD
R=S1/S0
G((ID+1)=G(ID+I1)*R
BETA=VD/S1
IF (R GT .4) GOTO 841
DO 81 J=I2,N
  G(IV+N)=G(IV+J)-V*A(J,I1)
  IF (I1 GT .M2) GOTO 83
  DO 82 J=I1,K2
    J1=J+1
    82 A(J,I)=A(J1,I1)+BETA*A(IV+J1)
  83 CONTINUE
    A(K,I)=BETA
    DO 84 J=K1,N
      84 A(J,I)=A(J,I1)+BETA*A(IV+J)
      GOTO 849
  841 CONTINUE
    IF (I1 GT .K2) GOTO 843
    DO 842 J=I1,K2
      J1=J+1
      842 A(J,I)=BETA*A(IV+J1)+A(J1,I1)/R
    843 CONTINUE
    A(K,I)=BETA
    DO 844 J=K1,N
      844 A(J,I)=BETA*A(IV+J)+A(J,I1)/R
      DO 845 J=I2,N
        G(IV+J)=G(IV+J)-V*A(J,I1)
      845 CONTINUE
      LT(I1)=LT(I1)
      S0=S1
      I1=I2
      85 SG=I1./S1
      LT(0)=LTIN
      G((ID+K)=SG
      IF (LTIN EQ 1) GOTO 861
      I1=LTIN-1
      DO 862 I=1,II
        Z=A(LTIN,I)
        DO 863 J=LTIN,K2
          863 A(J,I)=A(J+1,I)
        862 A(K,I)=Z
      851 CONTINUE
      86 CONTINUE
      DO 87 I=K1,N
        G(ICAC,I)=G(ICAC,I)+SG*A(IV+I)**2
      87 K=K
      K=K2
      I1N=0
      ALPHA=1E75
      SAS=G(ICAC+IOUT)
      IF (SAS GT .0) ALPHA=ABS(G(IOUT))/SAS
      IF (G(IOUT).LT.0) GOTO 899
      J=1
      Z=X(LIOUT)-BL(LIOUT)
      GOTO 899
  898 CONTINUE
      J=0
      Z=BU(LIOUT)-X(LIOUT)
      INV14380

```

```

36   L=I . A(I,J) • G(I,S+J)
36   G(I,S+I) = Z
37   CONTINUE
   G(I,S+I)OUT)=SAS
   IF(K.EQ.0)GOTO42
   G(I,S+K)=-A(I)OUT,K)
   IF(K.EQ.1)GOTO42
   I=K
DO 41  I=2,K
   I=I-1
   Z=-A(I)OUT,I)
   I=I+1
DO 40  J=I1,K
   DO 40  Z=L.G(I,S+J)•A(J,1)
   IF(SIG.EQ.1.)GOT061
   DO 50  I=1,N
   50   G(I,S+I)=-G(I,S+I)
42   CONTINUE
   IF(K.EQ.0)GOT062
DO 61  I=1,K
   IF(G(I,S+I).EQ.0.)GOT061
   LI=LT(I)
CONTINUE
Z=BL(LI)-X(LI)
IF(G(I,S+I).LT.0.)GOT060
J=0
Z=BU(LI)-X(LI)
30   CONTINUE
Z=L/G(I,S+I)
IF(Z.GE.ALPHA)GOT061
ALPHA=Z
LB=J
LIN=I
LIIN=LI
61   CONTINUE
62   CONTINUE
   X(LI)OUT)=X(LI)OUT)+SIG•ALPHA
   IF(K.EQ.0)GOT071
DO 70  I=1,K
   LI=LT(I)
   70   X(LI)=X(LI)+ALPHA•G(I,S+I)
71   CONTINUE
DO 72  I=K1,N
   72   G(I)=G(I)+ALPHA•G(IAS+I)
   IF(LIN.EQ.0)GOT098
   X(LIIN)=BL(LIIN)
   IF(LB.EQ.0)X(LIIN)=BU(LIIN)
   IF(LIN.EQ.I)OUT)GOT020
   K2=K-1
SG=G(ID+LIIN)
   I=LIN+1
DO 80  I=I1,N
   80   G(IIV+I)=A(I,LIIN)
   IF(LIN.EQ.K)GOT088
   I2=LIN+2
   S0=1./SG
   DO 86  I=LIN,K2
   V=G(IIV+I)

```

```
DC 100 L=I1,J1
100 Z=Z+A(J,L)*A(L,I)
101 A(C,J,I)=-Z
102 CONTINUE
AA=1./G(ID+I1)
C(N*I1)=AA
DO 111 J=1,I
Z=A(I1,J)*AA
C(N*J)=G(N*J)+Z*A(I1,J)
IF(I.EQ.1) GOTO 111
J1=J+1
DO 110 L=J1,I
110 A(L,J)=A(L,J)+A(I1,L)*Z
111 A(I1,J)=Z
RETURN
END
```

```
INV14990
INV15000
INV15010
INV15020
INV15030
INV15040
INV15050
INV15060
INV15070
INV15080
INV15090
INV15100
INV15110
INV15120
INV15130
INV15140
```

```

899 CONTINUE
  IF (Z .GE. ALPHA) GOT026
    ALPHA=Z
    LB=J
    IIN=IOUT
    LIIN=LIOUT
    GOT026
900 CONTINUE
  K2=K1+1
  IF (SIG.EQ.1.) GOT091
  DO 901 I=K1,N
    G(IAS+I)=-G(IAS+I)
901 CONTINUE
  IF (IOUT.EQ.K1) GOT097
  LT(IOUT)=LT(K1)
  LT(K1)=LIOUT
  G(IAS+IOUT)=G(IAS+K1)
  G(ICAC+IOUT)=G(ICAC+K1)
  G(ICAC+K1)=SAS
  G(IOUT)=G(K1)
  IF (K.EQ.0) GOT097
  DO 92 I=1,K
    Z=A(K1,I)
    A(K1,I)=A(IOUT,I)
92  A(IOUT,I)=Z
93 CONTINUE
  IF (IOUT.EQ.IOUT) GOT095
  I1=IOUT-1
  DO 94 I=K2,I1
    A(IOUT,I)=A(I,K1)
94  CONTINUE
  IF (IOUT.EQ.N) GOT097
  I1=IOUT+1
  DO 95 I=I1,N
    A(I,IOUT)=A(I,K1)
95  CONTINUE
  G(K1)=0.
  K=K1
  IF (K.EQ.N) GOT027
  DO 98 I=K2,N
    Z=G(IAS+I)/SAS
    A(I,K1)=Z
    G(ICAC+I)=G(ICAC+I)-Z*G(IAS+I)
98  K=K2
GOT026

```

```

  ENTRY VE04B(N,A,IA,G,K)
  IF (K.EQ.0) RETURN
  ID=N+N
  G(N+1)=1./G(ID+1)
  N1=K-1
  IF (K.EQ.1) RETURN
  DO 111 I=1,N1
    I1=I+1
    A(I1,I)=-A(I1,I)
    IF (I.EQ.N1) GOT0102
    I1=I-2
    DO 101 J=II,K
      Z=A(J,I)
      J1=J-1
      INV14390
      INV14400
      INV14410
      INV14420
      INV14430
      INV14440
      INV14450
      INV14460
      INV14469
      INV14470
      INV14480
      INV14490
      INV14500
      INV14510
      INV14520
      INV14530
      INV14540
      INV14550
      INV14560
      INV14570
      INV14580
      INV14590
      INV14600
      INV14610
      INV14620
      INV14630
      INV14640
      INV14650
      INV14660
      INV14670
      INV14680
      INV14690
      INV14700
      INV14710
      INV14720
      INV14730
      INV14740
      INV14750
      INV14760
      INV14770
      INV14780
      INV14790
      INV14800
      INV14810
      INV14820
      INV14830
      INV14840
      INV14850
      INV14860
      INV14870
      INV14880
      INV14890
      INV14900
      INV14910
      INV14920
      INV14930
      INV14940
      INV14950
      INV14960
      INV14970
      INV14980

```

## Introduction

The utilization of downhole current sources in resistivity mapping increases the resolution for detecting and delineating subsurface features. The effects of near surface inhomogeneities are immensely reduced as shown by Asch and Morrison (1988). Being sensitive to changes in resistivities, the surveys with downhole sources are well suited for monitoring surface processes such as injection or leakage of contaminants from a waste site, steam flooding for enhanced oil recovery, or production of geothermal reservoirs.

In most of these applications, the holes are steel-cased and the casing distorts the current flow in the medium. Holladay and West (1984) have shown that surface resistivity surveys are strongly affected by casings. Also, Kauahikaua et al. (1980) showed that if the casing itself is used as an electrode, the results are unpredictable because the current leaves the pipe irregularly due to the variability of the contact resistance between the pipe and the formation.

To study the casing effects in more detail, we have recently formulated the problem for a point source of current, either inside or outside the pipe, on the axis of a finite length metal pipe in a conductive half space. The first part of this study (Schenkel and Morrison, 1987) showed that only the region very near the pipe exerts any substantial influence on the potential fields for a point source 100 casing diameters beyond the end of the pipe (Figure 1). For a 5% or less field distortion, the surface measurements must not be closer than 1/2 the pipe's length. In cross-hole surveys, the affected area is greatly reduced; near the pipe's end, measurements as close as 1/6 the length of the pipe for a 5% or less distortion. If the pipe-source separation is sufficiently large, then the resistivity survey can be corrected for the casing effects (assuming that the target are not too close to the pipe).

This study showed that cross-hole and hole-surface studies may be conducted with very little effects; even when the pipe exerts some influence, e.g., when the current source is close to the end, time monitoring experiments could be carried out with very little reduction in the signal strength. Further, this study revealed the intriguing possibility that segments of pipe, separated by insulated couplings, could be used as electrodes.

### **Proposed Work**

The above study was only developed for a very simple case, i.e., a pipe in a homogeneous half-space. A more complex model is required to simulate field situations. Several aims are proposed to create a realistic model and to evaluate field measurements for downhole sources in steel cased wells. These objectives are:

- 1) To determine the effects of contact resistance between the pipe and the host medium. Contact resistance is used to describe the resistance of the pipe-medium contact. If there is a large contact resistance, the results will completely change. The currents in the pipe will only leak out of the pipe in areas where the pipe has made a good contact with the host medium, thus completely changing the potential fields around the pipe. The contact resistance may be found by assuming a very thin layer between the host and pipe for each segment (Figure 2). An equivalent layer can be used to represent the effects of the contact resistance for each segment. The calculated potential field is obtained from the integral equation solution of the pipe variables. With the additional layer included to the model, the effects of pipe coating, corrosion, and cement on the potential fields can be evaluated.
- 2) To use insulated pipe segments as downhole sources and receivers. Downhole current electrodes can be created by energizing isolated segments. Likewise, insulated segments could be used as potential electrodes. By insulating several segments in the well (Figure 3), multiple

downhole source locations could be used to image a target in a hole-surface survey. A pole-pole configuration can be achieved by attaching to different segments current and potential electrodes. The isolated segments in the well can be used for an AC vertical electric dipole. By attaching to adjacent segments a positive and negative AC source, a grounded electric dipole can be produced to study EM properties of the medium. If an additional well is drilled with multiple isolated segments, then cross-hole DC and AC measurements can be acquired. Thus, cross-hole DC tomography (Daily and Morely, 1988 and Shima and Saito, 1988) could be used to reconstruct an image of a target between the two wells.

- 3) To determine the interaction between the source, pipe, and the anomalous body (Figure 4). To monitor the changes in the body, the effects of the metal pipe-body interaction must be investigated. The extent of this interaction will greatly depend on the source separation from the pipe, the distance between the pipe and the body, and the conductivity of the body. The determination of the limiting values of these parameters in which the body and pipe has very little coupling will be the main objective. For this situation, the body can be modeled alone saving computational time.
- 4) To invert for the geometric parameters for a plume-like body. An integral equation solution of an ellipsoidal model will be used to represent the plume. The parameters of the three axial lengths will be obtained by a non-linear least squares inversion which will make use of the integral equation solution. Sensitivity analysis and minimum spatial coverage will be evaluated for various acquisition array configurations.

Computer models will be required to investigate the above proposed tasks. The current algorithm is flexible so that variable source locations, segment lengths, and segment conductivities can be used. The development of an algorithm which includes an anomalous body and an outer layer is

needed. The current integral equation solution can be extended to include an additional layer and a circular disk. The circular disk is a first order approximation to a plume and will give an estimate of the pipe-body interaction.

Various lengths and separations of the insulated segments will be investigated to determine when a point approximation of the segments can be used. The outer layer will be used to evaluate the role of contact resistance on the field distortion and may be included in the pipe-body coupling phenomenon. The spatial separation of the source, pipe, and body to decouple the pipe and the body will be studied.

Field test and model verification are also required. The test would be conducted at U.C Berkeley, Richmond Field Station where there exist several plastic-cased holes. Four additional 100 foot holes are also needed. Two of the wells will be composed of alternating steel and fiberglass segments. Another would be cased with steel with the last 20 feet perforated. The last well needs to be plastic cased and perforated at the bottom. A surface grid and/or radial arrays of potential electrodes would be installed over the area. Cross-hole and hole-surface measurements would be compared to calculated fields of various pipe models. An injection of the salt water in both the steel-cased and plastic-cased wells would be measured for hole-surface, cross-hole, and pole-pole configurations. These data would be forward modeled and inverted to determine the geometry of the plume. Lastly, other configurations for which models have been published can be field tested with this field setup.

## REFERENCES

Asch, T., and Morrison, H.F., 1988, Mapping and monitoring electrical resistivity with surface and subsurface electrode arrays: (*Submitted to Geophysics*).

Daily, W. and Yorkey, T.J., 1988, Evaluation of cross-borehole resistivity tomography: Presented at the *58th Annual International SEG meeting* in Anaheim.

Holladay, J.S. and West, G.F., 1984, Effect of well casings on surface electrical surveys: *Geophysics*, **49**, p. 177-188.

Kauahikaua, J., Mattice, M., and Jackson, D., 1980, Mise-a-la-masse mapping of the HGP-A geothermal reservoir, Hawaii: *Geothermal Resource Council Transactions*, **4**, p. 65-68.

Schenkel, C.J. and Morrison, H.F., 1988, Effects of the well casing on potential field measurements: (*Submitted to Geoexploration*).

Shima, H. and Saito, H., 1988, Application of resistivity tomography for detection of faults and evaluation of their hydraulic continuity: some numerical experiments: Presented at the *58th Annual International SEG meeting* in Anaheim.